

Nonequilibrium functional bosonization of quantum wire networks

Stéphane Ngo Dinh^{a,d}, Dmitry A. Bagrets^c, Alexander D. Mirlin^{a,b,d,e}

^a*Institut für Theorie der Kondensierten Materie, Karlsruhe Institute of Technology, 76128 Karlsruhe, Germany*

^b*Institut für Nanotechnologie, Karlsruhe Institute of Technology, 76021 Karlsruhe, Germany*

^c*Institut für Theoretische Physik, Universität zu Köln, Zùlpicher Str. 77, 50937 Köln, Germany*

^d*DFG Center for Functional Nanostructures, Karlsruhe Institute of Technology, 76128 Karlsruhe, Germany*

^e*Petersburg Nuclear Physics Institute, 188300 St. Petersburg, Russia*

Abstract

We develop a general approach to nonequilibrium nanostructures formed by one-dimensional channels coupled by tunnel junctions and/or by impurity scattering. The formalism is based on nonequilibrium version of functional bosonization. A central role in this approach is played by the Keldysh action that has a form reminiscent of the theory of full counting statistics. To proceed with evaluation of physical observables, we assume the weak-tunneling regime and develop a real-time instanton method. A detailed exposition of the formalism is supplemented by two important applications: (i) tunneling into a biased Luttinger liquid with an impurity, and (ii) quantum-Hall Fabry-Pérot interferometry.

Keywords: Luttinger liquid, Bosonization, Quantum Hall edge states, Aharonov-Bohm effect

1. Introduction

Non-equilibrium electronic phenomena in nanostructures represent one of central directions of the modern condensed matter physics [1, 2]. Advances of nanofabrication have allowed researchers to explore experimentally transport properties of a great variety of nanodevices. Many remarkable phenomena have been observed in far-from-equilibrium regimes, i.e. for sufficiently large applied bias voltages.

A particularly important class of nanostructures is represented by coupled one-dimensional (1D) channels (quantum wires). The coupling may be due to tunneling between the wires or due to impurity-induced backscattering. Realizations of 1D elements that may serve as building blocks of such networks include, in particular, semiconducting and metallic quantum wires, carbon nanotubes, and quantum Hall edge states.

The standard analytical approach to interacting 1D systems (Luttinger liquids) is the bosonization [3]. Recently, a nonequilibrium generalization of the bosonization framework [4] was developed for setups where a nonequilibrium fermionic distribution is created outside of the interacting region and “injected” into the Luttinger liquid. We will focus here on a more complicated situation when the tunneling or the impurity backscattering takes place inside the interacting part of the system. Such coupling terms represent in general a very serious complication for the full bosonization approach, and we are not aware of any way to solve the problem exactly. We choose instead an alternative route based on the functional bosonization formalism [5] that retains both fermionic and bosonic degrees of freedom. Combining the functional bosonization idea with the Keldysh nonequilibrium framework, we derive Keldysh action for the considered class of problems. This action has a structure reminiscent of that of the generating function of the full counting statistics [6, 7]. Our action generalizes that of Ref. [8] where a local scatterer under nonequilibrium conditions was explored.

To proceed with evaluation of the functional integral, we assume a weak tunneling and develop a real-time instanton (saddle-point) method. This allows us to determine Keldysh Green functions characterizing physical observables under interest (tunneling density of states, distribution functions, current-voltage characteristics, etc.).

The goal of this article is twofold. First, we give a detailed exposition of the theoretical framework. Second, to illustrate the method, we present application of this approach to two important problems: (i) tunneling into a biased Luttinger liquid with an impurity, and (ii) quantum-Hall Fabry-Pérot interferometry.

The structure of the paper is as follows. Our general formalism is presented in Sec. 2. In Sec. 3 we use the approach to calculate the tunneling density of states of a biased Luttinger liquid with an impurity. In Sec. 4 we apply the method to explore a nonequilibrium quantum-Hall Fabry-Pérot interferometer. Section 5 includes a summary of our results and a discussion of prospective research directions. Technical details are presented in five Appendices.

Some of the results of this article have been previously published in a concise form in short communications [9, 10].

2. General Framework

2.1. Model and Functional Bosonization

Let us consider a general model of the ballistic conductor, which can be represented as a network of one-dimensional (1D) chiral channels and point scatterers, as shown in Fig. 1. It is assumed that electrons propagate along the channels, denoted by lower Greek index μ , with constant velocity v_μ from source to drain reservoirs located at coordinates x_μ^S and x_μ^D , respectively. In the physical world such channels are realized by quantum Hall (QH) edge states or right/left-moving 1D states in quantum wires. At point scatterers, denoted by Latin index j , instantaneous tunneling between different channels occurs, which is described by the scattering matrix s^j . Typical examples of scatterers are quantum point contacts (QPCs) or impurities in nanowires. Somewhat less trivial type of scatterer is a multi-terminal junction that can be realized by a quantum dot under assumption that its Thouless energy is well above all typical energy scales of the problem such as the temperature and the voltage.

Albeit quite simple, our quantum-wire network model covers a broad class of mesoscopic ballistic devices, including QH interferometers and quantum wire junctions (See Fig. 1). We note also that the importance of network models has been well appreciated in the context of the integer QH effect, where the Chalker-Coddington network model [11] serves as a highly useful starting point for numerical and analytical investigation of the QH transition.

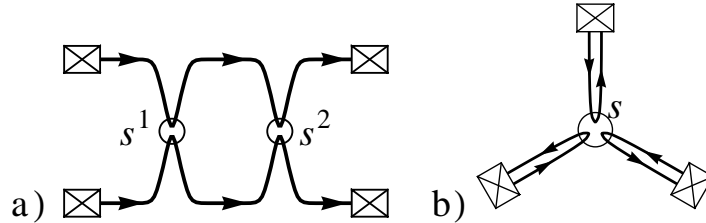


Figure 1: Two possible realizations of our model: (a) Mach-Zehnder quantum Hall interferometer and (b) junction of three quantum wires. Channels are represented by solid lines, point scatterers by white circles, reservoirs by boxes. Arrows indicate directions of motion.

To warm up, we briefly recall the construction of the bosonized Keldysh action in the absence of tunneling, i.e. when all scattering matrices are trivial, $s^j = 1$, and thus different chiral channels are fully disconnected from each other. We also require that each chiral channel in the absence of tunneling is connected to one source and one drain reservoir (rather than forms a loop). Following the logic of the Keldysh formalism [1, 2], all field degrees of freedom are doubled: upper Greek indices $\alpha = -/+$ denote fields ψ^α on the forward/backward branch of Keldysh's time contour \mathcal{C} ; integration along \mathcal{C} is to be understood as $\int_{\mathcal{C}} dt' A(t') = \int dt' (A^-(t') - A^+(t'))$.

The fermionic action of the 1D fermions reads

$$\mathcal{A}_0[\psi, \bar{\psi}] = \sum_{\mu} \int_{\mathcal{C}} dt dx \bar{\psi}_{\mu} (i\partial_t + iv_{\mu}\partial_x) \psi_{\mu} + \frac{1}{2} \sum_{\mu\nu} \int_{\mathcal{C}} dt dx dx' U_{\mu\nu}(x, x') \varrho_{\mu}(x) \varrho_{\nu}(x').$$

Electron-electron interaction is taken into account by potential $U_{\mu\nu}$, charge density in channel μ is $\varrho_{\mu}(x) = \bar{\psi}_{\mu}(x+0)\psi_{\mu}(x)$ with Grassmannian fields $\psi_{\mu}(x)$, $\bar{\psi}_{\mu}(x)$. Spatial integration extends along the corresponding

channels: $x_\mu^S < x < x_\mu^D$. To proceed we apply the method of functional bosonization [5] and decouple interaction via Hubbard-Stratonovich (HS) transformation, introducing the bosonic field φ_μ :

$$\mathcal{A}_0[\psi, \bar{\psi}, \varphi] = \sum_\mu \int_{\mathcal{C}} dt dx \bar{\psi}_\mu (i\partial_t + iv_\mu \partial_x - \varphi_\mu) \psi_\mu + \frac{1}{2} \sum_{\mu\nu} \int_{\mathcal{C}} dt dx dx' \varphi_\mu(x) U_{\mu\nu}^{-1}(x, x') \varphi_\nu(x').$$

The fact that we consider 1D chiral channels enables us to decouple $\bar{\psi}_\mu \psi_\mu$ and φ_μ by a gauge transformation $\psi_\mu^\mp \rightarrow e^{i\Theta_\mu^\mp} \psi_\mu^\mp$ requiring

$$(\partial_t + v_\mu \partial_x) \Theta_\mu^\mp = -\varphi_\mu^\mp. \quad (1)$$

While resolving this gauge condition, one should properly take the Keldysh structure into account, which yields

$$\begin{pmatrix} \Theta_\mu^- \\ \Theta_\mu^+ \end{pmatrix}_\xi = - \int d\xi' \begin{pmatrix} D_{0\mu}^T & D_{0\mu}^< \\ D_{0\mu}^> & D_{0\mu}^T \end{pmatrix}_{\xi-\xi'} \begin{pmatrix} \varphi_\mu^- \\ -\varphi_\mu^+ \end{pmatrix}_{\xi'} \quad (2)$$

with $\xi = (x, t)$. Here the blocks of the particle-hole propagator $D_{0\mu}$ satisfy the relations

$$\begin{aligned} (\partial_t + v_\mu \partial_x) D^{T/\bar{T}}(\xi, \xi') &= \pm \delta(\xi - \xi'), \\ (\partial_t + v_\mu \partial_x) D^{\lessgtr}(\xi, \xi') &= 0 \end{aligned} \quad (3)$$

and therefore Eq. (2) indeed solves the gauge condition (1). In the frequency-momentum representation the bare retarded/advanced particle-hole propagator $D_{0\mu}$ in channel μ is given by

$$D_{0\mu}^{r/a}(\omega, q) = \frac{i}{\omega_\pm - v_\mu q}, \quad \omega_\pm = \omega \pm i0. \quad (4)$$

The Keldysh propagator $D_{0\mu}^K$ depends on the nonequilibrium state of the system. In what follows, we consider the zero temperature limit. Under this assumption, the electron distribution functions, $f_\lambda^< = f_\lambda$, $f_\lambda^> = 1 - f_\lambda$, of source reservoirs λ are completely characterized by the applied bias $\mu_\lambda = eV_\lambda$,

$$f_\lambda^{\lessgtr}(t, t') = f_\lambda^{\lessgtr}(t - t') = e^{i\mu_\lambda(t-t')} f_0^{\lessgtr}(t - t') \quad \text{with} \quad f_0^{\lessgtr}(t) = \mp \frac{i}{2\pi} \frac{1}{t \mp ia}, \quad (5)$$

where $f_0(t)$ is the real-time representation of the Fermi distribution function and a is a short-time cutoff. The components of the bare particle-hole propagators are then

$$D_{0\mu}^{\lessgtr}(x, t) = |v_\mu|^{-1} n_B^{\lessgtr}(t - x/v_\mu), \quad D_{0\mu}^{T/\bar{T}}(x, t) = \theta(\pm t) D_{0\mu}^>(x, t) + \theta(\mp t) D_{0\mu}^<(x, t), \quad (6)$$

with equilibrium Bose function $n_B^{\lessgtr}(t) = -i/2\pi(t \mp ia)$. Further, the Keldysh particle-hole propagator is given by the equilibrium relation

$$D_{0\mu}^k(\omega, q) = (D_{0\mu}^r(\omega, q) - D_{0\mu}^a(\omega, q)) \text{sgn}(\omega). \quad (7)$$

The gauge transformation has a non-trivial Jacobian contributing to the action. According to the Dzyaloshinskii-Larkin theorem [12], this contribution is Gaussian, and the new action reads

$$\mathcal{A}_0[\varphi] = \frac{1}{2} \sum_{\mu\nu} \int_{\mathcal{C}} d\xi d\xi' \varphi_\mu(\xi) V_{\mu\nu}^{-1}(\xi, \xi') \varphi_\nu(\xi') - \sum_\lambda \int_{\mathcal{C}} d\xi \varphi_\lambda(\xi) \varrho_{0\lambda}(\xi), \quad (8)$$

with excess charge $\varrho_{0\lambda} = \mu_\lambda/(2\pi|v_\lambda|)$, effective interaction

$$V_{\mu\nu}^{-1}(\xi, \xi') = U_{\mu\nu}^{-1}(x, x') \delta(t - t') - \delta_{\mu\nu} \Pi_\mu(\xi - \xi'),$$

polarization operator $\Pi_\mu^{\alpha\beta}(\xi) = -iG_{0\mu}^{\alpha\beta}(\xi)G_{0\mu}^{\beta\alpha}(-\xi)$, and free Green's function

$$G_{0\mu}^{\geq}(\xi) = -\frac{1}{2\pi|v_\mu|} \frac{e^{-ieV_\mu(t-x/v_\mu)}}{t \mp ia - x/v_\mu}, \quad G_{0\mu}^{T/\tilde{T}}(\xi) = \theta(\pm t)G_{0\mu}^>(\xi) + \theta(\mp t)G_{0\mu}^<(\xi). \quad (9)$$

After the standard rotation in the Keldysh space [1, 2] and the transformation into frequency-momentum representation, one obtains the retarded/advanced components of the 1D polarization operator

$$\Pi_\mu^{r/a}(\omega, q) = \frac{1}{2\pi|v_\mu|} \frac{v_\mu q}{\omega_\pm - v_\mu q}. \quad (10)$$

With the action $\mathcal{A}_0[\varphi]$ being Gaussian, the respective average value $\langle\varphi_\mu(\xi)\rangle_0$ and the correlator of the fluctuations $\delta\varphi_\mu(\xi) \equiv \varphi_\mu(\xi) - \langle\varphi(\xi)\rangle_0$ are simply given by $\langle\varphi(\xi)\rangle_0 = \sum_\nu \int_{\mathcal{C}} d\xi' V_{\mu\nu}(\xi, \xi') \varrho_{0\nu}(\xi')$ and $\langle\delta\varphi_\mu(\xi)\delta\varphi_\nu(\xi')\rangle_0 = iV_{\mu\nu}(\xi, \xi')$.

From (2), or symbolically $\Theta_\mu = -D_{0\mu}\varphi_\mu$, one obtains for the correlator $iD_{\Theta,\mu\nu}(\xi, \xi') = \langle\delta\Theta_\mu(\xi)\delta\Theta_\nu(\xi')\rangle$ the relation

$$D_{\Theta,\mu\nu} = -D_{0\mu}V_{\mu\nu}D_{0\nu}. \quad (11)$$

After having reviewed the results for the action in the absence of tunneling, we are ready to consider the case of a connected quantum network. This will be the subject of Sec. 2.2.

2.2. Keldysh Action

With all preliminaries we are now in a position to formulate the Keldysh action of the connected quantum network when at least one node is characterized by a non-trivial scattering matrix $s^j \neq \mathbb{1}$. For the case of a single compact scatterer such an action has been constructed in Ref. [8] with the use of nonequilibrium Green's function method. The result bears connection with the solution of the problem of full counting statistics [6, 7]. In our paper we generalize this approach to the situation with many scatterers. It turns out that the Keldysh action in this case can be written in terms of a full time-dependent single-particle scattering matrix (S-matrix) of the system in a given configuration of field φ^α , which we denote $S^\alpha = S[\varphi^\alpha](t, t')$, where α is the Keldysh index. Let us emphasize that the S-matrix is non-local in time and takes different values on the forward and backward branches of the Keldysh contour. Our result reads:

$$\begin{aligned} \mathcal{A}[\varphi] = & \frac{1}{2} \sum_{\mu\nu} \int_{\mathcal{C}} d\xi d\xi' \varphi_\mu U_{\mu\nu}^{-1} \varphi_\nu - \sum_\mu \int d\xi d\xi' (\varphi_\mu^c, \varphi_\mu^q)_\xi \begin{pmatrix} 0 & \Pi_\mu^a(\xi - \xi') \\ \Pi_\mu^r(\xi - \xi') & 0 \end{pmatrix} \begin{pmatrix} \varphi_\mu^c \\ \varphi_\mu^q \end{pmatrix}_{\xi'} \\ & - i \ln \text{Det} [\mathbb{1} - f + S[\varphi^+]^\dagger S[\varphi^-] f]. \quad (12) \end{aligned}$$

The last term in Eq. (12) is a functional determinant with respect to (real) time and channel indices. It is understood that f in the expression for the corresponding operator has the structure $f_{\mu\nu}(t, t') = \delta_{\mu\nu} f_\mu(t - t')$, i.e., it is diagonal in channel representation, with $f_\mu(t)$ being the Fourier transform of the source distribution function connected to channel μ . The second term in (12) represent anomalous contributions (related to the Schwinger anomaly) that have been already encountered before, see Eq. (8). They are most transparently written in the rotated Keldysh representation: $\varphi^{c(q)} = (\varphi^- \pm \varphi^+)/2$, $\Pi_\mu^{r/a} = (\Pi_\mu^T - \Pi_\mu^{\tilde{T}} \pm (\Pi_\mu^> - \Pi_\mu^<))/2$ and integration is performed along the real time axis.

A detailed derivation of the result (12), which employs ideas of Ref. [7], is presented in Appendix A. In view of the importance of this result, we give also its alternative proof (Appendix B), which follows closely the method of Ref. [8].

Construction of Scattering Matrix

Let us now discuss how the S-matrix for the systems under consideration is constructed. The elements of $S_{\nu\mu}^\alpha(t, t')$ give the amplitude that a wave packet incident from source μ at time t' leaves the system at time t through the drain ν . They are sums $S_{\nu\mu}^\alpha(t, t') = \sum_p A_\mu^{(p)\alpha}(t, t')$ over all corresponding paths p formed by elements of the network.

Figure 2 shows an exemplary path p through a network of channels and point scatterers. It consists of an alternating sequence of two types of processes:

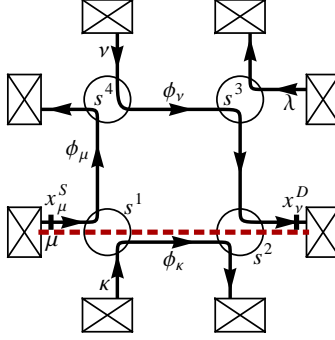


Figure 2: Network built out of four channels $\mu, \kappa, \nu, \lambda$ and point scatterers 1, 2, 3, 4. Counting fields measure outgoing currents. Along interior parts of channels classical phases $\phi_{\mu/\kappa/\nu}$, e.g. due to magnetic field, are accumulated. An exemplary path p is indicated by a dashed line.

Electron propagation in the potential φ_μ^α between x^i and x^j ,. leading to the accumulated phase

$$\vartheta_\mu^\alpha(x^j, x^i; t)(t) \equiv -v_\mu^{-1} \int_{x^i}^{x^j} dx \varphi_\mu^\alpha(x, t - (x^j - x)/v_\mu). \quad (13)$$

In addition to the Hubbard-Stratonovich field φ_μ^α , there may be other time-dependent phases ϕ_μ^α (e.g., induced by a magnetic field) contributing to Eq. (13). Note that $\vartheta_\mu^\alpha(x, x^i)$ satisfies the same differential equation $(\partial_t + v_\mu \partial_x) \vartheta_\mu^\alpha(x, x^i; t) = -\varphi_\mu^\alpha(x, t)$ as $\Theta_\mu^\alpha(x, t)$, but has a simpler (“incomplete”) Keldysh structure which involves only the retarded/advanced components of the bare particle-hole propagator $D_{0\mu}$. We refer to $\vartheta_\mu^\alpha(x, x^i)$ as a *kinematic* phase. To take a finite flight time of electron between x^i and x^j into account, we introduce a “delay operator”

$$\Delta_\mu(x^j, x^i; t', t) = \delta(t' - t - (x^j - x^i)/v_\mu) \quad (14)$$

Then the amplitude of this process reads

$$\mathcal{M}_\mu^\alpha(x^j, x^i; t, t') \equiv e^{i\vartheta_\mu^\alpha(x^j, x^i; t)} \Delta_\mu(x^j, x^i; t, t'). \quad (15)$$

Indeed, consider the 1D version of the Schrödinger equation on a directed link $x^i \rightarrow x^j$,

$$i\partial_t \psi_\mu = (-iv_\mu \partial_x + \phi_\mu^\alpha) \psi_\mu. \quad (16)$$

Using the definition of the kinematic phase (13), this equation can be solved independently on each branch of the Keldysh contour yielding the relation

$$\psi_\mu(x_j, t) = e^{i\vartheta_\mu^\alpha(x^j, x^i; t)} \psi_\mu(x_i, t - (x^j - x^i)/v_\mu), \quad (17)$$

which implies that the scattering matrix is given Eq. (15).

Scattering/tunneling at point scatterer j :. The amplitude of instantaneous scattering from channel μ to ν is

$$s_{\nu\mu}^j(t', t) = s_{\nu\mu}^j \delta(t' - t).$$

Passing the charge detector at drain μ , which is described by the counting field χ_μ .. As a special variant of a ., our formalism includes the theory of full counting statistics. A counting field residing in the drain lead μ measures the current flowing in that drain. The corresponding amplitude is

$$\mathcal{X}_\mu^\alpha(t', t) = e^{-i\frac{\alpha}{2} \chi_\mu} \delta(t' - t).$$

Then the action (12) enables us to express the cumulant generating function of the network as a functional integral over φ ,

$$\mathcal{Z}(\vec{\chi}) = \int \prod_{\mu} \mathcal{D}\varphi_{\mu}^{\pm}(x, t) \exp \{i\mathcal{A}(\varphi, \vec{\chi})\}, \quad (18)$$

where vector $\vec{\chi}$ combines counting fields χ_{μ} in all drains.

Finally, the amplitude $A_{\nu\mu}^{(p)\alpha}$ of a path p is the path-ordered (real) time convolution (“latest to the left”) of the amplitudes of its constituent processes. As an example, the amplitude indicated by the dashed line in Fig. 2 reads

$$\begin{aligned} A_{\nu\mu}^{(p)\alpha}(t, t') &= [\mathcal{X}_{\nu}^{\alpha} \mathcal{M}_{\nu}^{\alpha}(x_{\nu}^D, x_{\nu}^2) s_{\nu\kappa}^2 \mathcal{M}_{\kappa}^{\alpha}(x_{\kappa}^2, x_{\kappa}^1) s_{\kappa\mu}^1 \mathcal{M}_{\mu}^{\alpha}(x_{\mu}^1, x_{\mu}^S)](t, t') \\ &= \delta(t - t' - \tau) e^{-i\frac{\alpha}{2}\chi_{\nu} + i\phi_{\kappa}} s_{\nu\kappa}^2 s_{\kappa\mu}^1 \exp \{i\vartheta_{\nu}^{\alpha}(x_{\nu}^D, x_{\nu}^2; t) + i\vartheta_{\kappa}^{\alpha}(x_{\kappa}^2, x_{\kappa}^1; t - \tau_3) + i\vartheta_{\mu}^{\alpha}(x_{\mu}^1, x_{\mu}^S; t - \tau_3 - \tau_2)\}, \end{aligned}$$

where $\tau_{1/2/3}$ denote the flight times of the subpaths $x_{\mu}^S \rightarrow x_{\mu}^1$, $x_{\kappa}^1 \rightarrow x_{\kappa}^2$, $x_{\nu}^2 \rightarrow x_{\nu}^D$, and $\tau = \tau_1 + \tau_2 + \tau_3$ is the total flight time.

2.3. Weak Tunneling Expansion

Due to the complex temporal behavior of the scattering matrix analytical evaluation of the functional determinant (12) is not feasible in general. An approximate treatment is possible if a weak tunneling at the point scatterers is assumed (i.e. the scattering matrix $s_{\nu\mu}^j$ close to $\delta_{\nu\mu}$), and the ultimate goal of this section is the expansion of the action in the tunneling strength. Since in the absence of tunneling the network is described by the Gaussian action (8), one can introduce the tunneling action $\mathcal{A}_t[\varphi]$, so that $\mathcal{A}[\varphi] = \mathcal{A}_0[\varphi] + \mathcal{A}_t[\varphi]$, where the expansion of $\mathcal{A}_t[\varphi]$ starts from second-order terms with respect to the tunneling amplitudes at the point scatterers. In Appendix Appendix C we show that an exact representation of $\mathcal{A}_t[\varphi]$ is given in terms of a modified (“regularized”) functional determinant

$$\mathcal{A}_t[\varphi] = -i \ln \text{Det} \left[\mathbb{1} - f + \tilde{S}^{\dagger} \tilde{S}^{-} f \right]. \quad (19)$$

The new, “regularized” scattering matrix \tilde{S} here is constructed similarly to S . Each of its elements $\tilde{S}_{\nu\mu}^{\alpha}(t, t') = \sum_p \tilde{A}_{\nu\mu}^{(p)\alpha}(t, t')$ is a sum over the same paths p which contribute to $S_{\nu\mu}^{\alpha}(t, t')$ and connect the source μ with the drain ν . Full and regularized amplitudes, $A_{\nu\mu}^{(p)}$ and $\tilde{A}_{\nu\mu}^{(p)}$ respectively, differ in the partial amplitudes assigned to the elementary processes a . and b . which constitute a path p :

Propagation between x^i and x^j . Only the time delay is taken into account:

$$\tilde{\mathcal{M}}_{\mu}^{\alpha}(x^j, x^i) = \Delta_{\mu}(x^j, x^i),$$

while phase accumulation is shifted to

Tunneling at point scatterers j . The off-diagonal tunneling amplitudes become “dressed” by tunneling phases $\Phi_{\nu\mu}^{\alpha}(x^j, t) \equiv \Theta_{\mu}^{\alpha}(x_{\mu}^j, t) - \Theta_{\nu}^{\alpha}(x_{\nu}^j, t)$:

$$\tilde{s}_{\nu\mu}^{j\alpha}(t, t') = e^{i\Phi_{\nu\mu}^{\alpha}(x^j, t)} s_{\nu\mu}^j \delta(t - t').$$

The phases $\Theta_{\mu} = -D_{0\mu}\varphi_{\mu}$ are defined as in Sect. 2.1 and can be modified by additional time-independent phase contributions due to e.g. magnetic or counting fields as follows. If the additional phase accumulated by an electron which propagates along a channel μ from a position x to the drain lead μ is denoted as $\phi_{\mu, \text{out}}^{\alpha}(x)$, then the phase Θ_{μ}^{α} is modified according to

$$\Theta_{\mu}^{\alpha}(x, t) \mapsto \Theta_{\mu}^{\alpha}(x, t) - \phi_{\mu, \text{out}}^{\alpha}(x).$$

In our previous example, Fig. 2, the regularized scattering amplitudes read

$$\begin{aligned}\tilde{s}_{\kappa\mu}^{1\alpha}(t, t') &= e^{i\Phi_{\kappa\mu}^{\alpha}(x^1, t) - i(\phi_{\mu} - \phi_{\kappa}) + i\frac{\alpha}{2}(\chi_{\mu} - \chi_{\kappa})} s_{\kappa\mu}^2 \delta(t - t'), \\ \tilde{s}_{\nu\kappa}^{1\alpha}(t, t') &= e^{i\Phi_{\nu\kappa}^{\alpha}(x^2, t) + i\frac{\alpha}{2}(\chi_{\kappa} - \chi_{\nu})} s_{\nu\kappa}^2 \delta(t - t').\end{aligned}$$

The regularized scattering matrix becomes trivial in the “clean” limit, $\tilde{S} = \mathbb{1}$, since all effects of interaction are now contained in the phases of the off-diagonal elements of the regularized scattering matrices $\tilde{s}_{\nu\mu}^j$ of connectors. Thus Eq. (19) can be expanded in (even) powers of the tunneling amplitudes:

$$\mathcal{A}_t[\varphi] = i \sum_{n=1}^{\infty} \frac{1}{n} \text{Tr} \left[\left(\mathbb{1} - \tilde{S}^{+\dagger} \tilde{S}^- \right) f \right]^n.$$

We are now going to elaborate on the second-order terms in this series.

Second Order Expansion

We introduce a notation $\mathcal{A} \equiv \tilde{S}^{+\dagger} \tilde{S}^-$. Up to third order corrections in the tunneling amplitudes [that we denote as $\mathcal{O}(\text{tun}^3)$] the tunneling action is

$$\begin{aligned}\mathcal{A}_t[\varphi] &= i \text{Tr} \left[(\mathbb{1} - \mathcal{A})f + \frac{1}{2}(\mathbb{1} - \mathcal{A})f(\mathbb{1} - \mathcal{A})f \right] + \mathcal{O}(\text{tun}^3) \\ &= i \text{Tr} \left[(\mathbb{1} - \mathcal{A})_{\mu\mu} f_{\mu} + \frac{1}{2} \sum_{\mu \neq \nu} \mathcal{A}_{\mu\nu} f_{\nu} \mathcal{A}_{\nu\mu} f_{\mu} \right] + \mathcal{O}(\text{tun}^3).\end{aligned}\tag{20}$$

In the last expression, the trace is only taken with respect to time. To reduce the tunneling action to this form, we used $(\mathbb{1} - \mathcal{A})_{\mu\mu} = \mathcal{O}(\text{tun}^2)$ and $\mathcal{A}_{\nu\mu} = \mathcal{O}(\text{tun})$.

It can be shown (see Appendix Appendix D for a detailed derivation) that \mathcal{A}_t acquires contributions from paths which start in a certain source reservoir, evolve forward and backward in time, undergoing in total exactly 2 tunneling events, and eventually returning to the original source. Such paths involve exactly 2 different channels, μ and ν . Thus we can classify all paths according to the pair (μ, ν) of channels $\mu \neq \nu$ and the pair (i, j) of scatterers (possibly equal) at which the tunneling takes place: $\mu \rightarrow \nu$ at i and $\nu \rightarrow \mu$ at j . Of course, the class $(ij; \mu\nu)$ coincides with the class $(ji; \nu\mu)$. The second order expansion of the tunneling action then is a sum over these classes:

$$\mathcal{A}_t[\varphi] = -i \sum_{(ij; \mu\nu)} \int dt_1 dt_2 \begin{pmatrix} e^{-i\Phi_{\mu\nu}^-(x^i, t_1)} & e^{-i\Phi_{\mu\nu}^+(x^i, t_1)} \\ -\Pi_{ij; \mu\nu}^>(t_{12}) & \Pi_{ij; \mu\nu}^<(t_{12}) \end{pmatrix} \begin{pmatrix} \Pi_{ij; \mu\nu}^T(t_{12}) & -\Pi_{ij; \mu\nu}^<(t_{12}) \\ -\Pi_{ij; \mu\nu}^>(t_{12}) & \Pi_{ij; \mu\nu}^{\tilde{T}}(t_{12}) \end{pmatrix} \begin{pmatrix} e^{i\Phi_{\mu\nu}^-(x^j, t_2)} \\ e^{i\Phi_{\mu\nu}^+(x^j, t_2)} \end{pmatrix},\tag{21}$$

$t_{12} \equiv t_1 - t_2$, where the tunneling polarization operators are given by

$$\Pi_{ij; \mu\nu}^{\geq}(t) = -s_{\nu\mu}^i \tilde{s}_{\nu\mu}^j e^{i\Delta\phi_{\mu\nu}^{ij}} e^{\pm i(\chi_{\mu} - \chi_{\nu})} f_{\mu}^{\geq}(t + \tau_{\mu.\text{in}}^j - \tau_{\mu.\text{in}}^i) f_{\nu}^{\leq}(\tau_{\nu.\text{in}}^i - \tau_{\nu.\text{in}}^j - t),\tag{22}$$

$$\Pi_{ij; \mu\nu}^{T/\tilde{T}}(t) = [\theta(\pm t) \Pi_{ij; \mu\nu}^>(t) + \theta(\mp t) \Pi_{ij; \mu\nu}^<(t)]_{\chi \equiv 0},\tag{23}$$

where $\tau_{\lambda.\text{in}}^k$ is the flight time from the source to the scatterer k along a channel λ , $\tau_{\lambda.\text{in}}^k = (x_{\lambda}^k - x_{\lambda}^S)/v_{\lambda}$. We have also taken into account counting fields in the drain leads (which are not contained in $\Pi_{ij; \mu\nu}^{T/\tilde{T}}$) and classical phases,

$$\Delta\phi_{\mu\nu}^{ij} \equiv \phi_{\nu.\text{out}}(x^i) - \phi_{\mu.\text{out}}(x^i) - \phi_{\nu.\text{out}}(x^j) + \phi_{\mu.\text{out}}(x^j).$$

In the case $i = j$ we will also use the convention

$$\Pi_{ii; \mu\nu}^T(t) = \Pi_{ii; \mu\nu}^{\tilde{T}}(t) = \frac{1}{2} [\Pi_{ii; \mu\nu}^>(t) + \Pi_{ii; \mu\nu}^<(t)].\tag{24}$$

The comparison of this expression with the Eq. (23) shows that they differ from each other by the singular term proportional to $\text{sign}(t)h(t)\delta(t) = \pi\delta^2(t)$, where we put $h(t) = f_0^>(t) - f_0^<(t)$. It gives some constant (albeit infinite) contribution to the tunneling action (21) and therefore both representation for $\Pi_{ii;\mu\nu}^{T/\tilde{T}}$ are equivalent.

2.4. Real-Time Instanton Method

On the level of the second order expansion, the action $\mathcal{A}_t[\varphi]$ is expressed in terms of the tunneling phases Φ , which are linear functionals of φ :

$$\Phi_{\mu\nu}(\xi) = \sum_{\lambda} \int_C d\xi' \mathcal{D}_{\mu\nu;\lambda}(\xi, \xi') \varphi_{\lambda}(\xi'), \quad \mathcal{D}_{\mu\nu;\lambda} \equiv D_{0\mu}\delta_{\mu\lambda} - D_{0\nu}\delta_{\nu\lambda}. \quad (25)$$

The action $\mathcal{A}_t[\varphi]$ is non-Gaussian in Φ and, in fact, is quite similar to the Ambegaokar-Eckern-Schön (AES) action [13]. The difference is that the kernel appearing in Eq. (21) is not only non-local in time (as in the case of AES) but in general is non-local in space as well. In view of the non-Gaussian character of the action an exact evaluation of physical quantities does not seem feasible in general. For this reason, we will use a saddle-point approximation that catches correctly the relevant interaction-induced physics, including both the renormalization and the dephasing phenomena.

To explain the idea of the method, let us consider some physical quantity $\mathcal{O}[\varphi] = \mathcal{O}_0 e^{i\mathcal{A}_J[\varphi]}$, where $\mathcal{A}_J[\varphi] = -\sum_{\mu} \int_C d\xi J_{\mu}(\xi) \varphi_{\mu}(\xi)$ is a linear functional of φ , and the prefactor \mathcal{O}_0 is independent on φ . Important examples, which are treated in the next sections, include the electronic Green's function and the current. The quantum average value of \mathcal{O} is given by the functional integral

$$\langle \mathcal{O}[\varphi] \rangle = \int \mathcal{D}\varphi e^{i\mathcal{A}_0[\varphi] + i\mathcal{A}_t[\varphi] + i\mathcal{A}_J[\varphi]} \mathcal{O}_0, \quad (26)$$

which we estimate in the semiclassical approximation [14]. In this case the path integral is contributed by the saddle-point trajectory φ_{**} of the full action $\mathcal{A}_0[\varphi] + \mathcal{A}_t[\varphi] + \mathcal{A}_J[\varphi]$ and quantum fluctuations around it. Here free and tunneling actions $\mathcal{A}_0[\varphi]$, $\mathcal{A}_t[\varphi]$ are given by Eqs. (8) and (21), respectively. In the limit of weak tunneling between chiral channels the saddle-point trajectory (“instanton”) can be found approximately by requiring that it minimizes the Gaussian contributions to the action $\mathcal{A}_0[\varphi] + \mathcal{A}_J[\varphi]$, which gives

$$\varphi_{*\mu}(\xi) = \sum_{\nu} \int_C d\xi' V_{\mu\nu}(\xi, \xi') (\varrho_{0\nu}(\xi') + J_{\nu}(\xi')). \quad (27)$$

As shown in Appendix Appendix E, under such an approximation Eq. (26) simplifies to

$$\langle \mathcal{O}[\varphi] \rangle = \left\langle e^{i\mathcal{A}_J[\varphi]} \right\rangle_0 e^{i\tilde{\mathcal{A}}_t[\varphi_*]} \mathcal{O}_0, \quad (28)$$

with

$$\left\langle e^{i\mathcal{A}_J[\varphi]} \right\rangle_0 = \exp \left\{ i \langle \mathcal{A}_J[\varphi] \rangle_0 - \frac{1}{2} \left[\langle (\mathcal{A}_J[\varphi] - \langle \mathcal{A}_J[\varphi] \rangle_0)^2 \rangle_0 \right] \right\}, \quad (29)$$

$$\tilde{\mathcal{A}}_t[\varphi_*] = -i \sum_{\{\mu, \nu\}, \{i, j\}} \int dt_1 dt_2 \begin{pmatrix} e^{-i\Phi_{*\mu\nu}^-(x^i, t_1)} & e^{-i\Phi_{*\mu\nu}^+(x^i, t_1)} \end{pmatrix} \begin{pmatrix} \tilde{\Pi}_{ij;\mu\nu}^T(t_{12}) & -\tilde{\Pi}_{ij;\mu\nu}^<(t_{12}) \\ -\tilde{\Pi}_{ij;\mu\nu}^>(t_{12}) & \tilde{\Pi}_{ij;\mu\nu}^T(t_{12}) \end{pmatrix} \begin{pmatrix} e^{i\Phi_{*\mu\nu}^-(x^j, t_2)} \\ e^{i\Phi_{*\mu\nu}^+(x^j, t_2)} \end{pmatrix}, \quad (30)$$

where $t_{12} \equiv t_1 - t_2$ and $\langle \dots \rangle_0$ denotes averaging with respect to $\mathcal{A}_0[\varphi]$. We have introduced the instanton phases $\Phi_{*\mu\nu} = \mathcal{D}_{\mu\nu}\varphi_*$ and the *renormalized* tunneling polarization operators

$$\tilde{\Pi}_{ij;\mu\nu}^{\alpha\beta}(t_1 - t_2) = e^{i(D_{\Phi_{*\mu\nu}}^{\alpha\beta}(x^i, x^j; t_1 - t_2) - D_{\Phi_{*\mu\nu}}^{\alpha\beta}(0, 0))} \Pi_{ij;\mu\nu}^{\alpha\beta}(t_1 - t_2), \quad (31)$$

obtained by dressing of the bare tunneling polarization operators by phase-phase correlators

$$D_{\Phi\mu\nu}(\xi_1, \xi_2) = \sum_{\kappa\lambda} \int_C d\xi' d\xi'' \mathcal{D}_{\mu\nu;\kappa}(\xi_1, \xi') V_{\kappa\lambda}(\xi', \xi'') \mathcal{D}_{\mu\nu;\lambda}(\xi'', \xi_2).$$

The meaning of Eq. (31) is that quantum fluctuations of tunneling phases renormalize the temporal dependence of tunneling polarization operators which lead to non-trivial (usually power-law) energy-dependence of tunneling coefficients.

In the next two sections we consider two important applications of our general approach.

3. Tunneling Density of States of Luttinger Liquid with Single Impurity

In this section we show how our formalism can be applied to the evaluation of the tunneling density of states (TDOS) of a nonequilibrium quantum wire containing a single impurity [9], as depicted in Fig. 3. On the experimental side, the interest to such a theoretical study is motivated by the recent development of the nonequilibrium tunneling spectroscopy of 1D nanostructures, including carbon nanotubes [15] and quantum Hall edges [16, 17, 18].

3.1. Model and Results

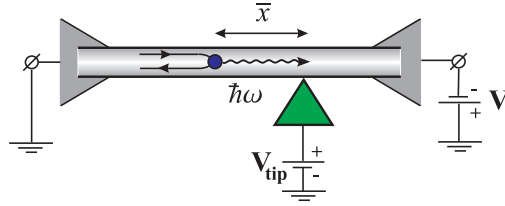


Figure 3: Tunneling experiment with a voltage-biased quantum wire.

The wire is modeled as a network of two channels: right- (left-) moving electrons, denoted with indices $\mu = +(-)$. Backscattering, i.e. tunneling between the two channels, occurs at the impurity (at $x = 0$) which is considered as a point scatterer with scattering matrix s . Non-equilibrium conditions are established by biasing the right reservoir with respect to the left one: $eV_+ = eV > 0$, $eV_- = 0$.

The interplay of interaction, nonequilibrium, and impurity scattering can be studied by placing a conducting tip held at a voltage V_{tip} near a position \bar{x} of the wire (we can assume without loss of generality that $\bar{x} > 0$) and measuring the current I_{tun} between tip and wire. Let us assume that the tip can be described in terms of fermionic quasiparticles with density of states $\nu_{\text{tip}}(\epsilon)$ and distribution function $f_{\text{tip}}(\epsilon)$, as is the case, e.g., in the absence of interaction within the tip. If the coupling $|t|^2$ between the tip and the wire is weak, a simple perturbative expansion yields the tunneling current

$$I_{\text{tun}} \propto |t|^2 \sum_{\mu=\pm} \int d\epsilon [\Gamma_{\mu}^{>}(\epsilon) f_{\text{tip}}(\epsilon) - \Gamma_{\mu}^{<}(\epsilon) (1 - f_{\text{tip}}(\epsilon))] \nu_{\text{tip}}(\epsilon).$$

The “rates” for tunneling into/out of the μ -channel of the wire are defined as

$$\Gamma_{\mu}^{\gtrless}(\epsilon) = \pm \frac{i}{2\pi} G_{\mu}^{\gtrless}(\bar{x}, \bar{x}, \epsilon). \quad (32)$$

Measurement of a differential tunneling conductance in the limit of a small temperature gives the access to the *tunneling* density of states, since

$$\left. \frac{\partial I_{\text{tun}}}{\partial V} \right|_{V_{\text{tip}}=\epsilon} \propto \Gamma_{\mu}^{>}(\epsilon) + \Gamma_{\mu}^{<}(\epsilon) = \nu_{\mu}(\epsilon) \equiv -\frac{1}{\pi} \text{Im} G_{\mu}^r(\bar{x}, \bar{x}, \epsilon). \quad (33)$$

In the absence of interaction, the rates would simplify to $\Gamma_{\mu}^{\geq}(\epsilon) = f_{\mu}^{\geq}(\epsilon)\nu_{\mu}(\epsilon)$ with the distribution functions $f_{\mu}^{<}(\epsilon) = f_{\mu}(\epsilon)$, $f_{\mu}^{>}(\epsilon) \equiv 1 - f_{\mu}(\epsilon)$ and the density of states $\nu_{\mu}(\epsilon)$ in the channel μ . Evaluation of tunneling rates and of the TDOS of the interacting problem is the goal of this section.

We consider a spinless LL model with a point-like repulsive interaction, $U_{\mu\nu}(x, x') = V_0\delta(x - x')$, that does not discriminate between different channels. The interaction strength in the LL model is conventionally characterized by the constant $K = (1 + V_0/\pi v_F)^{-1/2}$. The free electron spectrum is linearized around the Fermi points, which requires the introduction of a high-energy cutoff $\Lambda \sim E_F$ (which is of the order of the bandwidth). In the absence of backscattering, the tunneling rates exhibit the well-known zero bias anomaly, i.e. a power-law suppression near the Fermi edges,

$$\Gamma_{\mu}^{\geq}(\epsilon) = \frac{\nu_0}{\pi} \Gamma(1 + 2\gamma)^{-1} \times \theta(\pm(\epsilon - eV_{\mu})) \left| \frac{\epsilon - eV_{\mu}}{\Lambda} \right|^{2\gamma} \quad (34)$$

where $\nu_0 = (2\pi v_F)^{-1}$ is the non-interacting density of states, and the exponent γ is given by

$$\gamma = \frac{(1 - K)^2}{4K}. \quad (35)$$

As is shown in the remainder of this section the tunneling rates change considerably upon including the impurity. For $eV > 0$ the rates are given by

$$\Gamma_{\mu}^{\geq}(\epsilon) = \pm \frac{\nu_0}{\pi} \left(\frac{eV}{\Lambda} \right)^{2\gamma} \Gamma(-2\gamma) \operatorname{Im} [(\mp z_{\mu})^{2\gamma} + \mathcal{C}_{\mu} R_{*}(eV)(\pm 1)^{2\gamma} \Psi(-2\gamma, 1 - 2\gamma + 2\delta_{\mu}, -1 - z_{\mu})], \quad (36)$$

where we have introduced the following notations:

$$\mathcal{C}_{\pm} = \frac{\Gamma(2K)}{\Gamma(1/2 \pm K/2)^2}, \quad \delta_{+} = (1 - K)/2, \quad \delta_{-} = 1/2 - K, \quad z_{\mu} = (\epsilon - eV_{\mu} + \frac{i}{2}\tau_{\varphi}^{-1})/eV. \quad (37)$$

We have also introduced the renormalized reflection coefficient

$$R_{*}(eV) = \frac{|r_0|^2}{\Gamma(2K)} \left| \frac{\Lambda}{eV} \right|^{2(1-K)} \quad (38)$$

and the nonequilibrium dephasing rate

$$\tau_{\varphi}^{-1} \equiv R_{*}(eV) \frac{2 \sin^2 \pi \delta_{+}}{\pi} |eV|. \quad (39)$$

The energy dependence of rates $\Gamma_{\pm}^{\geq}(\epsilon)$ is shown in Fig. 4. The main feature of these plots is that the tunneling

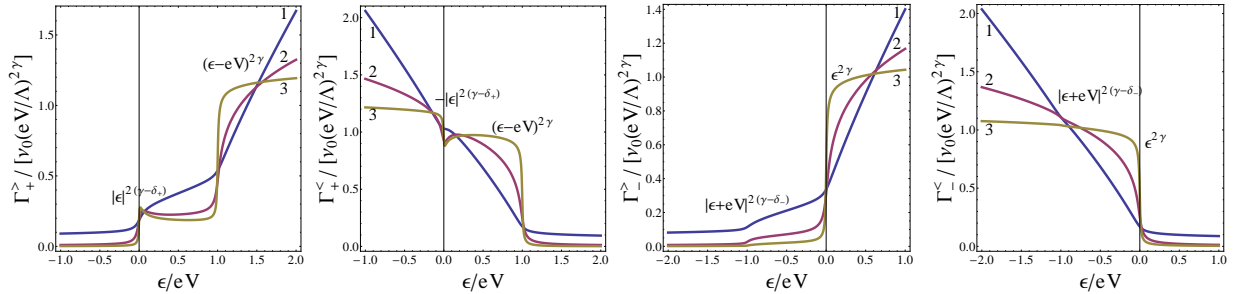


Figure 4: Tunneling rates for right- and left-movers with different interaction strengths: $K = 0.3$ (1), $K = 0.5$ (2), and $K = 0.75$ (3). Fermi edge for right-(left-) movers is at $eV_{+} = eV$ ($eV_{-} = 0$).

rates have split power-law singularities which are characterized by different exponents and are smeared by the

nonequilibrium dephasing rate $1/\tau_\varphi$. The main edges are located at the corresponding chemical potentials, i.e., at $\epsilon = eV_\pm$ in the case of right-/left-moving states, respectively, and are characterized by the exponent equal (in the considered weak-back-scattering regime) to its equilibrium value γ . The formation of the second (side) edge due to scattering off the impurity occurs at $\epsilon = e(V_\pm - V)$. If the interaction is repulsive ($K < 1$) then the corresponding exponent $2(\gamma - \delta_-)$ for left-moving electrons is always positive, hence the correction at the side edge $\epsilon = 0$ is smooth. For right-movers in the case of not too strong interaction, $K > 1/3$, the nonequilibrium exponent $2(\gamma - \delta_+)$ is negative, yielding a resonance in tunneling at the side edge $\epsilon = 0$.

The presence of side edges in the tunneling rates can be understood in the following way. Inelastic electron backscattering at the impurity at point $x = 0$ induces the emission of *real* nonequilibrium plasmons with typical frequencies $\hbar\omega \leq eV$, which in the non-dissipative LL can propagate to the distant point of tunneling \bar{x} . As the result, inelastic tunneling with absorption or stimulated emission of these real plasmons become possible. For example, an electron tunneling into the right/left moving state of the LL with the energy $\epsilon < eV_\pm$ can accommodate itself above the corresponding Fermi energy (eV_\pm) by picking up the quantum $\hbar\omega > |\epsilon|$ from the nonequilibrium plasmon bath. Since the energy of out-of-equilibrium plasmons is limited by the applied voltage, one has a threshold: $\epsilon > e(V_\pm - V)$, which is developed into the power-law singularity typical for the LL. The singularity at the side edge of the tunneling rate-out describes the inverse processes: the inelastic tunneling from the LL accompanied by the stimulated emission of nonequilibrium plasmons with typical energy $\hbar\omega \simeq eV$. Such side edge is pronounced in the case of right-moving states only, $\Gamma_+^<(\epsilon)$, and is not seen for the left-moving states, $\Gamma_-^<(\epsilon)$, since the associated exponent $2(\gamma - \delta_-)$ is always positive in the latter case.

Having announced the main results, we now turn to details of their derivation.

3.2. Calculations

3.2.1. Action

Since interaction does not discriminate between channels $\mu, \nu = \pm$, it can be decoupled by a Hubbard-Stratonovich transformation introducing a single field φ , i.e. $\varphi_+ = \varphi_- = \varphi$. For weak backscattering, i.e. weak tunneling between right- and left-moving states at the impurity, the action $\mathcal{A}[\varphi] = \mathcal{A}_0[\varphi] + \mathcal{A}_t[\varphi]$ is obtained according to Sect. 2.3. The free action (8) is

$$\mathcal{A}_0[\varphi] = \frac{1}{2} \int_C d\xi d\xi' \varphi(\xi) V^{-1}(\xi - \xi') \varphi(\xi') - \sum_\mu \int_C d\xi \varphi(\xi) (\varrho_{0+} + \varrho_{0-})$$

with $\xi = (x, t)$, non-local effective interaction $V^{-1}(\xi - \xi') = V_0^{-1} \delta(\xi - \xi') - \Pi(\xi - \xi')$ and the total polarization operator $\Pi(\xi) = \Pi_+(\xi) + \Pi_-(\xi)$. Using (10) one obtains for the retarded/advanced components of effective interaction

$$V^{r/a}(\omega, p) = V_0 \frac{\omega^2 - v_F^2 p^2}{\omega_\pm^2 - u^2 p^2} \quad (40)$$

with a plasmon velocity $u = v_F/K$. (For a repulsive interaction $K < 1$, so that $u > v_F$.)

Since we are dealing with a single scatterer, the tunneling (or, equivalently, backscattering) action \mathcal{A}_t , as given by (21), consists of one term [corresponding to class (11; +-)]:

$$\mathcal{A}_t[\varphi] = -i \int dt_1 dt_2 \begin{pmatrix} e^{-i\Phi^-(t_1)} & e^{-i\Phi^+(t_1)} \end{pmatrix} \begin{pmatrix} \Pi_{+-}^T & -\Pi_{+-}^< \\ -\Pi_{+-}^> & \Pi_{+-}^T \end{pmatrix}_{t_1-t_2} \begin{pmatrix} e^{i\Phi^-(t_2)} \\ e^{i\Phi^+(t_2)} \end{pmatrix}, \quad (41)$$

where $\Phi^\mp(t) = \Theta_-^\mp(0, t) - \Theta_+^\mp(0, t)$ is the tunneling phase evaluated at the impurity, $x = 0$. The phases are related to the Hubbard-Stratonovich field φ according to (2). The tunneling polarization operator $\Pi_{+-} = \Pi_{11;+-}$ is given by Eqs. (22), (23). The components of the polarization operator read

$$\Pi_{+-}^>(t) = -|r_0|^2 f_+^>(t) f_-^<(-t) = -|r_0|^2 e^{-ieVt} [f_0^>(t)]^2, \quad (42)$$

$$\Pi_{+-}^{T/\bar{T}}(t) = \frac{1}{2} [\Pi_{+-}^>(t) + \Pi_{+-}^<(t)]. \quad (43)$$

where $|r_0|^2 = |s_{+-}^1|^2 = |s_{-+}^1|^2$ is the bare reflection coefficient. We note that in Ref. [9] different notations were used: \mathcal{A}_b instead of $\mathcal{A}_0[\varphi]$, \mathcal{A}_{imp} instead of $\mathcal{A}_t[\varphi]$, and ϑ instead of Θ . We also note that Eq. (43) is slightly different from Eq. (23); however, this difference leads only to an additional constant contribution to the action that is physically irrelevant.

3.2.2. Green's Functions in Instanton Approximation

In order to find the tunneling rates, we represent the electron Green's function at the point of tunneling $\bar{x} > 0$ as a path integral over the field φ ,

$$G_\mu^{\gtrless}(\bar{x}, \bar{x}; \bar{t}) = \int \mathcal{D}\varphi e^{i\mathcal{A}[\varphi]} e^{i\Theta_\mu^\pm(\bar{x}, \bar{t})} G_\mu^{\gtrless}(\bar{x}, \bar{x}; \bar{t}; [\varphi]) e^{-i\Theta_\mu^\mp(\bar{x}, 0)}.$$

Here, $G_\mu(\bar{x}, \bar{x}; \bar{t}; [\varphi])$ denotes the Green's function for a given configuration of φ . It satisfies the Dyson equation with the spatially local self-energy

$$\Sigma_\mu[\varphi](x, x'; t, t') = i\delta(x)\delta(x')(|r_0|^2 v_F/2) e^{i\mu\Phi(t)} g_{-\mu}(t - t') e^{-i\mu\Phi(t')},$$

where g_μ are the quasiclassical Green's functions of the source reservoirs. Solving the Dyson equation to the first order in $|r_0|^2$, we get

$$G_\mu^{\alpha\beta}(\bar{x}, \bar{x}; \bar{t}) = \mathcal{G}_{0\mu}^{\alpha\beta} + \mathcal{G}_{1\mu}^{\alpha\beta}, \quad (44)$$

where

$$\begin{aligned} \mathcal{G}_{0\mu}^{\alpha\beta} &= \left\langle e^{i\Theta_\mu^\alpha(\bar{x}, \bar{t})} G_{0\mu}^{\alpha\beta}(\bar{x}, \bar{x}; \bar{t}) e^{-i\Theta_\mu^\beta(\bar{x}, 0)} \right\rangle, \\ \mathcal{G}_{1\mu}^{\alpha\beta} &= i \frac{|r_0|^2 v_F}{2} \sum_{\gamma\delta=\mp} \gamma\delta \int dt_1 dt_2 \end{aligned} \quad (45)$$

$$\left\langle e^{i\Theta_\mu^\alpha(\bar{x}, \bar{t})} G_{0\mu}^{\alpha\gamma}(\bar{x}, 0; \bar{t} - t_1) e^{i\mu\Phi^\gamma(t_1)} g_{-\mu}^{\gamma\delta}(t_1 - t_2) e^{-i\mu\Phi^\delta(t_2)} G_{0\mu}^{\delta\beta}(0, \bar{x}; t_2 - \bar{t}) e^{-i\Theta_\mu^\beta(\bar{x}, 0)} \right\rangle. \quad (46)$$

Here $G_{0\mu}^{\alpha\beta}$ are the Green's functions of free electrons; in particular,

$$G_{0\mu}^{\gtrless}(x, t) = \pm f^{\gtrless}(t - \mu x/v_F)/iv_F. \quad (47)$$

All averages $\langle \dots \rangle$ in Eq. (46) are taken with respect to the action $\mathcal{A}_0[\varphi] + \mathcal{A}_t[\varphi]$. They are of the form (26) and can be evaluated with the real-time instanton method described in Sect. 2.4. In this approximation the first term in Eq. (44) reads

$$\mathcal{G}_{0\mu}^{\alpha\beta} \approx e^{i\tilde{\mathcal{A}}_t[\varphi_*]} \times \left\langle e^{i\Theta_\mu^\pm(\bar{x}, \bar{t})} G_{0\mu}^{\gtrless}(\bar{x}, \bar{x}; \bar{t}) e^{-i\Theta_\mu^\mp(\bar{x}, 0)} \right\rangle_0. \quad (48)$$

The second factor here is the full Green's function of a *clean* LL,

$$\tilde{G}_{0\mu}^{\gtrless}(\bar{x}, \bar{x}; \bar{t}) = e^{-\frac{1}{2}\langle [\Theta_\mu^\pm(\bar{x}, \bar{t}) - \Theta_\mu^\mp(\bar{x}, 0)]^2 \rangle_0} G_{0\mu}^{\gtrless}(\bar{x}, \bar{x}; \bar{t}) = \pm \frac{a^{2\gamma}}{2\pi i v_F} e^{-i\mu_\mu \bar{t}} \frac{1}{(a \pm i\bar{t})^{2\gamma+1}}. \quad (49)$$

The first factor in Eq. (48) gives dephasing corrections due to the interplay of tunneling and interaction. The instanton action $\tilde{\mathcal{A}}_t[\varphi_*]$ is defined in (30) and obtained by substituting the dressed polarization operators into (41). The instanton phase φ_* is generated by the source $i\mathcal{A}_J[\varphi] = i\Theta_\mu^\alpha(\bar{x}, \bar{t}) - i\Theta_\mu^\beta(\bar{x}, 0)$,

$$\Phi_*^\mp(t) = \langle \Phi^\mp(t) \rangle_0 - D_{\Phi\Theta_\mu}^{\mp\alpha}(t - \bar{t}, -\bar{x}) + D_{\Phi\Theta_\mu}^{\mp\beta}(t, -\bar{x}) \text{ with } D_{\Phi\Theta_\mu}^{\gamma\delta}(t, x) = D_{\Theta, -\mu}^{\gamma\delta}(t, x) - D_{\Theta, +\mu}^{\gamma\delta}(t, x), \quad (50)$$

and depends on Keldysh indices α, β , the direction μ of the tunneling electron, as well as the time and the position of tunneling \bar{t}, \bar{x} . Since the average value $\langle \Phi^\mp(t) \rangle_0$ does not depend on the Keldysh index \mp and the time t it will drop out when the instanton phase is substituted into (41). Therefore it will be omitted in what follows.

3.2.3. Phase-phase Correlation Functions

To lay the groundwork for all further calculations we compute the correlation functions of the phases Θ_μ and $\Phi = \Theta_- - \Theta_+$. With the bare particle-hole propagator (4), the effective interaction (40), and the relation (11), the retarded/advanced components of the correlators $D_{\Theta,\mu\nu}$ can be easily evaluated in the (q, ω) representation:

$$D_{\Theta,\mu\mu}^{r/a}(\omega, q) = -\frac{2\pi}{\omega} \frac{\omega + \mu v_F q}{\omega} \mu \left[\frac{1+K}{4K} \frac{1}{q - \mu\omega_\pm/u} - \frac{1-K}{4K} \frac{1}{q + \mu\omega_\pm/u} - \frac{1}{2} \frac{1}{q - \mu\omega_\pm/v_F} \right], \quad (51)$$

$$D_{\Theta,-\mu\mu}^{r/a}(\omega, q) = -\frac{2\pi}{\omega} \frac{1-K^2}{4K} \left[\frac{1}{q - \omega_\pm/u} + \frac{1}{q + \omega_\pm/u} \right]. \quad (52)$$

Transforming the above relations into the mixed space-frequency representation, we obtain

$$D_{\Theta,\mu\nu}^{r/a}(\omega, x) = \mp \frac{2\pi i}{\omega} \left\{ \theta(\pm\mu x) \left[c_{\mu\nu}^+ e^{i\mu\omega x/u} - \delta_{\mu\nu} e^{i\mu\omega/v_F} \right] + \theta(\mp\mu x) c_{\mu\nu}^- e^{-i\mu\omega x/u} \right\} \quad (53)$$

with

$$c_{\mu\mu}^\pm = (1 \pm K)^2/(4K), \quad c_{\mu,-\mu}^\pm = (1 - K^2)/(4K). \quad (54)$$

The Keldysh component of the phase correlator is given at zero temperature by

$$D_{\Theta,\mu\nu}^k(\omega, x) = B(\omega) (D_{\Theta,\mu\nu}^r(\omega, x) - D_{\Theta,\mu\nu}^a(\omega, x)) = \text{sign } \omega (D_{\Theta,\mu\nu}^r(\omega, x) - D_{\Theta,\mu\nu}^a(\omega, x)). \quad (55)$$

Performing the Keldysh rotation, we then arrive at

$$\begin{aligned} D_{\Theta,\mu\nu}^{\geq}(\omega, x) &= \frac{1}{2} (D_{\Theta,\mu\nu}^k(\omega, x) \pm (D_{\Theta,\mu\nu}^r(\omega, x) - D_{\Theta,\mu\nu}^a(\omega, x))) = \pm \theta(\pm\omega) (D_{\Theta,\mu\nu}^r(\omega, x) - D_{\Theta,\mu\nu}^a(\omega, x)), \\ D_{\Theta,\mu\nu}^{T/\bar{T}}(\omega, x) &= \frac{1}{2} (D_{\Theta,\mu\nu}^k(\omega, x) \pm (D_{\Theta,\mu\nu}^r(\omega, x) + D_{\Theta,\mu\nu}^a(\omega, x))) = \pm \theta(\pm\omega) D_{\Theta,\mu\nu}^r(\omega, x) \pm \theta(\mp\omega) D_{\Theta,\mu\nu}^a(\omega, x). \end{aligned} \quad (56)$$

In the real-time representation (x, t) these phase-phase correlation functions can be decomposed into the plasmon (moving with velocity u) and particle-hole (having velocity v_F) contributions

$$iD_{\Theta,\mu\nu}^{\alpha\beta}(t, x) = c_{\mu\nu}^+ \mathcal{L}_{\mu u}^{\alpha\beta}(t, x) - c_{\mu\nu}^- \mathcal{L}_{-\mu u}^{\alpha\beta}(t, x) - \delta_{\mu\nu} \mathcal{L}_{\mu v_F}^{\alpha\beta}(t, x), \quad (57)$$

where for a given velocity v the functions $\mathcal{L}_v^{\alpha\beta}(t, x)$ read

$$\mathcal{L}_v^{\geq}(t, x) = \ln \frac{\mp ia}{t \mp ia - x/v}, \quad \mathcal{L}_v^{T/\bar{T}}(t, x) = \ln \frac{\mp ia \text{ sign } x/v}{t \mp ia \text{ sign } x/v - x/v}.$$

This follows from the Eqs. (56) after the Fourier transformation from ω to t with taking into account the high-energy cut-off. The functions $\mathcal{L}_v^{\alpha\beta}(t, x)$ satisfy

$$\partial_t \mathcal{L}_v^{\geq}(t, x) = -(t \mp ia - x/v)^{-1}, \quad \partial_t \mathcal{L}_v^{T/\bar{T}}(t, x) = -(t \mp ia \text{ sign } x/v - x/v)^{-1}.$$

It is worth mentioning that the appearance of both plasmon and particle-hole “light-cone” singularities in the phase-phase correlation function is a special feature of the functional bosonization approach.

For the $\Theta - \Phi$ phase-phase correlators we then obtain:

$$iD_{\Phi\Theta\mu}^{\alpha\beta}(t, x) \equiv \langle \delta\Phi^\alpha(t, x) \delta\Theta_\mu^\beta(0, 0) \rangle = i \left[D_{\Theta,-\mu}^{\alpha\beta}(t, x) - D_{\Theta,+\mu}^{\alpha\beta}(t, x) \right] \quad (58)$$

$$= -\mu \left[p \mathcal{L}_{\mu u}^{\alpha\beta}(t, x) - q \mathcal{L}_{-\mu u}^{\alpha\beta}(t, x) - \mathcal{L}_{\mu v_F}^{\alpha\beta}(t, x) \right]. \quad (59)$$

The correlation function of the tunneling phases $\Phi(t) = \Phi(t, 0)$ at the position of the impurity reads

$$iD_{\Phi}^{\alpha\beta}(t) \equiv \langle \delta\Phi^\alpha(t) \delta\Phi^\beta(0) \rangle = i \lim_{x \rightarrow 0} \left[D_{\Phi\Theta-}^{\alpha\beta}(t, x) - D_{\Phi\Theta+}^{\alpha\beta}(t, x) \right] = -2(1 - K) \mathcal{L}_{\Phi}^{\alpha\beta}(t), \quad (60)$$

where

$$\mathcal{L}_{\Phi}^{\geq}(t) = \ln \frac{\mp ia}{t \mp ia}, \quad \mathcal{L}_{\Phi}^{T/\bar{T}}(t) = \frac{1}{2} \left[\ln \frac{-ia}{t - ia} + \ln \frac{ia}{t + ia} \right]. \quad (61)$$

3.2.4. Instanton Action

The correlators obtained in the previous section reduce the “dressed” tunneling polarization operators (31) to the form

$$\tilde{\Pi}_{+-}^{\geqslant}(t) = -|r_0|^2 \frac{1}{(2\pi a)^2} e^{-ieVt} \left(\frac{a}{a \pm it} \right)^{2K}, \quad (62)$$

or in the frequency representation

$$\tilde{\Pi}_{+-}^{\geqslant}(\omega) = -\frac{R_*(eV)}{2\pi} \theta(\pm(\omega - eV)) \left| \frac{\omega - eV}{eV} \right|^{2K-1} |eV|,$$

where we used the definition (38) for the renormalized reflection coefficient R_* . With the mixed phase-phase correlation function (58) at hand we are also in a position to write down the instanton trajectories (50),

$$\begin{aligned} i\Phi_*^{\mp}(t) &= \mu \left\{ p \ln \left[\frac{t \pm ia + \mu\bar{x}/u}{t \pm ia - \bar{t} + \mu\bar{x}/u} \right] - q \ln \left[\frac{a - i\beta(t - \mu\bar{x}/u)}{a - i\alpha(t - \bar{t} - \mu\bar{x}/u)} \right] - \ln \left[\frac{t \pm ia + \mu\bar{x}/v_F}{t \pm ia - \bar{t} + \mu\bar{x}/v_F} \right] \right\}, \quad \mu\bar{x} > 0, \\ i\Phi_*^{\mp}(t) &= \mu \left\{ p \ln \left[\frac{a - i\beta(t + \mu\bar{x}/u)}{a - i\alpha(t - \bar{t} + \mu\bar{x}/u)} \right] - q \ln \left[\frac{t \pm ia - \mu\bar{x}/u}{t \pm ia - \bar{t} - \mu\bar{x}/u} \right] - \ln \left[\frac{a - i\beta(t + \mu\bar{x}/v_F)}{a - i\alpha(t - \bar{t} + \mu\bar{x}/v_F)} \right] \right\}, \quad \mu\bar{x} < 0, \end{aligned}$$

where we have introduced $p = (1 + K)/2$ and $q = (1 - K)/2$. It is worth emphasizing that these instantons represent non-classical solutions in the sense of the Keldysh nonequilibrium theory: the phases $\Phi_*(t)$ are different on the upper and lower time contours, so that the quantum part is non-zero, $\Phi_*^q(t) \neq 0$. Because of this the corresponding tunneling action $\tilde{\mathcal{A}}_t[\varphi_*]$, which we are going to evaluate, is non-zero.

To exemplify the evaluation of the instanton action $\tilde{\mathcal{A}}_t[\varphi_*]$, let us consider the case of tunneling into/out of a right-moving state with the tip being placed on the right from the impurity, $\mu = +$ and $\bar{x} > 0$. The phase factor is

$$e^{i\Phi_*^{\mp}(t)} = \kappa_+^{\mp}(t) \kappa_-^{\mp}(t) \kappa_0^{\mp}(t) \quad (63)$$

with

$$\kappa_+^{\mp}(t) = \left(\frac{t \pm ia + \bar{x}/u}{t \pm ia - \bar{t} + \bar{x}/u} \right)^p, \quad \kappa_-^{\mp}(t) = \left(\frac{a - i\alpha(t - \bar{t} - \bar{x}/u)}{a - i\beta(t - \bar{x}/u)} \right)^q, \quad \kappa_0^{\mp}(t) = \left(\frac{t \pm ia - \bar{t} + \bar{x}/v_F}{t \pm ia + \bar{x}/v_F} \right). \quad (64)$$

The instanton action reads

$$\begin{aligned} i\tilde{\mathcal{A}}_t[\varphi_*] &= \sum_{\zeta, \eta = \mp} \zeta \eta \int dt_3 dt_4 \tilde{\Pi}_{+-}^{\zeta\eta}(t_3 - t_4) \mathcal{K}_+^{\zeta\eta}(t_3, t_4) \mathcal{K}_-^{\zeta\eta}(t_3, t_4) \mathcal{K}_0^{\zeta\eta}(t_3, t_4) \\ &\text{with } \mathcal{K}_\sigma^{\zeta\eta}(t_3, t_4) = \kappa_\sigma^{\zeta}(t_3)^{-1} \kappa_\sigma^{\eta}(t_4) \quad \text{for } \sigma = +, -, 0. \end{aligned} \quad (65)$$

Since the polarization factor $\tilde{\Pi}_{+-}(t_3 - t_4)$ comes with the factor $e^{-ieV(t_3 - t_4)}$ the integral is dominated by the region $|t_3 - t_4| \lesssim |eV|^{-1}$. Furthermore, important contributions are expected to come from regions around the singularities of the phase factors, i.e. $t_3, t_4 \sim -\bar{x}/u$, $\bar{t} - \bar{x}/u$ for \mathcal{K}_+ , $t_3, t_4 \sim \bar{x}/u$, $\bar{t} + \bar{x}/u$ for \mathcal{K}_- , and $t_3, t_4 \sim -\bar{x}/v_F$, $\bar{t} - \bar{x}/v_F$ for \mathcal{K}_0 . These regions in the $t_3 - t_4$ -plane are sketched in Fig. 5.

We will assume that the singularities are well separated, which imposes the condition

$$|\bar{t}|, |eV|^{-1} \ll (1 - K)|\bar{x}|/v_F, \quad (66)$$

For interaction strength of order unity, the dephasing time τ_φ (which governs the relevant \bar{t}) is $\sim |eV|^{-1}$, so that the conditions (66) reduce simply to $|eV|^{-1} \ll |\bar{x}|/v_F$. This condition, implying a sufficiently large voltage and/or tip-to-impurity distance, can be easily satisfied.

Far from the singularities, the phase factors become trivial, $\mathcal{K}_\sigma(t_3, t_4) \rightarrow 1$, so that the integral (65) approximately splits into

$$i\tilde{\mathcal{A}}_t[\varphi_*] \approx \mathcal{I}[\mathcal{K}_+] + \mathcal{I}[\mathcal{K}_-] + \mathcal{I}[\mathcal{K}_0], \quad (67)$$

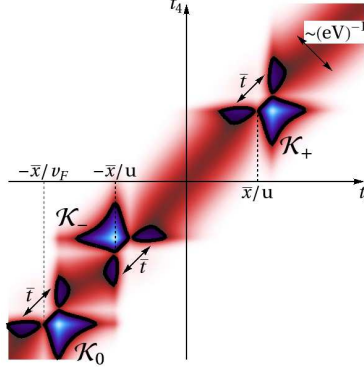


Figure 5: Regions in the $t_3 - t_4$ -plane providing dominant contributions to the integral for the instanton action, Eq. (3.2.4) .

with

$$\mathcal{I}[\mathcal{K}_\sigma] = \sum_{\zeta, \eta = \mp} \zeta \eta \int dt_3 dt_4 \tilde{\Pi}_{+-}^{\zeta\eta}(t_3 - t_4) (\mathcal{K}_\sigma^{\zeta\eta}(t_3, t_4) - 1). \quad (68)$$

We have added -1 to the phase factor \mathcal{K}_σ in Eq. (68) to make the convergence manifest. This does not change the value of the integral in view of $\sum_{\zeta, \eta} \zeta \eta \tilde{\Pi}_{+-}^{\zeta\eta}(t) = 0$. For the very same reason, the independence of $\mathcal{K}_\sigma^{\zeta\eta}(t_3, t_4)$ of the Keldysh indices ζ, η implies $\mathcal{I}[\mathcal{K}_-] = 0$.

According to Eqs. (64), (3.2.4), $\mathcal{K}_+, \mathcal{K}_0$ have the form $\mathcal{K}^{\zeta\eta}(t_3, t_4) \equiv \kappa^\zeta(t_3)^{-1} \kappa^\eta(t_4)$ with $\kappa^\mp(t) = \left(\frac{t - t_a \pm ia}{t - t_b \pm ia} \right)^r$ and some exponent $r > 0$. Therefore, $\mathcal{I}[\mathcal{K}]$ is dominated by the regions $|t_3 - t_4| \lesssim |eV|^{-1}$ (singularity of $\tilde{\Pi}_{+-}$) and $|t_3 - t_a|, |t_4 - t_b| \lesssim |eV|^{-1}$ (singularity of \mathcal{K}) which determine the long-time asymptotics $|eV\bar{t}| \gg 1$. This yields

$$\begin{aligned} \mathcal{I}[\mathcal{K}] &\approx \int dt \sum_{\zeta\eta} \zeta \eta \tilde{\Pi}_{+-}(t) \int dT (\kappa^\zeta(T)^{-1} \kappa^\eta(T) - 1) \\ &\quad + \sum_{\zeta\eta} \zeta \eta \tilde{\Pi}_{+-}^{\zeta\eta}(t_a - t_b) \Big|_{eV=0} \int dt_3 e^{-ieVt_3} \kappa^\zeta(t_3)^{-1} \int dt_4 e^{ieVt_4} \kappa^\eta(t_4) \\ &\approx -R_*(eV) \left\{ \frac{|eV(t_b - t_a)|}{2\pi} \left(1 - e^{-2\pi i r \operatorname{sign}[eV(t_b - t_a)]} \right) - \frac{\Gamma(2K)}{\Gamma(r)^2} e^{ieV(t_b - t_a)} [ieV(t_b - t_a)]^{2(r-K)} \right\}. \end{aligned} \quad (69)$$

Assuming for definiteness $\bar{x} > 0$ and considering first right-movers, $\mu = +$, we thus obtain for the instanton action $i\tilde{\mathcal{A}}_t[\varphi_*] = \mathcal{I}[\mathcal{K}_+] + \mathcal{I}[\mathcal{K}_0]$. The first contribution here,

$$\mathcal{I}[\mathcal{K}_+] = -\frac{|\bar{t}|}{2\tau_\varphi} - iR_*(eV) \frac{\sin 2\pi p}{2\pi} eV\bar{t} + \mathcal{C}_+ R_*(eV) e^{ieV\bar{t}} [ieV\bar{t}]^{2q}, \quad \mathcal{C}_+ = \Gamma(2K)/\Gamma(p)^2, \quad (70)$$

encodes effects of real plasmons on tunneling which are generated because of backscattering off the impurity. One of such effects is the shot-noise, which is represented by the first term in Eq. (70). This term is negative and linear in time \bar{t} and thus accounts for dephasing with the rate (39). The second term in Eq. (70) represents a perturbatively small renormalization of bias voltage and will be neglected in the following. The third term in Eq. (70) is subleading as compared to the first one and we will treat it perturbatively in R_* . It shows an oscillatory behavior accounting for an energy transfer $\sim eV$ between the nonequilibrium bath of plasmons and a tunneling electron. We will return to this point when discussing the tunneling rates.

We turn now to the contribution $\mathcal{I}[\mathcal{K}_0]$. In this case $r = 1$, so that the first term in (69) vanishes. Thus,

the the electron-hole pair contribution reads

$$\mathcal{I}[\mathcal{K}_0] = \sum_{\zeta\eta} \zeta\eta \tilde{\Pi}_{+-}^{\zeta\eta}(\bar{t}) \Big|_{eV=0} \int dt_3 e^{-ieVt_3} \kappa_0^\zeta(t_3)^{-1} \int dt_4 e^{ieVt_4} \kappa_0^\eta(t_4) \quad (71)$$

$$= R_*(eV) \Gamma(2K) e^{-ieV\bar{t}} [-ieV\bar{t}]^{2(1-K)}. \quad (72)$$

It is oscillatory and can be again treated perturbatively. In contrast to the plasmon contribution, however, it seemingly corresponds to an energy transfer of $\sim -eV$ and does not have a clear physical interpretation. We will see below that this term is an artifact of functional bosonization which will be canceled by the Born correction $\mathcal{G}_{1\mu}^{\alpha\beta}$. In total, we have

$$e^{i\tilde{\mathcal{A}}_t[\varphi_*]} \approx e^{-|\bar{t}|/2\tau_\varphi} \left(1 + \mathcal{C}_+ R_*(eV) e^{ieV\bar{t}} [ieV\bar{t}]^{2q} + \mathcal{I}[\mathcal{K}_0] \right) \quad \text{for } \bar{x} > 0, \mu = +. \quad (73)$$

The same considerations can be applied to left-movers, with the result

$$e^{i\tilde{\mathcal{A}}_t[\varphi_*]} \approx e^{-|\bar{t}|/2\tau_\varphi} \left(1 + \mathcal{C}_- R_*(eV) e^{ieV\bar{t}} [ieV\bar{t}]^{1-2K} \right), \quad \mathcal{C}_- = \Gamma(2K)/\Gamma(q)^2, \quad \text{for } \bar{x} > 0, \mu = -. \quad (74)$$

3.2.5. Born Correction

We evaluate the Born correction $\mathcal{G}_{1\mu}^{\alpha\beta}$ to the Green's function, (44), in leading order in $|r_0|^2$, which amounts to taking averages with respect to the clean action $\mathcal{A}_0[\varphi]$ only. Then Wick's theorem yields

$$\mathcal{G}_{1\mu}^{\alpha\beta} \approx i \frac{|r_0|^2 v_F}{2} \sum_{\gamma\delta=\mp} \gamma\delta \int dt_1 dt_2 G_{0\mu}^{\alpha\gamma}(\bar{x}, 0; \bar{t} - t_1) g_{-\mu}^{\gamma\delta}(t_1 - t_2) G_{0\mu}^{\delta\beta}(0, \bar{x}; t_2 - \bar{t}) \mathcal{J}_\mu^{\alpha\beta\gamma\delta}(\bar{x}, \bar{t}; t_1, t_2) \quad (75)$$

with

$$\begin{aligned} \mathcal{J}_\mu^{\alpha\beta\gamma\delta}(\bar{x}, \bar{t}; t_1, t_2) &= \left\langle e^{i\Theta_\mu^\alpha(\bar{x}, \bar{t})} e^{i\mu\Phi^\gamma(t_1)} e^{-i\mu\Phi^\delta(t_2)} e^{-i\Theta_\mu^\beta(\bar{x}, 0)} \right\rangle_0 \\ &= e^{-\frac{1}{2} \langle [\Theta_\mu^\alpha(\bar{x}, \bar{t}) - \Theta_\mu^\beta(\bar{x}, 0)]^2 \rangle_0 - \frac{1}{2} \langle [\Phi^\gamma(t_1) - \Phi^\delta(t_2)]^2 \rangle_0} e^{i\mu(\Phi_*^\gamma(t_1) - \Phi_*^\delta(t_2))} \end{aligned} \quad (76)$$

and the instanton (50). The appearance of the instanton makes the integral (75) quite similar to the instanton action and we will use an analogous approximations to deal with the time integrals.

We have already seen that the instanton phase factor factorizes into three contributions (63)—two governed by plasmons and one by electron-hole pairs—and one might expect the integral (75) to split into three contributions in a way akin to the instanton action. However, it will turn out that the presence of the bare Green's functions $G_{0\mu}^{\alpha\gamma}(\bar{x}, 0; \bar{t} - t_1)$ and $G_{0\mu}^{\delta\beta}(0, \bar{x}; t_2 - \bar{t})$ suppresses the plasmon contributions. Focusing again on $\mu = +$, $\bar{x} > 0$, we show that the remaining electron-hole pair term cancels $\mathcal{I}[\mathcal{K}_0]$ in (73).

The t_1, t_2 -dependent contributions to (75) are

$$\begin{aligned} G_{0+}^{\alpha\gamma}(\bar{x}, 0; \bar{t} - t_1) g_-^{\gamma\delta}(t_1 - t_2) G_{0+}^{\delta\beta}(0, \bar{x}; t_2 - \bar{t}) e^{-\frac{1}{2} \langle [\Phi^\gamma(t_1) - \Phi^\delta(t_2)]^2 \rangle_0} e^{i\Phi_*^\gamma(t_1) - i\Phi_*^\delta(t_2)} \\ = e^{-ieV\bar{t}} e^{ieV(t_1 - t_2)} \times \tilde{g}_-^{\gamma\delta}(t_1 - t_2) \times \kappa_0^\delta(t_2)^{-1} \kappa_+^\delta(t_2)^{-1} \kappa_-^\delta(t_2)^{-1} \times \tilde{\kappa}_0^\gamma(t_1) \kappa_+^\gamma(t_1) \kappa_-^\gamma(t_1). \end{aligned}$$

We combined terms with similar pole structure, defining

$$\begin{aligned} \tilde{g}_-^{\gamma\delta}(t_1 - t_2) &\equiv e^{-\frac{1}{2} \langle [\Phi^\delta(t_2) - \Phi^\gamma(t_1)]^2 \rangle_0} g_-^{\gamma\delta}(t_1 - t_2) \Big|_{eV=0}, \\ \tilde{\kappa}_0^\delta(t_2)^{-1} &\equiv G_{0+}^{\delta\beta}(-\bar{x}, t_2) \Big|_{eV=0} \kappa_0^\delta(t_2)^{-1}, \\ \tilde{\kappa}_0^\gamma(t_1) &\equiv G_{0+}^{\alpha\gamma}(\bar{x}, \bar{t} - t_1) \Big|_{eV=0} \kappa_0^\gamma(t_1). \end{aligned}$$

All voltage dependence has been singled out in the phase factors explicitly.

Let us examine the pole structure: $\tilde{g}_-^{\gamma\delta}(t_1 - t_2)$ is divergent for $t_1 \approx t_2$. This is reminiscent of $\tilde{\Pi}_{+-}(t_3 - t_4)$ in (65) which preferred $t_3 \approx t_4$. The plasmon contributions κ_+ and κ_- have been studied in the previous section where we already noted $\kappa_{\pm}(t) \rightarrow 1$ for t far from their singularities. This is no longer true for $\tilde{\kappa}_0$. Indeed, leaving the Keldysh indices and the corresponding short-time regularizations aside for a moment, we have

$$G_{0+}(x, t) \Big|_{eV=0} = -\frac{1}{2\pi v_F} \frac{1}{t - x/v_F} \quad \text{and} \quad \kappa_0(t) = \frac{t - \bar{t} + \bar{x}/v_F}{t + \bar{x}/v_F},$$

and hence,

$$\tilde{\kappa}_0^\delta(t_2)^{-1} \sim -\frac{1}{2\pi v_F} \frac{1}{t_2 - \bar{t} + \bar{x}/v_F}, \quad \tilde{\kappa}_0^\gamma(t_1) \sim \frac{1}{2\pi v_F} \frac{1}{t_1 + \bar{x}/v_F}.$$

Similarly to the original phase factors $\kappa_0^\delta(t_2)^{-1}$, $\kappa_0^\delta(t_1)$, these new ones have the poles at $t_1 \sim -\bar{x}/v_F$, $t_2 \sim \bar{t} - \bar{x}/v_F$; however, at variance with $\kappa_0^\delta(t_2)^{-1}$, $\kappa_0^\delta(t_1)$, the factors $\tilde{\kappa}_0^\delta(t_2)^{-1}$, $\tilde{\kappa}_0^\delta(t_1)$ vanish far from the poles instead of converging to unity. Therefore, the poles of $\tilde{\kappa}_0^\delta(t_2)^{-1}$, $\tilde{\kappa}_0^\delta(t_1)$ are dominating the integral (75), while the plasmonic poles give subleading contributions (suppressed by the factor $v_F \bar{t}/(1-K)\bar{x} \ll 1$). With only leading terms taken into account the integrals simplify to

$$\begin{aligned} \mathcal{G}_{1+}^{\alpha\beta} &\approx i \frac{|r_0|^2 v_F}{2} e^{-\frac{1}{2} \langle [\Theta_\mu^\alpha(\bar{x}, \bar{t}) - \Theta_\mu^\beta(\bar{x}, 0)]^2 \rangle} \\ &\sum_{\gamma, \delta = \mp} \gamma \delta e^{-\frac{1}{2} \langle [\Phi^\delta(\bar{t}) - \Phi^\gamma(0)]^2 \rangle} \left[G_{0+}^{\alpha\gamma}(\bar{x}, \bar{t} + \bar{x}/v_F) g_-^{\gamma\delta}(-\bar{t}) G_{0+}^{\delta\beta}(-\bar{x}, \bar{t} - \bar{x}/v_F) \right]_{eV=0} e^{-ieV\bar{t}} \\ &\int dt_2 e^{-ieVt_2} \kappa_0^\delta(t_2)^{-1} \int dt_1 e^{ieVt_1} \kappa_0^\gamma(t_1) \quad (77) \end{aligned}$$

For large times $|\bar{t}| \gg |eV|^{-1}$, the short-time regularization and thus the distinction between different Keldysh components becomes immaterial, e.g. $\Pi_{+-}^\delta = |r_0|^2 e^{-ieV\bar{t}}/(2\pi\bar{t})^2$, $G_{0+}^{\alpha\beta}(0, \bar{t}) = -1/(2\pi v_F \bar{t})$, and one obtains

$$\begin{aligned} i \frac{|r_0|^2 v_F}{2} \left[G_{0+}^{\alpha\gamma}(\bar{x}, \bar{t} + \bar{x}/v_F) g_-^{\gamma\delta}(-\bar{t}) G_{0+}^{\delta\beta}(-\bar{x}, \bar{t} - \bar{x}/v_F) \right]_{eV=0} e^{-ieV\bar{t}} \\ = i \frac{|r_0|^2 v_F}{2} \left(\frac{1}{2\pi v_F} \frac{1}{\bar{t}} \right)^2 \left(-\frac{i}{\pi} \frac{1}{\bar{t}} \right) e^{-ieV\bar{t}} = -G_{0+}^{\alpha\beta}(\bar{x}, \bar{x}; \bar{t}) \left[\Pi_{+-}^{\delta\gamma}(\bar{t}) \right]_{eV=0}. \end{aligned}$$

Substituting this into (77), taking into account the dressing of the Green functions (49) and polarization operators by phase factors and comparing with Eq. (71), we find

$$\begin{aligned} \mathcal{G}_{1+}^{\alpha\beta} &\approx -\tilde{G}_{0+}^{\alpha\beta}(\bar{x}, \bar{x}; \bar{t}) \sum_{\delta\gamma} \delta\gamma \tilde{\Pi}_{+-}^{\delta\gamma}(\bar{t}) \Big|_{eV=0} \int dt_2 e^{-ieVt_2} \kappa_0^\delta(t_2)^{-1} \int dt_1 e^{ieVt_1} \kappa_0^\gamma(t_1) \\ &\approx -\tilde{G}_{0+}^{\alpha\beta}(\bar{x}, \bar{x}; \bar{t}) \mathcal{I}[\mathcal{K}_0]. \quad (78) \end{aligned}$$

The very same analysis can be performed for $\mu = -$. In this case, however, $\tilde{\kappa}_0^\gamma$ does not depend on the Keldysh index γ . Because of $\sum_{\gamma\delta} \gamma\delta g_+^{\gamma\delta}(t_1 - t_2) = 0$ the contribution $\mathcal{G}_{1-}^{\alpha\beta}$ is negligible.

Concluding, we obtain

$$\mathcal{G}_{0+}^{\alpha\beta} \approx e^{-|\bar{t}|/2\tau_\varphi} \tilde{G}_{0+}^{\alpha\beta}(\bar{x}, \bar{x}; \bar{t}) \left(1 + \mathcal{C}_+ R_*(eV) e^{ieV\bar{t}} [ieV\bar{t}]^{2q} + \mathcal{I}[\mathcal{K}_0] \right), \quad (79)$$

$$\mathcal{G}_{0-}^{\alpha\beta} \approx e^{-|\bar{t}|/2\tau_\varphi} \tilde{G}_{0-}^{\alpha\beta}(\bar{x}, \bar{x}; \bar{t}) \left(1 + \mathcal{C}_- R_*(eV) e^{ieV\bar{t}} [ieV\bar{t}]^{1-2K} \right), \quad (80)$$

$$\mathcal{G}_{1+}^{\alpha\beta} \approx -\tilde{G}_{0+}^{\alpha\beta}(\bar{x}, \bar{x}; \bar{t}) \mathcal{I}[\mathcal{K}_0]. \quad (81)$$

In leading order in $|r_0|^2$, i.e. neglecting dephasing corrections, $G_{1+}^{\alpha\beta}$ cancels the $\mathcal{I}[\mathcal{K}_0]$ term of $\mathcal{G}_{0+}^{\alpha\beta}$, as was stated in the end of Sec. 3.2.4.

3.2.6. Tunneling Rates

We are now ready to evaluate the components of the Keldysh Green function and, in particular, the tunneling density of states controlling the tunneling current between the system and the tip. Let us note that because of the tunneling actions (73) and (74) the Green functions contain power-law terms $[ieV\bar{t}]^{2\delta}$, $r > 0$, which have apparent branchcut singularities near $\bar{t} = 0$. However, results (73) and (74) are only valid in the long-time limit $|eV\bar{t}| \gg 1$. A regularization which takes this into account and does not violate the symmetry relation $\left[iG_\mu^{\geq}(\bar{x}, \bar{x}; \bar{t}) \right]^* = iG_\mu^{\geq}(\bar{x}, \bar{x}; -\bar{t})$ is $[1 + ieV\bar{t}]^{2\delta}$, which yields the Green's functions

$$G_\mu^{\alpha\beta}(\bar{x}, \bar{x}; \bar{t}) = \tilde{G}_\mu^{\alpha\beta}(\bar{x}, \bar{x}; \bar{t}) e^{-|\bar{t}|/2\tau_\varphi} \left(1 + C_\mu R_*(eV) e^{ieV\bar{t}} [1 + ieV\bar{t}]^{2\delta_\mu} \right) \quad (82)$$

$$\text{with } C_+ = \Gamma(2K)/\Gamma(p)^2, \quad C_- = \Gamma(2K)/\Gamma(q)^2, \quad \delta_+ = (1 - K)/2, \quad \delta_- = 1/2 - K. \quad (83)$$

The tunneling rates are obtained by Fourier transformation to energy representation. Using the aforementioned symmetry property of the Green's function, we obtain

$$\begin{aligned} \Gamma_\mu^{\geq}(\epsilon) &= \pm \frac{1}{2\pi} \int_0^\infty d\bar{t} \left(e^{i\epsilon\bar{t}} iG_\mu^{\geq}(\bar{x}, \bar{x}; \bar{t}) + e^{-i\epsilon\bar{t}} iG_\mu^{\geq}(\bar{x}, \bar{x}; -\bar{t}) \right) = \mp \frac{1}{\pi} \text{Im} \int_0^\infty d\bar{t} e^{i\epsilon\bar{t}} G_\mu^{\geq}(\bar{x}, \bar{x}; \bar{t}) \\ &= \pm \frac{\nu_0}{\pi} \text{Im} \left[\mathcal{J}_0^{\geq}(\epsilon; eV_\mu) + C_\mu R_*(eV) \mathcal{J}_{\delta_\mu}^{\geq}(\epsilon; eV_\mu - eV) \right] \end{aligned} \quad (84)$$

with

$$\mathcal{J}_\delta^{\geq}(\epsilon; U) \equiv \pm i a^{2\gamma} \int_0^\infty d\bar{t} e^{i(\epsilon - U + i/2\tau_\varphi)\bar{t}} (1 + ieV\bar{t})^{2\delta} (a \pm i\bar{t})^{-(2\gamma+1)},$$

Since $\mathcal{J}_r^{\geq}(\epsilon; U)$ is an analytic function of all parameters $\epsilon, \delta, \gamma, U, eV \in \mathbb{C}$ as long as $\text{Im}(\epsilon - U + i/2\tau_\varphi) > 0$ and $\text{Im} eV \leq 0$, we can consider here $\text{Re } \delta > -1$, $\text{Re}(2\gamma + 1) < 1$, $\text{Im} eV < 0$ and $\text{Re}[(\epsilon - U + i/2\tau_\varphi)/eV] < 0$ and deduce all relevant cases by analytic continuation. Under these constraints, one can evaluate the integral by rotating the integration contour, $\bar{t} = -is/eV$, $0 < s < \infty$, into the complex plane, and put $a \rightarrow 0$. Writing $z = (\epsilon - U + i/2\tau_\varphi)/eV$ we get

$$\begin{aligned} \mathcal{J}_\delta^{\geq}(\epsilon; U) &= \pm \frac{a^{2\gamma}}{eV} \int_0^\infty ds e^{zs} (1 + s)^{2\delta} (\pm s/eV)^{-(2\gamma+1)} \\ &= \left(\pm \frac{eV}{\Lambda} \right)^{2\gamma} \Gamma(-2\gamma) \Psi(-2\gamma, 1 - 2\gamma + 2\delta, -z) \end{aligned} \quad (85)$$

with the confluent hypergeometric function $\Psi(a, b, z)$. In the case $\delta = 0$ one has $\Psi(-2\gamma, 1 - 2\gamma, z) = z^{2\gamma}$ and thus the term \mathcal{J}_0^{\geq} in Eq. (84) yields the equilibrium zero-bias anomaly. Taking into account the 2nd (impurity) contribution we arrive at the results that have been presented in Sec. 3.1 [see Eq. (36)]. We note here that the result for the physical (real) voltage eV is obtained from Eq. (85) by substituting there $eV - i0$. One can also note that at $\delta \neq 0$ one gets $\Psi(-2\gamma, 1 - 2\gamma + 2\delta, z) \sim z^{2(\gamma-\delta)}$ at $z \rightarrow 0$. Therefore Eq. (85) gives the impurity correction $\Delta\Gamma_\mu$ to tunneling rates which is singular at $\epsilon = eV_\pm - eV$. Explicitly one has

$$\Delta\Gamma_\mu^<(\epsilon) \propto -R_*(eV) |\epsilon - eV_\pm + eV|^{2(\gamma-\delta_\mu)} \sin \begin{cases} 2\pi\delta_\mu, & \epsilon > eV_\pm - eV \\ 2\pi\gamma, & \epsilon < eV_\pm - eV \end{cases} \quad (86)$$

in case of tunneling from the wire into the tip and

$$\Delta\Gamma_\mu^>(\epsilon) \propto R_*(eV) \theta(\epsilon - eV_\pm + eV) |\epsilon - eV_\pm + eV|^{2(\gamma-\delta_\mu)} \quad (87)$$

in case of tunneling from the tip into the wire.

4. Quantum Hall Fabry-Pérot Interferometer

In this section we study the role of Coulomb interaction in an electronic Fabry-Pérot interferometer realized with chiral edge states in the integer QHE regime. Electronic Fabry-Pérot (FPI) [26, 28, 27, 29] and Mach-Zehnder (MZI) [30, 31, 32, 33, 34, 35, 36, 37, 38, 39, 40, 41] interferometers are analogues of the optical interferometers, where the chiral edge states play the role of light beams while quantum point contacts (QPCs) act as beam splitters. Electron interferometry provides a powerful tool for studying the quantum interference and dephasing in mesoscopic semiconductor devices. Another motivation behind these experimental efforts stems from the recent interest in topological quantum computations, which propose to exploit the non-Abelian anyons in the fractional QHE regime [19].

The Coulomb interaction is of paramount importance in fractional QHE systems, where it gives rise to quasi-particles with fractional charge obeying anyonic statistics. It came as a surprise that e - e interaction plays a prominent role in integer QHE interferometers as well, even when their conductance is $\sim e^2/h$ so that the Coulomb blockade physics seems to be inessential. For instance, visibility in the MZIs and FPIs strongly depends on the source-drain voltage showing decaying oscillations, which have been termed “lobes”. The search for a resolution of this puzzle in the case of MZI has triggered a lot of attention [43, 44, 45, 42, 46, 47, 48]. On the contrary, the extent of theoretical works on FPIs operating in the integer QHE regime is rather small [49, 50, 51].

In this section we develop a capacitance model of the e - e interaction in a FPI and apply it to study the transport properties of the FPI in and out of equilibrium in the limit of weak backscattering. Our approach is inspired by the previous theoretical work [50]. Its essential idea is that a compressible Coulomb island can be formed in the center of the FPI between two constrictions (Fig. 1), which strongly affects Aharonov-Bohm oscillations. Starting from this model, we demonstrate that depending on the strength of the e - e interaction the FPI can fall into “Aharonov-Bohm” (AB) or “Coulomb-dominated” (CD) regimes observed in the experiments [28, 29]. We also analyze the suppression of nonequilibrium AB oscillations with the increase of a source-drain voltage and find regions of both power-law and exponential decays, which explains experiments of Refs. [26, 27].

The brief account on results of this section has been reported by two of us previously [10]. Here we present technical details of our calculations and further elaborate on the qualitative picture of the interplay of interference and e - e interaction in the FPI which explains well the plethora of experimental data on the flux and gate periodicity of Aharonov-Bohm oscillations.

4.1. Model

We consider an electronic FPI of size L formed by a Hall bar with ν edge channels and two constrictions (QPCs) that allow for electron backscattering between the innermost right/left moving edge channels with amplitudes $r_{1(2)}$ as shown in Fig. 6 (a). Right- and left-moving channels are connected to leads with different chemical potentials μ_+ and μ_- , respectively. In what follows, we take into account the backscattering in the lowest order, thus accounting for interference of maximally two different paths. For simplicity we assume the flight times along upper and lower arms (i.e. between two QPCs) to be the same, $\tau_+ = \tau_- = \tau = L/v_F$. We denote the magnetic flux threading the interferometer cell by ϕ , i.e. an electron which encircles the cell once accumulates the phase $2\pi\phi/\phi_0$, where $\phi_0 = hc/|e|$ is the flux quantum.

The 2DEG in the QHE regime is divided into compressible and incompressible strips [20]. The filling factor in the n -th incompressible strip is integer. These strips are separated by much wider regions of compressible Hall liquid with a non-integer filling factor (compressible strips). The corresponding sketch of electron density profile $\rho(y)$ in the FPI along y -axis is shown in Fig. 7. Let us denote by y_k^\pm the boundaries between compressible and incompressible regions. Then $a_k = y_k^+ - y_k^-$ is the width of the k -th incompressible strip while $b_k = y_{k-1}^- - y_k^+$ is the width of the k -th compressible one. As it was shown in Ref. [20], in the situation of gate-induced confinement of 2DEG in the QHE regime the widths $b_k \gg \lambda_B$, with λ_B being the magnetic length. At the same time a_k scales as $a_k \sim (b_k \lambda_B)^{1/2}$, so that in general the condition $b_k \gg a_k \gg \lambda_B$ is satisfied. In this picture compressible regions play the role of edge channels — the self-consistent electrostatic potential is constant through the compressible strips and can be controlled by connecting them to external leads.

We also assume that the filling fraction ν_0 in the center of the FPI exceeds ν , giving rise to a compressible droplet (Coulomb island). The reason for that can be smooth (on a scale λ_B) disorder potential fluctuations [21]. Let us denote by eN_i the excess charge on the island ($e < 0$), with N_i being integer. On the scheme in Fig. 7 the boundary of the island is given by y_ν^- . This value is quantized and changes abruptly when an electron tunnels between innermost compressible strips and the island through the incompressible strip. On the contrary, the boundaries of edge channels may change continuously because of a variation in external parameters, such as μ_\pm and V_g , or due to quantum fluctuations of electrostatic potentials on these compressible regions (see also discussion later).

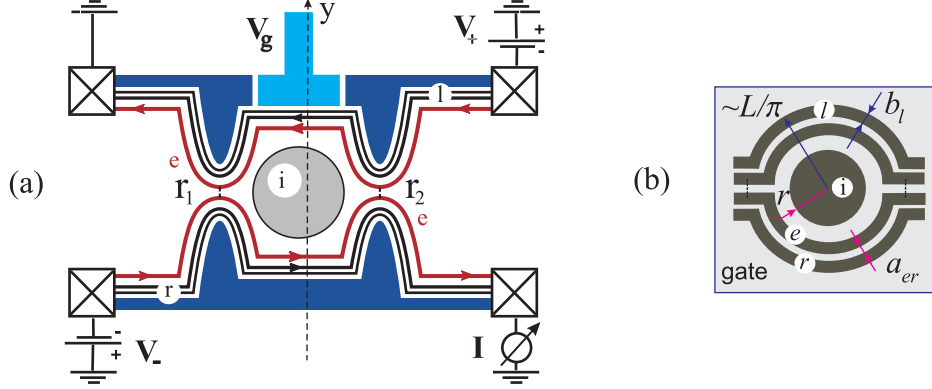


Figure 6: (a) Fabry-Pérot interferometer with compressible island i . The innermost edge channels e are subject to backscattering at the QPCs; the remaining $f_T = \nu - 1$ right(r)- and left(l)- moving channels are fully transmitted; their role is in screening of the interaction between the electrons of the channel e . Right- and left-moving channels are connected to reservoirs with different chemical potentials $\mu_\eta = eV_\eta$, $\eta = \pm$. Here, the gate g is depicted as a “plunger” gate. (b) Simple capacitance model, which uses geometry of the compressible regions. Right(r)- and left(l)-channels are each joined into one conductor with the widths b_r and b_l , respectively.

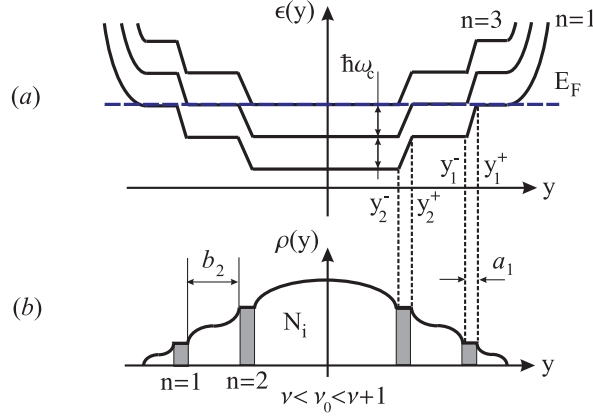


Figure 7: The structure of the edge states in the FPI. Cut through the center of an interferometer cell: (a) Landau level energies as the function of vertical coordinate y and (b) electron density $\rho(y)$ (see also Fig. 6). Besides ν completely filled LLs, the central region can sustain a partially filled Landau level whose occupation N_i changes by tunneling. Here we denoted by $a_k = y_k^+ - y_k^-$ the width of the k -th incompressible strip (shown by grey), which has the integer filling factor k . Compressible regions (white) represent the regions with non-integer filling fraction and have the width $b_k = y_{k-1}^- - y_k^+$. The picture above corresponds to the case $\nu = 2$.

Electrostatics of the FPI

In the framework of the above model, we treat the e - e interaction in the FPI by using the constant interaction model with mutual capacitances $C_{\alpha\beta}$ between four compressible regions — the interfering channel

(e); right- and left-moving fully transmitted channels (r , l); the compressible island (i) — and the gate (g). These capacitances are denoted by C_{eg} , C_{ei} etc. We assume a large capacitance between counter-propagating innermost channels — thus they share the same electrostatic potential φ_e — and also consider $f_T = \nu - 1$ right- and left-moving channels as joint conductors with potentials φ_r (φ_l). Defining a capacitance matrix \tilde{C} with elements $\tilde{C}_{\alpha\alpha} = \sum_{\gamma} C_{\alpha\gamma} + C_{\alpha g}$, and $\tilde{C}_{\alpha\beta} = -C_{\alpha\beta}$ ($\alpha \neq \beta$), where Greek indices span the set $\{e, r, l, i\}$ and $q_{\alpha} = -C_{\alpha g}V_g$ is an offset charge on the α 's conductor, the electrostatic energy reads

$$E = \frac{1}{2} \sum_{\alpha\beta} (Q_{\alpha} - q_{\alpha}) \left(\tilde{C}^{-1} \right)_{\alpha\beta} (Q_{\beta} - q_{\beta}). \quad (88)$$

Total charge $Q_i = e(N_i + \nu\phi/\phi_0)$ on the island is distributed on the highest partially filled Landau level (LL) and on ν fully occupied underlying LLs (cf. Fig. 7). Single electron tunneling is possible between interfering channels (e) and the island. We assume the rate of such tunneling process to be much smaller than all other energy scales in the problem, $\Gamma \ll \epsilon_{\text{th}}$, hence N_i is quantized and is fixed for given external parameters (ϕ , V_g , μ_{\pm}).

The mutual capacitances $C_{\alpha\beta}$ can be estimated from geometrical considerations [22]. We regard the island as a disc of radius r and represent the compressible edge channels as concentric rings of the width b_{α} and diameter L (here $\alpha = e, r, l$) as depicted in Fig. 6 (b). The edge channels are assumed to be thin, $b_{\alpha} \ll L$. Therefore for estimation of capacitances we can neglect the difference between the radii of the island and those of edge channels, i.e. $L \simeq \pi r \simeq \pi y_k^{\pm}$. A top gate, if present, is modeled by a plane situated at distance d from the 2DEG. Since the size of FPI cell is much larger than d , we treat C_{ig} , C_{eg} and $C_{r(l)g}$ as a parallel-plate capacitors and find an estimate

$$C_{ig} \simeq \epsilon \frac{r^2}{4d}, \quad C_{eg} \simeq \epsilon \frac{Lb_e}{2\pi d}, \quad C_{rg} \simeq \epsilon \frac{Lb_r}{4\pi d}, \quad (89)$$

where $\epsilon = 12.6$ is the dielectric constant for GaAs. The estimate for edge-to-edge (C_{er} and C_{el}) and edge-to-island (C_{ei}) capacitances can be found as a mutual capacitance of two conducting rings. In the limit $b \ll a$ we obtain with logarithmic accuracy [23]

$$C_{er} \simeq \frac{\epsilon L}{2\pi^2} \ln \left(\frac{b_e b_r}{a_{er}^2} \right), \quad C_{ei} \simeq \frac{\epsilon r}{\pi} \ln \left(\frac{r b_e}{a_{ei}^2} \right). \quad (90)$$

Here $b_{r(l)} = \sum_k^{\nu-1} b_k$ are the total widths of fully transmitted edge channels. Finding the mutual capacitance between a plunger gate and the island or the interfering edge channel is in general more difficult. Because of geometry, one can expect that C_{ig} and C_{eg} in this case will be substantially smaller than the above estimate (89) for the case of a top gate.

Let us now comment on the flux dependence of the electrostatic energy, Eq. (88). When the magnetic flux through the island is increased, $\delta\phi = \pi r^2 \delta B$, the LLs are squeezed and the charge on the island (for a fixed boundary y_{ν}^-) varies as $\delta Q_i = e\nu \delta\phi/\phi_0$. A similar effect of magnetic field on charges $Q_{e,r,l}$ distributed on compressible circular strips is negligibly small because of the condition $b \ll r$. Indeed, for a typical variation δB , such that $\delta\phi/\phi_0 \sim 1$, the corresponding modulation of these charges are

$$\frac{\delta Q_{e,r,l}}{e} \sim \frac{\delta\phi}{\phi_0} \left(\frac{b}{\pi r} \right) \ll 1, \quad (91)$$

and we do not include them into Eq. (88).

4.2. Results

In this subsection we summarize our results and give their physical interpretation. The detailed derivation is presented in the next subsection. The qualitative behavior of the FPI crucially depends on the relative coupling strength of the interfering edge (e) to the fully transmitted channels (l , r), to the island, and to the gate. The essential parameters are the number of transmitted channels ν^* which screen the bare

e - e interaction in the interfering channel — as we demonstrate in the section 4.3, one has $\nu^* \simeq 1$ in the case of strong and $\nu^* \simeq \nu$ in the case of weak inter-edge interaction — and the effective edge capacitance \bar{C}_e as defined below by Eq. (98). There are also two characteristic energy scales in our problem: (i) charging energy $E_C = e^2/\bar{C}_e$, or charge relaxation frequency $\omega_C = (\nu^*/\pi)E_C$; and (ii) the Thouless energy $\epsilon_{\text{th}} = \tau^{-1} = v_F/L$. A relation between these two parameters depends essentially on the geometry of the experiment (most importantly, on the geometry of the gates). We will assume that the condition $\epsilon_{\text{th}} \ll \omega_C$ is always satisfied, which simplifies a lot our subsequent calculations and enables us to get analytical results. This appears to be a proper assumption for most of available experiments. In particular, the value of the Thouless energy that can be deduced from the experiment of the Harvard group is $\epsilon_{\text{th}} \sim 50 \mu\text{V}$ [26], whereas the charging energy is in the mV range [28].

4.2.1. Visibility, dephasing and the “lobe” structure

In the limit of weak backscattering, $r_j \ll 1$, the differential conductance of the FPI, $g = g_{\text{inc}} + g_{\text{AB}}$, is the sum of incoherent and coherent contributions. The incoherent contribution is

$$g_{\text{inc}}(V) = \nu - R_{1*}(eV) - R_{2*}(eV), \quad (92)$$

where $R_{j*}(eV)$ are the renormalized reflection coefficients (see Eq. (96) below). The dependence of the AB conductance on external parameters — the gate voltage V_g , the variation of the magnetic field ΔB and the bias V — factorizes into

$$g_{\text{AB}}(\mu_+, \mu_-, \phi, V_g) = \tilde{g}(V) \cos[\varphi_{\text{AB}}(V_g, \Delta B)]. \quad (93)$$

The AB phase φ_{AB} will be discussed in the details shortly. The amplitude of the oscillations is

$$\tilde{g}(V) = e^{-\tau/\tau_\varphi} R_{12*}(eV) 2 \left| \cos \left(|eV\tau| + \frac{\pi}{4\nu^*} \right) \right| \quad (94)$$

with the nonequilibrium dephasing rate given by

$$\tau_\varphi^{-1} = |eV| (R_{1*}(eV) + R_{2*}(eV)) \frac{2}{\pi} \sin^2 \frac{\pi}{2\nu^*}. \quad (95)$$

In Eqs. (92) and (94) we have introduced the renormalized reflection coefficients defined as

$$\begin{aligned} R_{j*}(eV) &= R_j \left| \frac{\omega_C}{eV} \right|^{1/\nu^*} \frac{e^{\gamma/\nu^*}}{\Gamma(2 - 1/\nu^*)} = R_{j*}(\epsilon_{\text{th}}) \left| \frac{\epsilon_{\text{th}}}{eV} \right|^{1/\nu^*}, \\ R_{12*}(eV) &= R_{12} |\omega_C \tau|^{1/2\nu^*} \left| \frac{\omega_C}{eV} \right|^{1/2\nu^*} \frac{2^{1/2\nu^*} e^{\gamma/\nu}}{\Gamma(1 - 1/2\nu^*)} = R_{12*}(\epsilon_{\text{th}}) \left| \frac{\epsilon_{\text{th}}}{eV} \right|^{1/2\nu^*}. \end{aligned} \quad (96)$$

Remarkably, in the last equation the amplitudes r_1, r_2 do not renormalize separately, rather the renormalization operates non-locally. A similar result was found for FPIs in the fractional QHE regime in Ref. [49]. The relations (96) are valid for bias in the range $\epsilon_{\text{th}} \ll eV \ll \omega_C$. The above renormalization comes from *virtual* electron-hole excitations (being a precursor of weak Coulomb blockade [24, 25]) and stops at $eV \simeq \epsilon_{\text{th}}$. On the contrary, the dephasing rate τ_φ^{-1} is caused by *real* e-h pairs excited by backscattered electrons and is proportional to the shot noise of the QPCs. There a simple linear dependence of the shot noise on voltage, which is valid in the absence of interaction, is modified because of the renormalization of reflection coefficients.

A functional dependence on bias in the conductance amplitude (94) stems from an oscillatory prefactor which has a characteristic scale $\pi\epsilon_{\text{th}}$. As a consequence, the amplitude or, equivalently, the visibility $v(V) = |\tilde{g}(V)|/g_{\text{inc}}(V)$ vanishes for certain equidistantly distributed values of bias. The resulting characteristic “lobe” structure of visibility is shown in Fig. 8 and is in agreement with experiments reported in Refs. [27, 26].

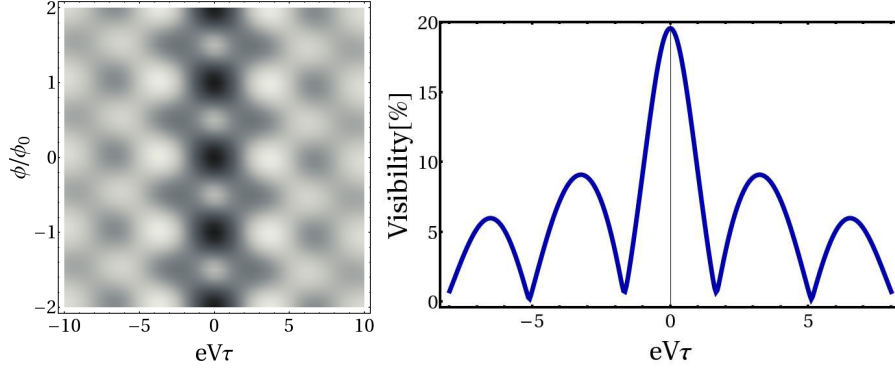


Figure 8: Total differential conductance g as a function of bias and magnetic flux (left panel), and visibility (right panel). Parameters are: $\nu^* = 2$, $\omega_C \tau = 25$, $R_{1*}(\epsilon_{th}) = R_{2*}(\epsilon_{th}) = 0.2$.

4.2.2. Aharonov-Bohm oscillations

In experiment one usually characterizes the FPI in terms of a pattern of its equilibrium conductance in the (B, V_g) - plane, which is governed by AB phase. We have identified four different regimes where the behavior of AB oscillations is qualitatively different (see Table 1). In this table the parameter ν^* — the effective number of transmitted channels which screen the Coulomb interaction in the interfering channel — depends on the relative strength of the inter-edge e - e interaction. To distinguish between the limits of weak and strong e - e interaction we compare an inter-channel interaction energy $\sim e^2/C_{e\alpha}$ (here $\alpha = r, l$) with a screened by the gate charging energy of the interfering edge itself given by $\sim e^2/C_{\alpha g}^*$. Here the edge-to-gate capacitance is effectively increased by the so-called “quantum capacitance”:

$$C_{\alpha g}^* = C_{\alpha g} + (\nu - 1)\tau e^2/(\hbar\pi). \quad (97)$$

In the weak coupling limit one has $C_{e\alpha} \gg C_{\alpha g}^*$. In this case the electrostatic potentials on all edge channels (r, l , and e) are approximately equal to each other and we set $\nu^* \simeq \nu$. In the opposite strong coupling limit we have $C_{e\alpha} \ll C_{\alpha g}^*$. The potential φ_e here fluctuates independently of potentials on other edge channels (r and l), thus screening of e - e interaction by the latter channels is not effective and one gets $\nu^* \simeq 1$. To

Table 1: “Phase diagram” of the FPI, which discriminate between two Aharonov-Bohm (AB and AB*) and two Coulomb dominated (CD I and CD II) regimes.

	$C_{e\alpha} \gg C_{\alpha g}^*$ $\nu^* = \nu$ $\bar{C}_{ei} = C_{ei} + C_{ri} + C_{li}$ $\bar{C}_{eg} = C_{eg} + C_{rg} + C_{lg}$	$C_{e\alpha} \ll C_{\alpha g}^*$ $\nu^* = 1$ $\bar{C}_{ei} = C_{ei}$ $\bar{C}_{eg} = C_{eg}$
$C_{ei} \ll C_{ig}$	AB	AB*
$C_{ei} \gg C_{ig}$	CD II	CD I

make a distinction between the “Aharonov-Bohm” (AB) and “Coulomb-dominated” (CD) regimes we now define an effective edge-to-island capacitance \bar{C}_{ei} by the relation $\bar{C}_{ei} = C_{ei} + C_{ri} + C_{li}$ in the weak coupling limit, i.e. at $\nu^* \simeq \nu$, and set it to be $\bar{C}_{ei} = C_{ei}$ in the opposite case of strong coupling. Then the FPI falls into AB or CD regimes depending on a ratio \bar{C}_{ei}/C_{ig} , as it is shown in the Table 1. As one can see from Eqs. (89) and (90), for the device with a top gate the capacitance C_{ig} scales like r^2 when the FPI size grows, while \bar{C}_{ei} increases only as $r \ln r$. This suggests a simple rule of thumb: the AB regime occurs primary in large FPIs with a top gate (in experiment “large” means a cell area $\sim 20 \mu\text{m}^2$). In this situation, i.e. at $\bar{C}_{ei}/C_{ig} \ll 1$, fluctuations of charge on the island are screened by the gate electrode and do not affect

the AB conductance. In the case of opposite ratio between the capacitances ($\bar{C}_{ei}/C_{ig} \gg 1$), as one will see shortly, the AB conductance becomes linked to the Coulomb blockade on the compressible island. This explains a terminology choice — "Coulomb-dominated" — for the above regime.

For a device without the top gate a bare edge-to-gate capacitance C_{eg} is due to only a plunger gate (see Fig. 6). Such gate is used to control the size of the interference loop and because of geometry C_{eg} typically is very small, so that one has $C_{eg}^* \simeq (\nu - 1)\tau e^2/(\hbar\pi)$. In this case our first condition of weak versus strong inter-edge e - e coupling can be simplified. Defining the dimensionless coupling constant as

$$\alpha_\nu \equiv \frac{(\nu - 1)e^2}{\epsilon\hbar v_F}$$

and using the estimate (90) for capacitances C_{er} and C_{el} one obtains the crossover value

$$\alpha^* \sim \frac{1}{2\pi} \ln \left(\frac{b_e b_r}{a_{er}^2} \right),$$

which sets the boundary between the weak and strong coupling regimes.

We name four regimes AB, AB*, CD I and CD II according to the Table 1 above which for the benefit of the reader lists the values of parameters ν^* , \bar{C}_{ei} and \bar{C}_{eg} . The capacitance \bar{C}_{eg} here is defined in analogy to \bar{C}_{ei} . In addition to these effective edge-to-island and edge-to-gate capacitances we now define full island and edge capacitances as

$$\bar{C}_i = \bar{C}_{ei} + C_{ig}, \quad \bar{C}_e = \bar{C}_{eg} + \bar{C}_{ei}C_{ig}/\bar{C}_i. \quad (98)$$

Then the AB phase in Eq. (93) reads

$$\varphi_{AB} = 2\pi\phi/\phi_0 - \frac{2\pi}{\nu^*} \frac{\bar{C}_{ei}}{\bar{C}_i} (N_{i*} + \nu\phi/\phi_0) + \frac{|e|}{\omega_C} (2V_g - V_+ - V_-) \quad (99)$$

with integer N_{i*} minimizing the charging energy of the Coulomb island

$$E_i = \frac{e^2}{2\bar{C}_i} (N_{i*} + \nu\phi/\phi_0 - C_{ig}V_g/|e|)^2, \quad (100)$$

and we have defined $\omega_C = \nu^* E_C/\pi$ and $E_C = e^2/\bar{C}_e$.

In Fig. 9 we show the conductance $g_{AB}(\phi, V_g)$ in the (B, V_g) -plane for three regimes: AB, CD-I and CD-II. The plots display significant differences. In particular, the lines of constant phase have a different slope in the AB and type-I CD regimes. The flux periodicity is also different in these two cases. The AB conductance in the case of type-II CD regime shows the "rhomb-like" pattern. The pattern of equilibrium conductance in the AB* case is the same as in the AB regime, provided one sets $\nu^* = 1$.

4.2.3. Discussion and comparison with experiment

Let us now discuss the physics which underlies the rich phenomenology of our rather simple model. To appreciate the role of interaction we consider first the non-interacting case, where the interfering channel couples neither to the fully transmitted ones nor to the island. Consider electron contributing to the tunneling current which is, say, incident from the left source and leaks into the left drain. It may tunnel either at the left or right QPC. The latter path is longer than the first by $2L = 2v_F\tau$ and encircles a magnetic flux ϕ . Along this path the electron accumulates a dynamic ("Fabry-Pérot") phase $2\epsilon\tau$ (ϵ is the energy of the electron) and a magnetic AB phase $2\pi\phi/\phi_0$. According to quantum mechanics, the current results from interference of both paths. Integration over all energies in the range $\mu_- < \epsilon < \mu_+$ gives the back-scattering current

$$I_b = -e \int_{\mu_-}^{\mu_+} \frac{d\epsilon}{2\pi} \left| r_1 + e^{2\pi i\phi/\phi_0 + 2i\epsilon\tau} r_2 \right|^2 = I_{\text{inc}} + I_{AB}, \quad (101)$$

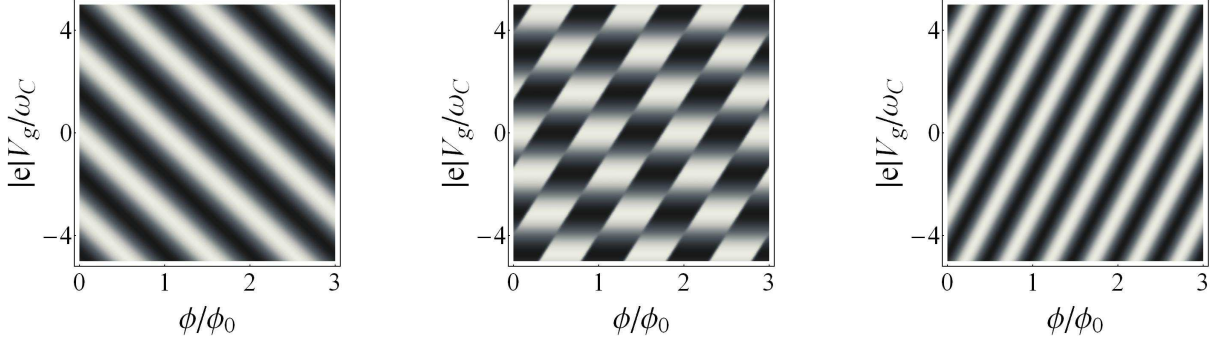


Figure 9: Aharonov-Bohm conductance: AB regime (left), $\nu^* = \nu = 2$, stripes of constant conductance have a negative slope, flux and gate voltage periods are $\Delta\phi = \phi_0$ and $\Delta V_g = \nu E_C/|e|$; type-I CD regime (middle), $\nu^* = 1$, $\nu = 3$, stripes of constant conductance have now a positive slope, flux and gate voltage periods are $\Delta\phi = \phi_0/(1-\nu)$ and $\Delta V_g = E_C/|e|$; type-I CD regime (right), $\nu^* = \nu = 2$, $C_{ig}/\bar{C}_e = 0.6$, at fixed gate voltage V_g conductance depends discontinuously on flux — phase jumps occurs at every $\Delta\phi = \phi_0/\nu$.

that we have split into incoherent and coherent contributions,

$$I_{\text{inc}} = -\frac{e^2}{2\pi}V(R_1 + R_2), \quad I_{\text{AB}} = \frac{e}{2\pi} \frac{2R_{12}}{\tau} \cos[(\mu_+ + \mu_-)\tau - 2\pi\phi/\phi_0] \sin[eV\tau]. \quad (102)$$

While the incoherent part of the current I_{inc} is expected already on the classical level, I_{AB} stems from interference and is sensitive to magnetic flux. The dynamic phase accumulated by an electron depends on its “absolute” energy ϵ , and hence the current I_{AB} depends on both chemical potentials μ_+ , μ_- , but not just on their difference $eV = \mu_+ - \mu_-$. Clearly, the sum $(\mu_+ + \mu_-)$ enters only into the phase shift of the AB pattern, but not in the amplitude. However, this independence of the amplitude of oscillations on the bias does not in general hold for the differential conductance g_{AB} . Specifically, when the differential conductance is calculated in the framework of the model of non-interacting electrons, the amplitude of the corresponding AB oscillations \tilde{g} does depend on the manner in which bias is applied.

Experimentally, the bias is applied asymmetrically: $\mu_+ = eV$, $\mu_- = 0$. The expected conductance then is

$$g_{\text{AB}} = G_Q^{-1} \partial_V I_{\text{AB}} = -2R_{12} \cos[2eV\tau + 2\pi\phi/\phi_0],$$

i.e. bias merely controls the phase shift of the AB oscillation pattern. The amplitude $\tilde{g} = -2R_{12}$ is independent of bias. This clearly contradicts to our results presented above as well as to experimental observations.

The situation would change essentially if the bias were applied symmetrically: $\mu_+ = eV/2$, $\mu_- = -eV/2$. Then the conductance would be

$$g_{\text{AB}} = -2R_{12} \cos[eV\tau] \cos[2\pi\phi/\phi_0]. \quad (103)$$

Now, the amplitude would oscillate with bias on the scale $\pi\epsilon_{\text{th}}$, yielding a visibility with a “lobe” structure. This result is apparently much more similar to our findings (albeit without dephasing and renormalization of R_{12}) as well to the experimental observations. On the basis of the similarity between Eq. (103) and the experimental observations it was conjectured in Ref. [28] that the electron-electron interaction effectively symmetrizes the bias even if the latter is applied asymmetrically.

To see how this works, assume that a charge within the interferometer cell produces a (for simplicity constant) self-consistent potential φ_0 . An electron which propagates in this potential during a time 2τ accumulates the “electrostatic” AB phase $-2\varphi_0\tau$. Hence, the dynamic phase would be $2(\epsilon - \varphi_0)\tau$ and instead of the bare chemical potentials the relative potentials $(\mu_{\pm} - \varphi_0)$ enter the result (102). Such a mean-field potential is indeed generated within our model. For instance, in the generic limit of large charging energy

$E_C \gg \epsilon_{\text{th}}$ our calculations in the subsection 4.3 yield $\varphi_0 \simeq (\mu_+ + \mu_-)/2$ in the case of AB regime. Therefore without a need of any fine tuning, the bias is effectively symmetrized, which explains the appearance of the “lobe” structure.

The mean-field potential φ_0 on the compressible strip corresponding to the interfering edge channel is in general the function of applied chemical potentials μ_{\pm} , the gate voltage V_g and the magnetic flux ϕ . The most general expression found in the subsection 4.3 reads

$$\varphi_0(\mu_{\pm}, V_g, \phi) = \frac{1}{1 + \omega_C \tau} \left[eV_g + \frac{\mu_+ + \mu_-}{2} \omega_C \tau + E_C \frac{\bar{C}_{ei}}{C_i} (N_{i*} + \nu \phi / \phi_0) \right]. \quad (104)$$

Here N_{i*} , as before, provides the minimum for the Coulomb energy E_i of the island given by Eq. (100). If we introduce the electrochemical potential

$$\tilde{\varphi}_0 = \varphi_0 - (\mu_+ + \mu_-)/2, \quad (105)$$

then the AB phase, given by Eq. (99), is equivalently represented by relation

$$\varphi_{AB}(\mu_{\pm}, V_g, \phi) = 2\pi\phi/\phi_0 - 2\tau\tilde{\varphi}_0(\mu_{\pm}, V_g, \phi). \quad (106)$$

The first contribution here is the magnetic AB phase accumulated along a fixed reference loop with area A_0 , i.e. $\phi = A_0 \delta B$, with $\delta B \ll B$ being a weak modulation of magnetic field on top of the high field B which drives the 2DEG into the QHE regime. Because of the condition $b \ll L$ (see Fig. 6 b) imposed in our model, and since a typical variation δB is such that ϕ changes on a scale of a few flux quanta only, one can use any boundary y_k^{\pm} to define A_0 . For example, one can set $A_0 = \pi(y_{\nu}^+)^2$. Let us further show, that the second “electrostatic” contribution $(-2\tau\tilde{\varphi}_0)$ to the phase φ_{AB} can be interpreted in terms of a motion of edge states which leads to the variation of a relevant FPI area when the magnetic field B or gate voltage V_g are varied.

First, we note that in a stationary limit an imbalance of electron density per unit length on the interfering edge channel $\delta\rho_e$ is related with the corresponding electrochemical potential (105) by a simple relation $\delta\rho_e = -\tilde{\varphi}_0/(2\pi v_F)$, since $(2\pi v_F)^{-1}$ is just but the 1D thermodynamic density of states in our model. As it is always the case in QHE systems, this charge density can be translated into the variation h_{ν} of the boundary between the compressible and incompressible strips (Fig. 10), $\delta\rho_e = n_L h_{\nu}$, where $n_L = B/\phi_0 = (2\pi\lambda_B^2)^{-1}$ is the electron concentration on one completely filled LL, and we have assumed the fluctuations of inner and outer boundaries of the compressible strip to be the same, $\delta y_{\nu+1}^+ = \delta y_{\nu}^- = h_{\nu}$. Therefore “electrostatic” part of the AB phase reads

$$-2\tau\tilde{\varphi}_0 = 4\pi L \delta\rho_e = 4\pi n_L (L h_{\nu}) = 2\pi(B/\phi_0) \delta A. \quad (107)$$

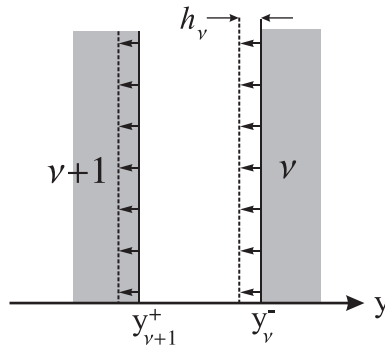


Figure 10: When the boundaries of the compressible strip (white) separating incompressible regions (gray) with filling factors ν and $\nu + 1$ move towards the $(\nu + 1)$ -liquid (indicated by arrows), the latter shrinks while the ν -liquid’s area grows: as the result the charge on the incompressible strip, defined by the boundaries $y_{\nu+1}^-$ and y_{ν}^+ , decreases (in this figure $h_{\nu} < 0$).

Here $\delta A = 2Lh_\nu$ is the change in area enclosed by interfering edge state. To recapitulate the logic, we have thus related the self-consistent electrostatic potential φ_0 to a variation of the FPI area. With these arguments at hand one can now rewrite Eqs. (104) and (106) in the equivalent form

$$\phi_{AB} = 2\pi(A_0\delta B + B\delta A)/\phi_0 + \text{const}, \quad (108)$$

where the variation of area reads

$$\delta A = -\frac{1}{\nu^*} \frac{\bar{C}_{ei}}{\bar{C}_i} \left(\nu \frac{A_0}{B} \delta B + \frac{\phi_0}{B} \Delta N_i \right) + \frac{|e|}{\omega_C} \frac{\phi_0}{\pi B} \delta V_g. \quad (109)$$

In the last equation we have introduced an integer ΔN_i which is a deviation in excess number of electrons on the Coulomb island with respect to the excess charge corresponding to some initially chosen reference gate voltage V_g . We have also took into account the source-drain bias is small on a scale of the charging energy, $|e|V \ll E_C$.

Let us now discuss our theory of the FPI in relation to the recent experiments by considering separately each of the four regimes in the Table 1. In the *AB regime* one has $\bar{C}_{ei}/C_i \ll 1$, thus the coupling of the interfering edge to the Coulomb island is negligible and the area A does not change with B . The AB phase then simplifies to

$$\varphi_{AB} = 2\pi\phi/\phi_0 + \frac{2\pi}{\nu} \frac{|e|V_g}{E_C}, \quad (110)$$

yielding the lines of constant phase with a negative slope (Fig. 9, left) and a magnetic field period $\Delta B = \phi_0/A_0$ which is independent of ν . The second term in the above equation describes a modulation in space of electron trajectory under variation of the gate voltage. If $\delta V_g > 0$ then the interfering edge state moves outwards and thus encloses a larger flux as it is seen from Eq. (109). The AB regime was observed in large devices (cell area $\sim 18\mu\text{m}^2$) with a top gate [26, 28, 29], where the condition $\bar{C}_{ei} \ll C_{gi}$ is satisfied. In Ref. [28] it has been also found that magnetic field period ΔB is independent of B but gate voltage periodicities (both top- and plunger- ones) scale as $\Delta V_g \propto 1/B \propto \nu$. These observation are consistent with our Eq. (110) if the charging energy $E_C = e^2/\bar{C}_e$ is ν -independent. It is so, provided the full edge capacitance $\bar{C}_e \simeq C_{eg} + \bar{C}_{ei}$ stays approximately the same at each Hall plateau.

In the *CD regime* one has $\bar{C}_{ei}/C_i \simeq 1$ and the area of the interfering loop shrinks with the magnetic field. This is because interfering edge is now electrostatically coupled to the charge $Q_i = e(N_i + \nu\phi/\phi_0)$ on the Coulomb island, which has explicit dependence on flux. The AB phase in this regime reads

$$\varphi_{AB} = 2\pi(1 - \nu/\nu^*)\phi/\phi_0 - \frac{2\pi}{\nu^*} N_i + \frac{2\pi}{\nu^*} \frac{|e|V_g}{E_C},$$

In the type-II CD regime $\nu^* \simeq \nu$ and at fixed V_g the AB phase stays piecewise constant when the magnetic field is varied. The dependence of phase on B exclusively enters via N_i . Indeed, as it follows from Eq. (109) the shrinkage of the interfering loop in this case, $\delta A = -(A_0/B)\delta B$, exactly compensates a change in magnetic phase $\varphi = A_0\delta B$. When the FPI is brought close to a charge degeneracy point of the island by varying V_g or B , electron tunneling becomes possible between the droplet and interfering channels (i.e. $\Delta N_i = \pm 1$) resulting in abrupt change of A . This creates a phase lapse (or jump) $\Delta\phi_{AB} = \pm 2\pi/\nu$ giving rise to the “rhomb-like” pattern shown in Fig. 9 (middle) at $\nu \geq 2$.

In the type-I CD regime $\nu^* \simeq 1$ and a change in AB phase caused by area shrinkage when rising B overcompensates the magnetic AB phase, since now $\delta A = -\nu(A_0/B)\delta B$. Counterintuitively, the phase decreases for increasing the magnetic field. At the same time, whenever an electron tunnels into the island from the interfering edge channel (e), the boundary of this edge state contracts so as to expel exactly one flux quantum from the AB loop. The phase lapse, being equal to $\Delta\phi_{AB} = (-2\pi)$ in this tunneling process, is therefore invisible in the interference conductance. As the result, one has the diagonal stripe pattern with lines of constant phase having positive slope (Fig. 9, right). The periods are $\Delta B = \phi_0/(f_TA)$ and $\Delta V_g = e/(C_{eg} + C_{gi})$, with $f_T = \nu - 1$ being the number of fully transmitted edge channels (note, that at $\nu = 1$ the lines of constant phase are vertical).

In the limit of weak backscattering at QPCs, the Coulomb-dominated regime has been observed in Ref. [29]. In this work measurements were performed with the set of edge state configurations (including fractional fillings), classified by bulk filling f_b and number f_T of fully transmitted edges. We focus on the results obtained with a $4.4\,\mu\text{m}^2$ -device without a top (but with plunger-) gate. They indicate that interaction plays a major role (i.e. CD-I and CD-II regimes). For integer f_b and $f_T = f_b - 1$ the results coincide with our Fig. 9 (right), including the period in magnetic field which scales as $\Delta B \propto 1/f_T$. The gate period in Ref. [29] was found to be weakly increasing with f_T . We can explain this dependence if one assumes that the full edge capacitance, which equals to $\bar{C}_e = C_{gi} + C_{eg}$ in the CD-I regime, decreases with f_T , since a mutual coupling of the plunger-gate to the inner interfering edge channel (C_{eg}) becomes less efficient at high ν . Quite “exotic” behavior was observed for more than one number of channels trapped in the interferometer cell. In case of $f_b = 4$ and $f_T = 1$ experimental findings resemble very much Fig. 9 (middle) corresponding to our CD-II regime. In such setting one fully transmitted and one partially reflected edge channel can be described by our model with $\nu = 2$ assuming that other two inner trapped channels play a role of a compressible island, where the excess charge is quantized.

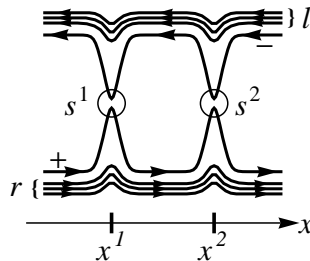
Non-equilibrium transport measurements in the FPIs in the AB regime have been performed in Refs. [26, 27]. Their main findings can be summarized as follows: (i) the dependence of AB conductance versus B and the bias V factorizes into a product of two terms yielding a “checkerboard” pattern in the $(\delta B, V)$ -plane (cf. Fig. 8, left); (ii) the scale of the “lobe”-structure is set by $\epsilon_{\text{Th}} \sim v_D/L$; (iii) a visibility decay with bias is stronger at higher magnetic fields. Results of our theory, Eqs. (93) - (96), are in full accord with these observations. In particular, a suppression of visibility in our model at $|r_j|^2 \ll 1$ is mainly due to a power-law decay with the *negative* exponent $(-1/2\nu^*)$. Since in the AB regime $\nu^* = \nu \propto 1/B$, this decay is stronger in case of a small number of edge channels, i.e. at higher B , in agreement with Ref. [26].

It is interesting to note, that our theory predicts a fourth regime (AB*, see Table 1). It is characterized by the same equilibrium conductance pattern as the AB regime (Fig. 9, left), but in contrast to the latter, the power-law decay of the visibility oscillations corresponds to $\nu^* = 1$, and thus is independent of B . Such a behavior of the FPI has not yet been observed in the experiment.

Closing this section we have to mention that a crossover from the AB to the type-I CD regime (in our terminology has been recently discussed in details in Ref. [51]. We note that our capacitance model is very similar in spirit to the one used in that paper. However, the important difference is that our approach takes explicitly into account quantum corrections to classical geometrical capacitances, given by Eq. (97). As the result we obtain the extra type-II CD regime which may arise because of screening of Coulomb interaction by the fully transmitted edge channels.

4.3. Calculations

We show here how to derive the above results using the formalism developed in Sect. 2. For simplicity we assume all edge channels to have the same length L and same velocity $|v_\mu| = v_F$ (with $v_\mu > 0$ in right-moving channels and $v_\mu < 0$ in left-moving ones). Consequently, all flight times $\tau = L/v_F$ are the same. Further, the scatterer 1 has a coordinate x^1 and scatterer 2 has the coordinate $x^2 = x^1 + L$ for each of the edges, see Fig. 11.



We remind that two characteristic energy scales play an important role in our analysis, namely, Thouless energy $\epsilon_{\text{th}} = \tau^{-1}$ and charging energy $E_C = e^2/\bar{C}_e$ (or charge relaxation frequency $\omega_C = \frac{\nu^*}{\pi} E_C$), see Sec. sec:FPI-results. As has been discussed there, we will assume that the charging energy is much higher than the Thouless energy, and will consider the range of voltages intermediate between these two scales, $\omega_C \gg |eV| \gg \epsilon_{\text{th}}$.

4.3.1. Electrostatic Action

Our network consists of ν right-moving and ν left-moving chiral channels which we label with index μ , see Fig. 11. The innermost right-moving channel ($\mu = +$) is coupled to the innermost left-moving channel ($\mu = -$) by two scatterers $i = 1, 2$ with 2×2 -scattering matrices s^i . The remaining chiral channels (right-moving ones labeled $\mu = r1, \dots, r(\nu - 1)$, left-moving ones by $\mu = l1, \dots, l(\nu - 1)$) connect sources to drains without any possibility of tunneling.

Interaction is taken into account by the electrostatic model (88) described in the beginning. For simplicity we assumed that electrostatic coupling between all fully transmitted right-moving channels ($\mu = r1, \dots, r(\nu - 1)$) is strong such that they share a common electrostatic potential V_r . This enables us to merge them into one conductor (labeled $\alpha = r$). We proceeded in the same way with the fully transmitted left-moving ones ($\mu = l1, \dots, l(\nu - 1)$) are now merged into $\alpha = l$) and the two innermost channels ($\mu = +, -$ are merged into $\alpha = e$). This reduces the number of charge degrees of freedom characterizing the edge channels down to three:

$$Q_e = \int dx \bar{\psi}_+ \psi_+ + \int dx \bar{\psi}_- \psi_-, \quad Q_r = \sum_{\kappa=1}^{\nu-1} \int dx \bar{\psi}_{r\kappa} \psi_{r\kappa}, \quad Q_l = \sum_{\kappa=1}^{\nu-1} \int dx \bar{\psi}_{l\kappa} \psi_{l\kappa}.$$

As a fourth conducting element, we introduce a central compressible island with total charge $Q_i = e(N_i + \nu\phi/\phi_0)$. While the second contribution, the charge in the ν fully occupied LLs of the central region, is fixed by external parameters, the occupation N_i of the partially filled LL of the island is an (integer) degree of freedom to begin with. Since it is assumed to fluctuate via very slow tunneling, $\Gamma \ll \epsilon_{\text{th}}$, we will, however, treat it in a mean-field approximation.

The fermionic action we start with reads as follows

$$\mathcal{A}_0[\psi, \bar{\psi}, N_i] = \sum_{\mu} \int_C dt dx \bar{\psi}_{\mu} (i\partial_t + iv_{\mu}\partial_x) \psi_{\mu} - \frac{1}{2} \sum_{\alpha\beta} (Q_{\alpha} - q_{\alpha}) \left(\tilde{C}^{-1} \right)_{\alpha\beta} (Q_{\beta} - q_{\beta}),$$

where the first sum extends over the 2ν chiral channels $\mu = r1, \dots, r(\nu - 1), l1, \dots, l(\nu - 1), +, -$ and the second one over the 4 conductors $\alpha, \beta = e, r, l, i$. The electrostatic part of $\mathcal{A}_0[\psi, \bar{\psi}, N_i]$ is, of course, a direct consequence of (88) and we refer to the corresponding section for definitions of q_{α} and \tilde{C} . Charges Q_{α} are, of course, dynamic, i.e. time-dependent, quantities, but for the sake of readability we leave time-dependence implicit (as we did with time integration in the above electrostatic action).

Our interest lies in interference effects which manifest themselves in tunneling corrections to current. Tunneling phases respond only to the Hubbard-Stratonovich field $\varphi = eV_e$ on the interfering edges (note that the electrostatic merging of channels $\mu = +, -$ allows us to use just one field $\varphi = \varphi_+ = \varphi_-$). The short-term goal of the present section is to integrate out all other degrees of freedom.

Potentials $V_c = (V_e, V_r, V_l)^t$: . First, we decouple the quadratic charge terms via a (multidimensional) Hubbard-Stratonovich transformation, thereby (re)introducing the potentials V_{α} on the conductors. Since we do not need the potential V_i on the island, we single out the island degrees of freedom beforehand, writing

$$\tilde{C}^{-1} = \begin{pmatrix} p_{cc} & p_{ci} \\ p_{ic} & p_{ii} \end{pmatrix}, \quad V_{ci} = p_{ci}(Q_i - q_i). \quad (111)$$

The index c refers to the 3 indices e, r, l , that means $p_{cc}, p_{ci} = p_{ic}^t, p_{ii}$ are 3×3 -, 3×1 -, and 1×1 -matrices. With that the action reads

$$\mathcal{A}_{\text{int}}[\psi, \bar{\psi}, N_i] = -\frac{1}{2}(Q_i - q_i)^2 p_{ii} - \frac{1}{2}(Q_c - q_c)^t p_{cc}(Q_c - q_c) - V_{ci}^t(Q_c - q_c)$$

and becomes upon Hubbard-Stratonovich decoupling:

$$\mathcal{A}_{\text{int}}[\psi, \bar{\psi}, V_c, N_i] = \frac{1}{2}(Q_i - q_i)^2 p_{ii} + \frac{1}{2}(V_c - V_{ci})^t p_{cc}^{-1} (V_c - V_{ci}) - V_c^t (Q_c - q_c) \\ \text{with } V_c = (V_e, V_r, V_l)^t.$$

Integrating out Q_e, Q_r, Q_l : . Next, we integrate out the charges Q_e, Q_r, Q_l . As explained in Sect. 2.1 and 2.2 charges and potentials are decoupled by a gauge transformation (2) which generates a tunneling term \mathcal{A}_t (see below) and, according to the Dzyaloshinskii-Larkin theorem, quadratic and linear (in voltages) terms $V_\alpha^2 S_\alpha$ and $\bar{Q}_\alpha V_\alpha$. The former is given by the polarization operators (10) and amounts for screening, thus an “enhancement” of the capacitances (in fact, the capacitances become complex, “Keldysh”- and energy-dependent, but in the static limit the corrections are indeed positive). Then the retarded/advanced components of the “screening capacitances” read

$$S_\alpha^{r/a}(\omega) = -e^2 \sum_{\kappa=1}^{\nu-1} \int d\xi_1 d\xi_2 \Pi_{\alpha\kappa}^{r/a}(\omega, \xi_1, \xi_2) = \pm i(\nu-1)e^2 \frac{1 - e^{\pm i\omega\tau}}{2\pi\omega}, \quad \alpha = r, l, \\ S_e^{r/a}(\omega) = -e^2 \sum_{\mu=\pm} \int d\xi_1 d\xi_2 \Pi_\mu^{r/a}(\omega, \xi_1, \xi_2) = \pm i2e^2 \frac{1 - e^{\pm i\omega\tau}}{2\pi\omega}. \quad (112)$$

Charges injected from the reservoirs due to nonequilibrium boundary conditions (in excess of the equilibrium charge which is canceled by the positive background charge) are

$$\bar{Q}_r = (\nu-1)e^{\frac{\mu_+ \tau}{2\pi}}, \quad \bar{Q}_l = (\nu-1)e^{\frac{\mu_- \tau}{2\pi}}, \quad \bar{Q}_e = e^{\frac{(\mu_+ + \mu_-) \tau}{2\pi}}. \quad (113)$$

We collect them in the diagonal matrix $S = \text{diag}(S_e, S_r, S_l)$ and the vector $\bar{Q}_c = (\bar{Q}_e, \bar{Q}_r, \bar{Q}_l)^t$. Subsequent elimination of charge degrees of freedom transforms $\mathcal{A}_{\text{int}}[\psi, \bar{\psi}, V_c, N_i]$ into

$$\mathcal{A}_0[V_c, N_i] = -\frac{1}{2}\bar{p}_{ii}(Q_i - q_i)^2 + \frac{1}{2}V_c^t(p_{cc}^{-1} + S)V_c - V_c^t(\bar{Q}_c - q_c + p_{cc}^{-1}V_{ci}) \\ \text{with } \bar{p}_{ii} = p_{ii} - p_{ic}p_{cc}^{-1}p_{ci}. \quad (114)$$

Integrating out V_r, V_l : . The final, and somewhat cumbersome step is to integrate out the voltages V_r, V_l . In order to do that we again split the degrees of freedom, writing

$$p_{cc}^{-1} = \begin{pmatrix} c_{ee} & c_{et} \\ c_{te} & c_{tt} \end{pmatrix}, \quad S = \begin{pmatrix} S_e & \\ & S_t \end{pmatrix}, \quad (115)$$

where the index t refers to the 2 indices r, l , and $c_{ee}, c_{et} = c_{te}^t, c_{tt}$ are corresponding 1×1 -, 1×2 -, and 2×2 -matrices. The action then reads

$$\mathcal{A}_0[V_c, N_i] = -\frac{1}{2}\bar{p}_{ii}(Q_i - q_i)^2 + \frac{1}{2}(c_{ee} + S_e)V_e^2 - V_e(\bar{Q}_e - q_e + c_{ee}V_{ei} + c_{et}V_{ti}) \\ + \frac{1}{2}V_t^t(c_{tt} + S_t)V_t - V_t^t(\bar{Q}_t - q_t + c_{te}V_{ei} + c_{tt}V_{ti} - c_{te}V_e).$$

Performing the Gaussian integration over V_r, V_l is a straightforward, albeit cumbersome calculation which in the end yields,

$$\mathcal{A}_0[V_e, N_i] = -\frac{1}{2\bar{C}_i}(Q_i - q_i)^2 - (\bar{Q}_t - q_t)^t \bar{p}_{ti}(Q_i - q_i) + \frac{1}{2}\bar{C}_e^* V_e^2 - V_e(\bar{Q}_e - q_e + x_{et}(\bar{Q}_t - q_t) + x_{ei}(Q_i - q_i)) \quad (116)$$

where we have introduced the effective capacitances and coupling strengths

$$\begin{aligned}\bar{C}_i^{-1} &\equiv p_{ii} - p_{ic} p_{cc}^{-1} p_{ci} + (p_{ie} c_{et} + p_{it} c_{tt})(c_{tt} + S_t)^{-1} (c_{te} p_{ei} + c_{tt} p_{ti}), \\ \bar{C}_e^* &\equiv c_{ee} + S_e - c_{et}(c_{tt} + S_t)^{-1} c_{te}, \quad \bar{C}_e \equiv \bar{C}_e^* \Big|_{S_e=S_r=S_l=0} \\ x_{et} &\equiv -c_{et}(c_{tt} + S_t)^{-1}, \\ x_{ei} &\equiv c_{ee} p_{ei} + c_{et} p_{ti} - c_{et}(c_{tt} + S_t)^{-1} (c_{te} p_{ei} + c_{tt} p_{ti}), \\ \bar{p}_{ti} &\equiv (c_{tt} + S_t)^{-1} (c_{te} p_{ei} + c_{tt} p_{ti}).\end{aligned}$$

Regimes ABI, CDI, CDII: . In the limits of very strong, i.e.

$$C_{\alpha e} \ll C_{eg} + S_e,$$

and very weak, i.e.

$$C_{\alpha e} \gg \frac{(C_{\alpha g} + S_{\alpha})^2}{C_{eg} + C_{rg} + C_{lg} + S_e + S_r + S_l},$$

coupling between fully transmitted edges $\alpha = r, l$ and interfering edge e the expressions simplify to

	Strong coupling	Weak coupling
C_i	$C_{ei} + C_{ig}$	$C_{ei} + C_{ri} + C_{li} + C_{ig}$
\bar{C}_e^*	$C_{eg} + S_e + C_{ig} - C_{ig}^2 / \bar{C}_i$	$C_{eg} + C_{rg} + C_{lg} + S_e + S_l + S_r + C_{ig} - C_{ig}^2 / \bar{C}_i$
x_{et}	$\begin{pmatrix} 0 & 0 \end{pmatrix}$	$\begin{pmatrix} 1 & 1 \end{pmatrix}$
x_{ei}	C_{ei} / \bar{C}_i	$(C_{ei} + C_{ri} + C_{li}) / \bar{C}_i$
\bar{p}_{ti}	0	0,

and using Eqs. (111)-(115), the action becomes

$$\mathcal{A}_0[\varphi, N_i] = \frac{1}{2} \int_C dt dt' \varphi(t) V^{-1}(t - t') \varphi(t') - \int_C dt \varphi(t) N_0(t) - \frac{1}{2\bar{C}_i} (Q_i - q_i)^2 \quad (117)$$

$$\begin{aligned}\text{with } V^{r/a}(\omega) &= E_C \frac{\omega}{\omega \pm i\omega_C(1 - e^{\pm i\omega\tau})}, \\ N_0 &\equiv \frac{\nu^*}{\pi} \frac{\mu_+ + \mu_-}{2} \tau - \frac{|e|V_g}{E_C} - \frac{\bar{C}_{ei}}{\bar{C}_i} Q_i / |e|\end{aligned} \quad (118)$$

Here \bar{C}_i , \bar{C}_e , \bar{C}_{eg} , \bar{C}_{ei} , and ν^* are given in Sect. 4.2.2 (Eq. (98) and table above).

4.3.2. Tunneling Action

To construct the tunneling action $\mathcal{A}_t[\varphi]$ in lowest order we use Eq. (20) which makes it necessary to identify the paths $(ij; \mu\nu)$. Only the innermost chiral channels $\mu, \nu = \pm$ allow for tunneling between each other at scatterers $i, j = 1, 2$ which gives 4 classes: (11; +−), (22; +−), (12; +−), and (21; +−). Classical phases are accumulated due to magnetic flux ϕ :

$$\Delta\phi_{+-}^{11} = \Delta\phi_{+-}^{22} = 0, \quad \Delta\phi_{+-}^{12} = -\Delta\phi_{+-}^{21} = -2\pi\phi/\phi_0.$$

At zero temperature the distribution functions read $f_{\pm}^{\gtrless}(t) = e^{-i\mu_{\pm}t} f_0^{\gtrless}(t)$ with Fermi distribution function $f_0^{\gtrless}(t)$. Writing for short $r_i \equiv s_{-+}^i$, $\chi \equiv \chi_+ - \chi_-$, $\epsilon_{ij} = \epsilon_{ij3}$ (the right-hand side being the 3-dimensional Levi-Civita symbol), and $\Pi_{ij} \equiv \Pi_{ij;+-}$ we obtain the tunneling operators (22, 23)

$$\Pi_{ij}^{\gtrless}(t) = -r_i \bar{r}_j e^{\pm i\chi} e^{-i\epsilon_{ij}[2\pi\phi/\phi_0 + (\mu_+ + \mu_-)\tau]} e^{-ieVt} f_0^{\gtrless}(t + \epsilon_{ij}\tau) f_0^{\lesseqgtr}(t - \epsilon_{ij}\tau), \quad (119)$$

$$\Pi_{ij}^{T/\bar{T}}(t) = [\theta(\pm t) \Pi_{ij}^{\gtrless}(t) + \theta(\mp t) \Pi_{ij}^{\lesseqgtr}(t)]_{\chi=0}. \quad (120)$$

Writing the tunneling phases $\Phi \equiv \Phi_{+-}$ the tunneling action reads

$$\mathcal{A}_t[\varphi] = -i \sum_{i,j=1,2} \int dt_1 dt_2 \begin{pmatrix} e^{-i\Phi^-(x^i, t_1)} & e^{-i\Phi^+(x^i, t_1)} \end{pmatrix} \begin{pmatrix} \Pi_{ij}^T(t_{12}) & -\Pi_{ij}^<(t_{12}) \\ -\Pi_{ij}^>(t_{12}) & \Pi_{ij}^T(t_{12}) \end{pmatrix} \begin{pmatrix} e^{i\Phi^-(x^j, t_2)} \\ e^{i\Phi^+(x^j, t_2)} \end{pmatrix} \quad (121)$$

with $t_{12} \equiv t_1 - t_2$. According to Sect. 2.3 and Eq. (2) the tunneling phases are related to the potential φ via

$$\Phi(x^i, t) = \Theta_-(x^i, t) - \Theta_+(x^i, t) = \int_C dt' \mathcal{D}_{+-}(x^i; t, t') \varphi(t') \quad (122)$$

with $\mathcal{D}_{+-}(x; t, t') \equiv \int_{x_1}^{x_2} dx' D_{0-}(x - x'; t, t') - \int_{x_1}^{x_2} dx' D_{0+}(x - x'; t, t')$

with bare particle-hole propagator $D_{0\mu}$ (Eq. (4)). Note that x' is integrated over because potential $\varphi(x', t) = \varphi(t)$ in our model does not vary in space.

Defining $\epsilon_i = \pm$ for $i = 1, 2$ retarded and advanced components of \mathcal{D}_{+-} read in energy representation

$$\mathcal{D}_{+-}^{r/a}(\omega; x^i) = \pm i \epsilon_i \frac{e^{\pm i \omega \tau} - 1}{\omega}. \quad (123)$$

4.3.3. Current in Instanton Approximation

Current is measured via the counting fields χ in the tunneling polarization operators (119). We use the adiabatic approximation where measuring time t_0 is much larger than all intrinsic time scales of the system and transient effects due to switching of the counting fields are negligible. The tunneling correction to current is the derivative

$$I_t = -i \frac{e}{t_0} \partial_\chi \ln \mathcal{Z} \Big|_{\chi=0} = \sum_{i,j=1,2} (I_{ij}^< - I_{ij}^>) \quad (124)$$

$$\text{with } I_{ij}^{\alpha\beta} = \frac{e}{t_0} \int dt_1 dt_2 \int \mathcal{D}\varphi \sum_{\{N_i\}} e^{i\mathcal{A}_0[\varphi, N_i] + i\mathcal{A}_t[\varphi]} e^{-i\Phi^\alpha(x^i, t_1)} \Pi_{ij}^{\alpha\beta}(t_{12}) e^{i\Phi^\beta(x^j, t_2)} \Big|_{\chi=0}. \quad (125)$$

The average $\int \mathcal{D}\varphi \sum_{\{N_i\}}$ is treated in real-time instanton approximation as outlined in Sect. 2.4:

$$\begin{aligned} I_{ij}^{\alpha\beta} &\approx \frac{e}{t_0} \int dt_1 dt_2 e^{i\tilde{\mathcal{A}}_t[\varphi_*]} \left\langle e^{-i\Phi^\alpha(x^i, t_1)} \Pi_{ij}^{\alpha\beta}(t_{12}) e^{i\Phi^\beta(x^j, t_2)} \right\rangle_0 \Big|_{\chi=0, N_i=N_{i*}} \\ &= \frac{e}{t_0} \int dt_1 dt_2 e^{i\tilde{\mathcal{A}}_t[\varphi_*]} e^{-i\Phi_0(x^i) + i\Phi_0(x^j)} \tilde{\Pi}_{ij}^{\alpha\beta}(t_{12}) \Big|_{\chi=0, N_i=N_{i*}} \end{aligned} \quad (126)$$

As always $\langle \dots \rangle_0$ denotes averaging with respect to $\mathcal{A}_0[\varphi, N_{i*}]$ given in (117). Because of the linear-in- φ contribution potential φ and hence tunneling phase Φ have non-vanishing expectation values $\varphi_0 = \varphi_0[N_i]$, $\Phi_0 = \Phi_0[N_i]$ which minimize $\mathcal{A}_0[\varphi, N_i]$ for given N_i . At the saddle-point N_{i*} in turn minimizes $\mathcal{A}_0[\varphi_0[N_i], N_i]$. For strong coupling $\omega_C \tau \gg 1$ the mean-field reads

$$\begin{aligned} \varphi_0 &= \frac{1}{1 + \omega_C \tau} \left[eV_g + \frac{\mu_+ + \mu_-}{2} \omega_C \tau + E_C \frac{\bar{C}_{ei}}{\bar{C}_i} (N_{i*} + \nu \phi / \phi_0) \right], \\ \Phi_0(x^{1/2}) &= \mp \tau \varphi_0 \quad \Rightarrow \quad -i\Phi_0(x^k) + i\Phi_0(x^l) = 2i\epsilon_{kl} \tau \varphi_0 \end{aligned} \quad (127)$$

with $N_{i*} \in \mathbb{Z}$ minimizing the electrostatic energy E_i , (100).

Due to the presence of the source term $i\mathcal{A}_J[\varphi] = -i\Phi^\alpha(x^i, t_1) + i\Phi^\beta(x^j, t_2)$ the instanton phase $\Phi_* = \Phi_0 + \delta\Phi_*$, (27), deviates from the mean-field by

$$\delta\Phi_*^\gamma(x^k, t) = D_{\Phi}^{\gamma\alpha}(t - t_1, x^k, x^i) - D_{\Phi}^{\gamma\beta}(t - t_2, x^k, x^j). \quad (128)$$

The instanton action thus reads

$$i\tilde{\mathcal{A}}_t[\varphi_*] = \sum_{kl} \sum_{\gamma\delta} \gamma\delta \int dt_3 dt_4 e^{-i\Phi_0(x^k)+i\Phi_0(x^l)} e^{-i\delta\Phi_*^\gamma(x^k,t_3)+i\delta\Phi_*^\delta(x^l,t_4)} \tilde{\Pi}_{kl}^{\gamma\delta}(t_3-t_4) \quad (129)$$

We will evaluate the time integrals in (126) and (129) approximately. They will be dominated by the singularities of the instanton and the polarization operators. To identify and characterize them more precisely it is indispensable to compute the phase correlator $D_\Phi \equiv -i \langle (\Phi - \Phi_0)(\Phi - \Phi_0) \rangle_0$. It will turn out that the singularities (branchcuts) of $\tilde{\Pi}_{kk}(t)$ around $t \sim 0$ and of $\tilde{\Pi}_{kl}(t)$, $k \neq l$, around $t \sim \pm\tau$ dominate all integrals.

4.3.4. Correlation Functions

In this section we calculate the correlation function of the tunneling phases $\Phi(x^i)$ which according to (122) is $D_\Phi = -\mathcal{D}_{+-} V \mathcal{D}_{+-}$. Details of the calculation are not important for the rest of the paper and may be safely skipped. The final results for zero temperature and the strong coupling limit, $\omega_C \tau \gg 1$, are

$$D_\Phi^{\geq}(t=0, x^i, x^j) = D_\Phi^{T/\tilde{T}}(0, x^i, x^j) \equiv D_\Phi(0; x^i, x^j) = A_{ij} \frac{i}{\nu^*} (\gamma + \ln[\omega_C \tau]) \quad (130)$$

and

$$D_\Phi^{\geq}(t, x^i, x^j) = A_{ij} \frac{i}{2\nu^*} \left\{ \ln \left[\frac{a \pm i(t-\tau)}{a \pm it} \right] + \ln \left[\frac{a \pm i(t+\tau)}{a \pm it} \right] \right\}. \quad (131)$$

for large times, $|\omega_C t| \gg 1$.

We start the computation by combining (118) and (123),

$$D_\Phi^r(\omega, x_i, x_j) = -\mathcal{D}_{+-}^r(\omega; x^i) V^r(\omega) \mathcal{D}_{+-}^r(\omega; x^j) = -i A_{ij} \frac{\pi}{\nu^*} \frac{i\omega_C (1 - e^{i\omega\tau})}{\omega [\omega + i\omega_C (1 - e^{i\omega\tau})]} (e^{i\omega\tau} - 1)$$

with $A_{ij} = \epsilon_i \epsilon_j$. In time representation the relevant correlation functions are the \geq -components which, at zero temperature, read

$$\begin{aligned} D_\Phi^{\geq}(t) &= \pm \int \frac{d\omega}{2\pi} e^{-i\omega t} [D_\Phi^r(\omega) - D_\Phi^a(\omega)] \theta(\pm\omega) \\ &= -A_{ij} \frac{i}{2\nu^*} \left\{ J^{\geq}(t-\tau) - J^{\geq}(t) + [J^{\geq}(-t^*-\tau)]^* - [J^{\geq}(-t^*)]^* \right\} \end{aligned} \quad (132)$$

$$\text{with } J^{\geq}(t) \equiv \int d\omega [\pm\theta(\pm\omega)] \frac{i\omega_C (1 - e^{i\omega\tau})}{\omega [\omega + i\omega_C (1 - e^{i\omega\tau})]} (e^{-i\omega t} - 1). \quad (133)$$

The integral defining $J^>$ ($J^<$) is perfectly convergent for all times with non-positive (non-negative) imaginary part, $\text{Im } t \leq 0$ ($\text{Im } t \geq 0$), thus ensuring the analyticity of J^{\geq} in this region. Apparently, we have $J^{\geq}(t)^* = J^{\leq}(t^*)$.

First, we perform the integration for $\text{Re } t < 0$. Under this assumption the contour of integration can be rotated into the upper half of the complex ω -plane where the integrand is analytic (see Fig. 12). Defining dimensionless time and charging frequency, $z \equiv -t/\tau$, and $y \equiv \omega_C \tau$, respectively, and integrating along the imaginary axis, one obtains for $y \gg 1$

$$\begin{aligned} J^{\geq}(t) &= \int_0^\infty ds (e^{-zs} - 1) \frac{y(1 - e^{-s})}{s[s + y(1 - e^{-s})]} \approx \int_0^\infty ds (e^{-zs} - 1) \frac{y}{s(s + y)} \\ &= -e^{yz} \Gamma(0, yz) - \gamma - \ln yz \equiv g(yz) \end{aligned} \quad (134)$$

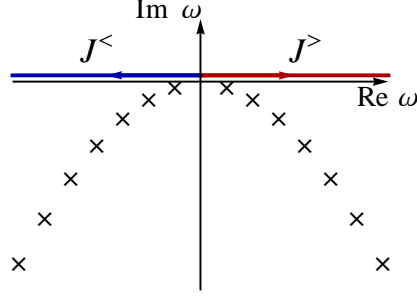


Figure 12: Analytic structure of the integrand in (133): it is analytic in the upper half of the ω -plane and possesses poles in the lower half. Contours of integration for $J^>$ and $J^<$ are indicated by arrows.

with the incomplete Gamma function $\Gamma(\alpha, x) = \int_x^\infty ds e^{-s} s^{\alpha-1}$, $x \in \mathbb{R}$, and the Euler-Mascheroni constant γ .

The asymptotic behavior of g is

$$\begin{aligned} g(yz) &\equiv (-1 + \gamma + \ln yz) yz, & yz &\rightarrow 0+, \\ &\rightarrow -\gamma - \ln yz - \frac{1}{yz}, & yz &\rightarrow \infty. \end{aligned} \quad (135)$$

We now proceed with the case $\text{Re } t > 0$ where the contour of integration can be rotated into the lower half of the complex plane ω -plane. In contrast to the previous case the integrand does possess poles in this region (see Fig. 12), around which, therefore, the integral has to be taken additionally. Since both pole and imaginary axis contribution, J_0^\geq and J_1^\geq respectively, separately diverge for large ω we have to introduce an auxiliary ultraviolet cutoff, $e^{\mp a\omega}$, $a = \tilde{a}\tau$. Then, defining $z \equiv t/\tau$, the imaginary axis contribution reads for $y = \omega_C \tau \gg 1$

$$J_1^\geq(t) = -y \int_0^\infty ds \frac{1 - e^s}{s[s - y(1 - e^s)]} (e^{-sz} - 1) e^{\pm is\tilde{a}} \approx \int_0^\infty ds \frac{e^{-sz} - 1}{s} e^{\pm is\tilde{a}} = -\ln \frac{\tilde{a} \pm iz}{\tilde{a}}.$$

The poles are defined as roots of equation $\omega + i\omega_C(1 - e^{i\omega\tau}) = 0$, $\omega \neq 0$, and writing $x = i\omega\tau$, they are given by $x_n = y - W_{-n}(ye^y)$, $n \in \mathbb{Z} \setminus \{0\}$, where the product log function is defined by $W_n(x)e^{W_n(x)} = x$. We choose the numbering such that $\text{Im } x_{n+1} > \text{Im } x_n$, $\text{Im } x_1 > 0 > \text{Im } x_{-1}$. As can be deduced already from the defining equation the roots satisfy $\text{Re } x_n \geq 0$. One may show that in two limiting cases one has

$$x_n \rightarrow 2\pi i n \frac{y}{1+y} + 2 \left(\frac{n\pi}{y} \right)^2, \quad |n| \ll \frac{y}{2\pi}, \quad (136)$$

$$\rightarrow 2\pi i n + \ln \left[-i \frac{2\pi n}{y} \right], \quad |n| \gg \frac{y}{2\pi}. \quad (137)$$

To proceed further, we note that $\frac{d}{d\omega} [\omega + i\omega_C(1 - e^{i\omega\tau})]_{\omega_n} = 1 + y - x_n$. Therefore the residues read

$$\text{Res}_{\omega_n} \left[\frac{i\omega_C(1 - e^{i\omega\tau})}{\omega[\omega + i\omega_C(1 - e^{i\omega\tau})]} (e^{-i\omega\tau} - 1) e^{\mp a\omega} \right] = -\frac{1}{1 + y - x_n} (e^{-zx_n} - 1) e^{\pm i\tilde{a}x_n}.$$

Taking into account that for $J^>$ ($J^<$) only poles ω_n with positive (negative) real part contribute, $n \geq 1$ ($n \leq -1$), we obtain for the pole contribution

$$J_0^\geq(t) = -\sum_{n=1}^{\infty} \frac{\mp 2\pi i}{1 + y - x_n} (e^{-zx_{\pm n}} - 1) e^{\pm i\tilde{a}x_{\pm n}}.$$

This expression cannot be evaluated analytically further, but analytical approximations are possible by substituting the poles x_n by their asymptotic behavior, Eqs. (136), (137).

We convince ourselves that the short-time divergence, which forced us to introduce the ultraviolet cutoff \tilde{a} , is in fact merely an artifact of our method of calculation, and is cured by taking the sum of $J_1^{\geq} + J_0^{\geq}$. In other words, J_0^{\geq} has to diverge logarithmically for $z \rightarrow 0$ as well. Of course, any divergence originates from terms with large $|n| \rightarrow \infty$, such that for our present purpose we may safely use the approximation (137) which yields for $z \rightarrow 0$

$$J_0^{\geq}(t) \sim - \sum_{n=1}^{\infty} \left[\left(\pm i \frac{2\pi n}{y} \right)^z e^{-2\pi n(\tilde{a} \pm iz)} - e^{-2\pi n\tilde{a}} \right] \frac{1}{n} \approx - \ln \frac{1 - e^{-2\pi\tilde{a}}}{1 - e^{-2\pi(\tilde{a} \pm iz)}} \approx \ln \frac{\tilde{a} \pm iz}{\tilde{a}},$$

which is exactly what we expected to find. Although the approximation is good enough to estimate the divergency, it is not reliable for obtaining finite offsets. Using $\ln \tilde{a} = \ln \frac{1 - e^{-2\pi\tilde{a}}}{2\pi}$ we can single out all \tilde{a} -dependencies,

$$J_0^{\geq}(t) + J_1^{\geq}(t) = - \ln [\pm 2\pi iz] - \sum_{n=1}^{\infty} \frac{\mp 2\pi i}{1 + y - x_{\pm n}} e^{-zx_{\pm n}} + \sum_{n=1}^{\infty} \left[\frac{\mp 2\pi i}{1 + y - x_{\pm n}} \left(e^{\pm i\tilde{a}(x_{\pm n} \mp 2\pi in)} - 1 \right) + \frac{x_{\pm n} \mp 2\pi in - 1 - y}{(1 + y - x_{\pm n})n} \right] e^{-2\pi\tilde{a}n}.$$

The \tilde{a} -contribution is just a constant about which we will not care too much presently. For the moment we will fix it manually, by requiring a good agreement between $J_0^{\geq}(t) + J_1^{\geq}(t)$ and the analytical continuation $g(-\omega_C(t \mp i0))$ of the result (134) obtained for $\text{Re } t < 0$. Fig. 13 shows the corresponding plots for $y = 5$ and $y = 25$.

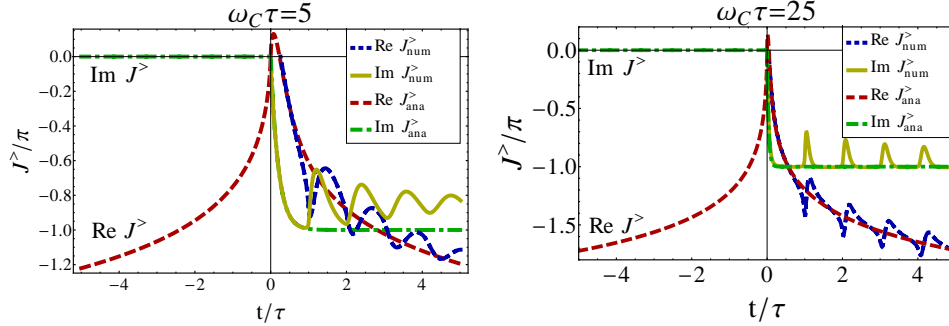


Figure 13: $J^>$ (real (blue) and imaginary (yellow) part), numerically evaluated and manually fixed, and analytical continuation $\sim g(-\omega_C(t - i0))$ (real (red) and imaginary (green) part).

A numerical study shows that the oscillating contributions decrease in width for large y (while their amplitude remains in the order of unity) and may be therefore neglected in the following. We approximate J^{\geq} by smooth functions g^{\geq} , required to be analytical for $\text{Im } t \leq 0$ ($\text{Im } t \geq 0$) and

$$g^{\geq}(t) = -e^{-\omega_C t} \Gamma(0, -\omega_C t) - \gamma - \ln[-\omega_C t], \quad \text{Re } t < 0.$$

Since the voltage is assumed to be low $|eV| \ll \omega_C$ one needs correlation functions for long times $|\omega_C t| \gg 1$ only and we can use the asymptotic expression (135) for g . Therefore introducing a short-time cutoff $a \sim \omega_C^{-1}$ and writing $t_{\mp} \equiv t \mp ia$ we use the following approximate relation in our subsequent analysis

$$J^{\geq}(t) \approx g^{\geq}(t) = -\gamma - \ln[-\omega_C t_{\mp}],$$

which together with (132) and $J^{\geq}(t = 0) = 0$ gives Eqs. (131) and (130).

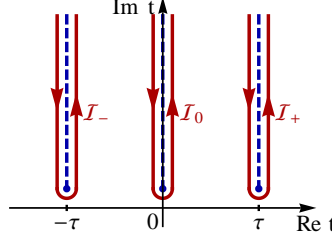


Figure 14: Analytic structure of \mathcal{I} in the complex t -plane: while the function is analytic in the lower half, it has poles or branchcuts in the upper half, residing at $t^* = 0, \tau, -\tau$. Integrating $\tilde{\Pi}_{kl}^{\geq}(t)$ “around” these, i.e. along drawn contours, gives $\tilde{P}_{kl}^{\geq}(t^*)$.

4.3.5. Renormalized Polarization Operators

In the real-time instanton approximation, Sect. 2.4, virtual fluctuations around the instanton are taken into account by dressing the tunneling polarization operators, Eq. (31). The phase factor is

$$e^{i[D_{\Phi\infty}^{\geq}(t, x_k, x_l) - D_{\Phi}(0)]} = e^{\frac{\gamma}{\nu^*}} (\omega_C \tau)^{\frac{1}{\nu^*}} \left[\frac{a \pm it}{a \pm i(t - \tau)} \right]^{\frac{A_{kl}}{2\nu^*}} \left[\frac{a \pm it}{a \pm i(t + \tau)} \right]^{\frac{A_{kl}}{2\nu^*}}.$$

and dressing of the bare polarization operators (119) yields (f_0 can be found in (5); χ is put to 0)

$$\begin{aligned} \tilde{\Pi}_{kl}^{\geq}(t) = & -r_k \bar{r}_l \frac{(\omega_C \tau)^{\frac{1}{\nu^*}}}{(2\pi)^2} e^{\frac{\gamma}{\nu^*}} e^{-i\epsilon_{kl}[2\pi\phi/\phi_0 + (\mu_+ + \mu_-)\tau]} e^{-ieVt} \\ & \times \begin{cases} [a \pm it]^{\frac{1}{\nu^*}-2} [a \pm i(t - \tau)]^{-\frac{1}{2\nu^*}} [a \pm i(t + \tau)]^{-\frac{1}{2\nu^*}}, & k = l, \\ [a \pm it]^{-\frac{1}{\nu^*}} [a \pm i(t - \tau)]^{\frac{1}{2\nu^*}-1} [a \pm i(t + \tau)]^{\frac{1}{2\nu^*}-1}, & k \neq l, \end{cases} \end{aligned}$$

The dressed polarization operators exhibit non-analytic behavior (poles or branchcuts) around $t \approx 0, \pm\tau$. The double time-integrals (126) and (129) can be approximately expressed in terms of the integrals $\tilde{P}_{kl}^{\geq} \equiv \int dt \tilde{\Pi}_{kl}^{\geq}(t)$. Before we demonstrate this statement in the next section, we will devote the remainder of the current section to the evaluation of \tilde{P}_{kl}^{\geq} .

We focus first on \tilde{P}_{kl}^{\geq} . To deal with both $k = l$ and $k \neq l$ simultaneously we generically consider the function

$$\begin{aligned} \mathcal{I}(t, eV) \equiv & e^{-ieVt} [a + it]^{\eta} [a + i(t - \tau)]^{\lambda} [a + i(t + \tau)]^{\lambda}, \\ & 0 > \eta > -2, \quad 0 > \lambda > -1, \quad 2\lambda + \eta = -2. \end{aligned}$$

Apparently, \mathcal{I} has branchcuts only in the upper half of the complex t -plane (Fig. 14), i.e. the integral $\int dt \mathcal{I}(t, eV)$ vanishes whenever the integration contour can be closed in the lower half. Therefore, we assume the nontrivial case $eV < 0$. The real-time integrals $\int dt \mathcal{I}(t, eV) = \mathcal{I}_- + \mathcal{I}_0 + \mathcal{I}_+$ consist of three contributions which correspond to integrals along closed contours in the complex t -plane. With $z \equiv |eV\tau| \gg 1$ the contour integral around $-\tau$ is

$$\mathcal{I}_- \approx -2\pi \frac{2^{\lambda}}{\Gamma(-\lambda)} e^{-iz} e^{i\frac{\pi}{2}\lambda} |eV| z^{-2-\lambda}.$$

Similarly, one obtains the integral around $+\tau$, $\mathcal{I}_+ = \mathcal{I}_-$.

The situation is slightly less trivial for the integral around $t \approx 0$, since it may be that $\eta = -1$, i. e. we have a first order pole, or $\eta > -1$, giving rise to a strong divergence. In the first case the integral gives

$$\mathcal{I}_0 = 2\pi [a - i\tau]^{\lambda} [a + i\tau]^{\lambda} \approx \frac{2\pi}{\tau}.$$

In the second case we have to go around the singularity with care. We explicitly kept the distance $\delta \ll a$ to the integration contour from the branchcut in the calculations. After weakening the degree of divergence by partial integration we may safely put $\delta \rightarrow 0$ and obtain

$$\mathcal{I}_0 \approx 2\pi\Gamma(-\eta)^{-1}|eV|z^{2\lambda}.$$

Note that in this approximation \mathcal{I}_0 is continuous in $\eta = -1$.

For the direct terms, $k = l$, we have $\eta = \frac{1}{\nu^*} - 2$, $\lambda = -\frac{1}{2\nu^*}$, i. e. $\eta + \lambda = \frac{1}{2\nu^*} - 2$, $2\lambda = -\frac{1}{\nu^*}$, hence for large voltages, $z \gg 1$, \mathcal{I}_0 is dominant. For the interference terms, $k \neq l$, we set $\eta = -\frac{1}{\nu^*}$, $\lambda = \frac{1}{2\nu^*} - 1$, i. e. $\eta + \lambda = -\frac{1}{2\nu^*} - 1$, $2\lambda = \frac{1}{\nu^*} - 2$, hence the contributions \mathcal{I}_{\pm} dominate over \mathcal{I}_0 if and only if $\nu^* > \frac{3}{2}$.

As $\int dt \mathcal{I}(t, eV)$ splits into three contributions, so do $\tilde{P}_{kl}^{\geq} = \tilde{P}_{kl}^{\geq}(-\tau) + \tilde{P}_{kl}^{\geq}(0) + \tilde{P}_{kl}^{\geq}(+\tau)$. Note that $\tilde{\Pi}^<(t) = \tilde{\Pi}^>(-t) \Big|_{eV \mapsto -eV}$ implies $\tilde{P}_{kl}^<(t^*) = \tilde{P}_{kl}^>(-t^*) \Big|_{eV \mapsto -eV}$.

Summarizing, for $z \gg 1$ the dominant integrals of the dressed polarization operators are

$$\tilde{P}_{kk}^{\geq}(t^* = 0) = -\theta(\mp eV) \frac{|eV|}{2\pi} R_{k*}(eV), \quad (138)$$

$$\tilde{P}_{kl}^{\geq}(t^* = \kappa\tau) = -\theta(\mp eV) \frac{1}{2\pi\tau} R_{12*}(eV) \frac{1}{2} e^{i\kappa[|eV\tau| - \frac{\pi}{2}(1 + \frac{1}{2\nu^*})]} e^{-i\epsilon_{kl}[2\pi\phi/\phi_0 + (\mu_+ + \mu_-)\tau]}, \quad (139)$$

$$\tilde{P}_{kl}^{\geq}(t^* = 0) = -\theta(\mp eV) \frac{1}{2\pi\tau} r_k \bar{r}_l |eV\tau|^{\frac{1}{\nu^*}-1} \frac{(\omega_C\tau)^{\frac{1}{\nu^*}} e^{\frac{\gamma}{\nu^*}}}{\Gamma(\frac{1}{\nu^*})} e^{-i\epsilon_{kl}[2\pi\phi/\phi_0 + (\mu_+ + \mu_-)\tau]} \quad (140)$$

with $k \neq l$, $\kappa = \pm$. In case of $\nu^* > \frac{3}{2}$ the contribution (139) is dominant, while in the case $\nu^* < \frac{3}{2}$ it is (140). We have used definitions (96) of the renormalized reflection coefficients and assumed for simplicity $r_1 \bar{r}_2$ to be real.

4.3.6. Instanton Action and Current

We have now everything in place to finalize the calculation of the instanton action (129) and the current (126). The instanton phases $\delta\Phi_*^\gamma(x^k, t) = D_\Phi^{\gamma\alpha}(t - t_1, x^k, x^i) - D_\Phi^{\gamma\beta}(t - t_2, x^k, x^j)$ and thus $i\tilde{\mathcal{A}}_t[\varphi_*]$ are functions of the times t_1, t_2 over which to integrate in (126). A shift of integration variables $t_{3/4} \mapsto t_{3/4} + t_2$ in (129) immediately shows that the action $i\tilde{\mathcal{A}}_t[\varphi_*]$ is a function of the difference $t \equiv t_1 - t_2$. Hence, the whole integrand of (126) is purely a function of $t = t_1 - t_2$. Performing a change of integration variables $(t_1, t_2) \mapsto (t = t_1 - t_2, T = (t_1 + t_2)/2)$, the integral over the center-of-mass time T is seemingly divergent. This simply amounts to infinite transferred charge $Q = \int_0^{t_0} dT I$ for a steady current I and an infinite measuring time $t_0 \rightarrow \infty$. Since our interest lies in the steady current (not on transient effects due to switching of the measuring device) we identify $\int dt_1 dt_2 = \int dT dt = t_0 \int dt$ upon which the current becomes

$$I_{ij}^{\alpha\beta} = e \int dt e^{i\tilde{\mathcal{A}}_t[\varphi_*]} \Big|_{t_1 - t_2 = t} e^{2i\epsilon_{ij}\tau\varphi_0} \tilde{\Pi}_{ij}^{\alpha\beta}(t) \Big|_{\chi=0}. \quad (141)$$

Given that $i\tilde{\mathcal{A}}_t[\varphi_*]$ is non-divergent, large contributions to this current stem from the singularities of $\tilde{\Pi}_{ij}^{\alpha\beta}(t)$ which we identified in the previous section. The case $\nu^* = 1$, i.e. $\nu^* < \frac{3}{2}$, needs to be treated more carefully and will be considered towards the end of this section. Focussing for now on $\nu^* \geq 2$, dominant contributions are then

$$e^{-1} I_{ij}^{\alpha\beta} \approx \begin{cases} e^{i\tilde{\mathcal{A}}_t[\varphi_*]} \Big|_{t_1 - t_2 \approx 0} \tilde{P}_{ii}^{\alpha\beta}(t^* = 0), & i = j, \\ e^{i\tilde{\mathcal{A}}_t[\varphi_*]} \Big|_{|t_1 - t_2| \approx \tau} e^{2i\epsilon_{ij}\tau\varphi_0} \left(\tilde{P}_{ij}^{\alpha\beta}(t^* = +\tau) + \tilde{P}_{ij}^{\alpha\beta}(t^* = -\tau) \right), & i \neq j. \end{cases} \quad (142)$$

We evaluate the t_3, t_4 -integrals in (129) using a similar approximation scheme. Within the given constraints $t_1 - t_2 \approx 0$ for $i = j$ and $|t_1 - t_2| \approx \tau$ for $i \neq j$, the singularity of

$$\tilde{\Pi}_{kk}(t_3 - t_4) \sim \frac{1}{(t_3 - t_4)^{2-1/\nu^*}}$$

dominates over the ones of

$$\tilde{\Pi}_{kl}(t_3 - t_4) \sim \frac{1}{[(t_3 - t_4 - \tau)(t_3 - t_4 + \tau)]^{1-1/2\nu^*}}, \quad k \neq l,$$

and of the instantons

$$\begin{aligned} e^{i\delta\Phi_*(x^k, t' + t_2)} &= e^{iD_\Phi(t' - t_1 + t_2, x^k, x^i) - iD_\Phi(t', x^k, x^j)} \\ &\sim \left(\frac{(t' - t_1 + t_2)^2}{(t' - t_1 + t_2 - \tau)(t' - t_1 + t_2 + \tau)} \right)^{A_{ki}/2\nu^*} \left(\frac{(t' - \tau)(t' + \tau)}{t'^2} \right)^{A_{kj}/2\nu^*}. \end{aligned}$$

Hence, again transforming to relative and center-of-mass times, $t = t_3 - t_4$, $T = (t_3 + t_4)/2$, the dominant contribution to the instanton action stems from the $t \approx 0$ -singularity of $\tilde{\Pi}_{kk}(t)$:

$$\begin{aligned} i\tilde{\mathcal{A}}_t[\varphi_*] &\approx \sum_{k=1,2} \sum_{\gamma, \delta=\mp} \gamma\delta \int dt \tilde{\Pi}_{kk}^{\gamma\delta}(t) \int dT e^{-i\delta\Phi_*^\gamma(x^k, T) + i\delta\Phi_*^\delta(x^k, T)} \\ &= - \sum_{k=1,2} \sum_{\gamma \neq \delta} \int dt \tilde{\Pi}_{kk}^{\gamma\delta}(t) \int dT \left(e^{iJ^{\gamma\delta}(T)} - 1 \right) \quad \text{with } J^{\gamma\delta}(T) = -\delta\Phi_*^\gamma(x^k, T) + \delta\Phi_*^\delta(x^k, T) \\ &\approx \sum_{k=1,2} \sum_{\gamma \neq \delta} \tilde{P}_{kk}^{\gamma\delta}(t^* = 0) \int dT \left(e^{iJ^{\gamma\delta}(T)} - 1 \right). \end{aligned}$$

The second equality follows from $\tilde{\Pi}_{kl}^>(t) + \tilde{\Pi}_{kl}^<(t) = \tilde{\Pi}_{kl}^T(t) + \tilde{\Pi}_{kl}^{\tilde{T}}(t)$. The integrals $\tilde{P}_{kl}^{\gamma\delta} = \int dt \tilde{\Pi}_{kl}^{\gamma\delta}(t)$ have been studied in the previous section.

Using the definition (128) of the instanton and the relation $(D_\Phi^T - D_\Phi^>)(t, x^k, x^l) = (D_\Phi^< - D_\Phi^{\tilde{T}})(t, x^k, x^l) = A_{kl} \frac{\pi}{\nu^*} \theta(-t) \theta(t + \tau)$ one obtains (independent of α and β !)

$$J^{\geq}(T) = \pm \frac{\pi}{\nu^*} [A_{ki} \theta(t_1 - T) \theta(T - t_1 + \tau) - A_{kj} \theta(t_2 - T) \theta(T - t_2 + \tau)] \quad (143)$$

With constraints $|t_1 - t_2| \ll \tau$ for $i = j$ and $|t_1 - t_2| = \tau$ for $i \neq j$ (cf. Eq. (142)), the instanton action thus reads

$$i\tilde{\mathcal{A}}_t[\varphi_*] = \begin{cases} -|t_1 - t_2|/\tau_\varphi, & i = j \\ -\tau/\tau_\varphi - ieV\tau\epsilon_{ij}(R_{1*}(eV) - R_{2*}(eV))\pi^{-1} \sin \frac{\pi}{\nu^*}, & i \neq j \end{cases} \quad (144)$$

with dephasing rate

$$\tau_\varphi^{-1} = -4 \sin^2 \frac{\pi}{2\nu^*} \sum_{k=1,2} \left(\tilde{P}_{kk}^>(0) + \tilde{P}_{kk}^<(0) \right) \quad (145)$$

which due (138) to becomes the expression (95) in the limit $|eV\tau| \gg 1$, see Fig. 15. The purely imaginary contributions to (144) correspond to (perturbatively small) renormalization corrections to bias voltage and will be neglected further on. We will also neglect the instanton action for $i = j$.

Combining these results with (142) we obtain for the incoherent and interference corrections to current due to tunneling

$$\Delta I_{\text{inc}} = I_{11} + I_{22} = -\frac{e^2}{2\pi} (R_{1*}(eV) + R_{2*}(eV)) V, \quad (146)$$

$$I_{AB} = -\frac{e}{\pi\tau} R_{12*}(eV) \text{sign } V e^{-\tau/\tau_\varphi} \sin(|eV\tau| - \pi/4\nu^*) \cos \varphi_{AB} \quad (147)$$

with Aharonov-Bohm phase

$$\varphi_{AB} = 2\pi\phi/\phi_0 + (\mu_+ + \mu_-)\tau - 2\tau\varphi_0 \quad (148)$$

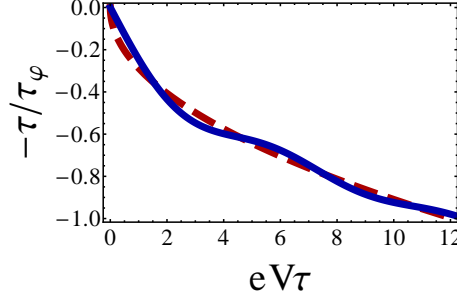


Figure 15: Dephasing rate as a function of source-drain voltage shown for $\nu^* = 2$, $\omega_C\tau = 25$ and $R_{1*}(\epsilon_{\text{th}}) = R_{2*}(\epsilon_{\text{th}}) = 0.2$. The solid line gives the numerical result for (145). The dashed line is the power-law asymptotic given by Eq. (95).

which in the limit $\omega_C\tau \gg 1$ gives (99). For large bias, $\omega_C \gg |eV| \gg \epsilon_{\text{th}}$, this yields the dimensionless conductances given in (92) and (93).

Concluding this section we turn to the case $\nu^* = 1$. According to Eq. (140) the dominant contribution to current is

$$e^{-1} I_{ij}^{\alpha\beta} \approx e^{i\tilde{\mathcal{A}}_t[\varphi_*]} \Big|_{t_1-t_2 \approx 0} e^{2i\epsilon_{ij}\tau\varphi_0} \tilde{P}_{ij}^{\alpha\beta}(t^* = 0). \quad (149)$$

The $i \neq j$ -contribution of Eq. (142) is also present, but subleading. The instanton action $i\tilde{\mathcal{A}}_t[\varphi_*]$ can be evaluated following the same line of reasoning as for $\nu^* \geq 2$, yielding $i\tilde{\mathcal{A}}_t[\varphi_*] = -|t_1 - t_2|/\tau_\varphi$ which can be neglected. The dominant contribution to current is thus

$$I_{\text{AB}}^{\nu^*=1} = -\frac{e}{\pi\tau} r_1 \bar{r}_2 \omega_C \tau e^\gamma \cos \varphi_{\text{AB}}.$$

In the limit $\omega_C\tau \gg 1$ its bias dependence is negligible, in contrast to the contribution I_{AB} , Eq. (147). Therefore, while the latter is subleading in *current* for $\nu^* = 1$, it yields the leading contribution to *conductance*: $g_{\text{AB}} = \partial I_{\text{AB}}^{\nu^*=1}/\partial V + \partial I_{\text{AB}}/\partial V \approx \partial I_{\text{AB}}/\partial V$, i.e. giving the previous result (93).

5. Summary and Outlook

In this article, we have developed a general theoretical framework for investigation of electronic properties of a broad class of nonequilibrium nanostructures consisting of one-dimensional channels coupled by tunnel junctions and/or by impurity scattering. Our formalism is based on nonequilibrium version of functional bosonization.

We have derived a nonequilibrium (Keldysh) action for this class of systems, Eq. (12), that has a form reminiscent of the theory of full counting statistics. In order to make the further analytical progress possible, we have developed a method based on a combination of a weak-tunneling approximation and an instanton (saddle-point) approach.

We have supplemented a detailed exposition of the formalism by two important applications: (i) tunneling spectroscopy of a biased Luttinger liquid with an impurity, and (ii) nonequilibrium quantum Hall Fabry-Pérot interferometry. One more application, quantum Hall Mach-Zehnder interferometry, has been presented recently by two of us with Schneider in a separate publication, Ref. [48].

The developed Keldysh-action formalism has allowed us to explore the rich interaction-induced physics of all the above problems, which includes, in particular, renormalization and dephasing far from equilibrium as well as an oscillatory voltage dependence of visibility of Aharonov-Bohm oscillations (“lobe structure”). The theoretical results are in good agreement with experiments on Fabry-Pérot and Mach-Zehnder interferometers.

We close the paper by identifying future research perspectives; a work in some of these directions is currently underway.

- (i) It is important to see under what conditions and how can one proceed in a controllable way
- (ii) A further important direction is the analysis of asymptotic behavior of relevant types of Fredholm determinants. Recently, such an analysis has been carried out for Toeplitz determinants arising in the problem of nonequilibrium Luttinger liquids and related models [53]. Required generalizations include, in particular, block Toeplitz determinants which arise naturally in the case of models with several channels coupled by tunneling.
- (iii) One of prospective applications of our formalism is related to edge states of quantum spin Hall topological insulators. Of great interest is a generalization on setups based on fractional quantum Hall (or, more generally, fractional topological insulator) edge states.

6. Acknowledgements

We thank S.T. Carr, L.I. Glazman, I.V. Gornyi, M. Heiblum, A. Kamenev, N. Ofek, D.G. Polyakov, and B. Rosenow for useful discussions. This work was supported by the German-Israeli Foundation and by the Deutsche Forschungsgemeinschaft via CFN and SFB/TR 12.

Appendix A. Derivation of Keldysh Action

The first two Appendices, Appendix A and Appendix B, are devoted to the proof of (12) and more specifically to the calculation of the Jacobian $J[\varphi, \psi, \bar{\psi}]$ corresponding to the gauge transformation $\psi_\mu^\mp \rightarrow e^{i\Theta_\mu^\mp} \psi_\mu^\mp$ with (2). Since this is a linear transformation in $\psi, \bar{\psi}$, its Jacobian is independent of $\psi, \bar{\psi}$ and can be therefore computed as

$$J[\varphi] \equiv e^{i\mathcal{A}_f[\varphi]} \equiv \int \mathcal{D}(\psi, \bar{\psi}) e^{i\mathcal{A}[\varphi, \psi, \bar{\psi}]} = \text{Tr} \left\{ \hat{\rho}_0 \hat{U}[\varphi^+]^\dagger \hat{U}[\varphi^-] \right\} \quad (\text{A.1})$$

with density operator $\hat{\rho}_0$ and the (many-particle) time evolution operators $\hat{U}[\varphi^\mp]$. The latter describes any *single-particle* dynamics the electrons undergo in the system *and the leads* (see Fig. A.16), say scattering and propagation through time-dependent potentials $\varphi^\alpha(t)$. These potentials may have a non-trivial Keldysh structure, thus the superindex $\alpha = \mp$ which refers to the forward/backward branch of the Keldysh contour, respectively.

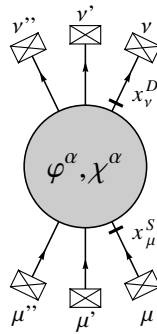


Figure A.16: Sketch of the system (shaded blob) which is connected to reservoirs (rectangles) via source (drain) leads, depicted by incoming (outgoing) lines. The leads μ (ν) enter (leave) the systems at contact positions x_μ^S (x_ν^D).

Appendix A.1. Integrating out Fermions with Klich's Formula

There are several ways to evaluate the many-particle trace (A.1). Here we employ an approach that generalizes a derivation of the full counting statistics in Ref. [7]. In Appendix B we present an alternative derivation which keeps closely to the spirit of Ref. [8] where an analogous action was derived for the case of a single compact scatterer.

A central mathematical statement proven in Ref. [7] relates traces of certain *many*-particle operators with determinants of associated *single*-particle operators. We denote the (many-particle) Fock space representation of single-particle operators C by $\Gamma(C) \equiv \sum c_i^\dagger \langle i | C | j \rangle c_j$. Here, $\{|i\rangle\}_i$ is some single-particle basis, and c_i (c_i^\dagger) annihilates (creates) an electron in state $|i\rangle$. Then, the following identity holds:

$$\text{Tr} \left(e^{\Gamma(A_1)} \dots e^{\Gamma(A_n)} \right) = \det \left(\mathbb{1} + e^{A_1} \dots e^{A_n} \right). \quad (\text{A.2})$$

To proceed we write the density operator in the form

$$\hat{\rho}_0 = \frac{e^{\Gamma(F)}}{\det(\mathbb{1} + e^F)} \quad (\text{A.3})$$

where the single-particle operator $F = \sum \alpha_i N_i$ is a suitable linear combination of (single-particle!) “number operators” $N_i = |i\rangle \langle i|$ in the reservoirs. E.g. in thermal equilibrium $F = -\beta H_0$ with some appropriate Hamiltonian $H_0 = \sum \epsilon_i N_i$. The many-particle time-evolution operator is canonically discretized as

$$\hat{U}[\varphi^\alpha] = \text{Texp} \left[-i \int_{-\infty}^{\infty} dt \hat{H}[\varphi^\alpha(t)] \right] = \lim_{\substack{\Delta t \rightarrow 0 \\ N \rightarrow \infty}} \prod_{i=1}^N e^{-i \Delta t \Gamma(H[\varphi^\alpha(t_i)])}.$$

Hence, Eq. (A.1) is a trace over a (infinite) product of operator exponentials which, according to (A.2), is

$$\begin{aligned} J[\varphi] &= \frac{\text{Tr} \left[e^{\Gamma(F)} \hat{U}[\varphi^+]^\dagger \hat{U}[\varphi^-] \right]}{\det(\mathbb{1} + e^F)} = \frac{\det(\mathbb{1} + e^F U[\varphi^+]^\dagger U[\varphi^-])}{\det(\mathbb{1} + e^F)} \\ &= \det(\mathbb{1} + f (U[\varphi^+]^\dagger U[\varphi^-] - \mathbb{1})) \end{aligned} \quad (\text{A.4})$$

with the single-particle time-evolution operator $U[\varphi^\alpha]$ (not to be confused with $\hat{U}[\varphi^\alpha]$) and the occupation number operator $f = [\mathbb{1} + e^{-F}]^{-1}$.

Appendix A.2. Wave packet representation

In a next step, we follow Landauer's original idea[55] and represent the time-evolution operators with respect to the wave packet bases, relating them to the single-particle scattering matrices. Using a more compact notation for the single-particle time-evolution operator

$$U^\alpha(t_1, t_0) = \text{Texp} \left[-i \int_{t_0}^{t_1} dt H[\varphi^\alpha(t)] \right], \quad t_0 < t_1,$$

(hence $U[\varphi^\alpha] = U^\alpha(\infty, -\infty)$), Eq. (A.4) can be brought into the form

$$J[\varphi] = \lim_{t_\pm \rightarrow \pm\infty} \det \left\{ \mathbb{1} + f \left[U^+(t_+, t_-)^\dagger U^-(t_+, t_-) - \mathbb{1} \right] \right\}. \quad (\text{A.5})$$

We fix some time-independent reference Hamiltonian, say $H_0 \equiv H[\varphi \equiv 0]$, which contains the lead kinematics as well as scattering, but no interaction or current counting. Then the incoming/outgoing scattering states with respect to H_0 form two natural bases of the single-particle Hilbert space, see Fig. A.17. Each state is characterized by its energy ϵ and the lead μ through which it enters/leaves the system: $H_0 |\epsilon\mu\rangle^{\text{in/out}} = \epsilon |\epsilon\mu\rangle^{\text{in/out}}$. The two bases are hence $(|\epsilon\mu\rangle^{\text{in}})_{\epsilon;\mu}$ and $(|\epsilon\mu\rangle^{\text{out}})_{\epsilon;\mu}$.

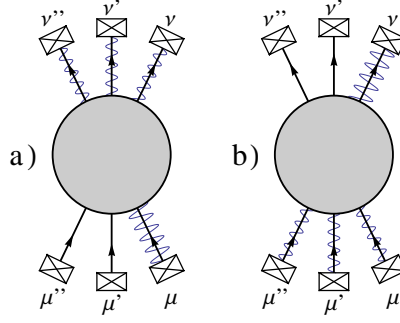


Figure A.17: (a) Spatial distribution of incoming scattering state $|\epsilon\mu\rangle^{\text{in}}$ (wavy lines). It extends in source lead μ and arbitrary drain leads ν , but in no other source leads. (b) Spatial distribution of outgoing scattering state $|\epsilon\nu\rangle^{\text{out}}$ (wavy lines). It extends in drain lead ν and arbitrary source leads μ , but in no other drain leads.

For the sake of argument we will assume the lead channels μ to be one-dimensional (1D), semi-infinite and non-dispersive with constant velocity v_μ . We use the convention $v_\mu > 0$, i.e. for source channels $-\infty < x < x_\lambda^S$ and for drain channels $x_\lambda^D < x < \infty$, and choose the normalization such that ${}^{\text{in/out}}\langle\epsilon'\mu'|\epsilon\mu\rangle^{\text{in/out}} = \delta_{\mu\mu'}\delta(\epsilon - \epsilon')$ is satisfied.

The incoming state $|\epsilon\mu\rangle^{\text{in}}$ is a *plane wave* in source lead μ and spreads into drain leads ν . It vanishes in all other source leads μ' : ${}^{\text{in}}\langle x\mu'|\epsilon\mu\rangle^{\text{in}} = \delta_{\mu'\mu} \frac{1}{\sqrt{2\pi v_\mu}} e^{i\epsilon x/v_\mu}$ (where $|x\mu\rangle$ is the eigenstate of the position operator in channel μ). Analogous statements hold for the outgoing states.

Let us now construct the incoming (outgoing) wave packet basis at reference time t_- (t_+). For that we define

$$|t\mu\rangle^{\text{in}} \equiv \int \frac{d\epsilon}{\sqrt{2\pi}} e^{i\epsilon(t-t_- - x_\mu^S/v_\mu)} |\epsilon\mu\rangle, \quad |t\lambda\rangle^{\text{out}} \equiv \int \frac{d\epsilon}{\sqrt{2\pi}} e^{i\epsilon(t-t_+ - x_\lambda^D/v_\lambda)} |\epsilon\lambda\rangle.$$

Note that t is not a parameter which describes the time-evolution of a state “ $|\mu\rangle$ ” but labels the state $|t\mu\rangle$ similar to ϵ in $|\epsilon\mu\rangle$. The two new bases are thus $(|t\mu\rangle^{\text{in}})_{t;\mu}$ and $(|t\mu\rangle^{\text{out}})_{t;\mu}$.

To shed light on the meaning of label t , we study the time-evolution of the newly constructed states with respect to the reference Hamiltonian H_0 . For time t' one has

$${}^{\text{in}}\langle x\mu'|e^{-iH_0(t'-t_-)}|t\mu\rangle^{\text{in}} = \delta_{\mu'\mu} \sqrt{v_\mu} \delta(x - x_\mu^S + v_\mu(t - t')).$$

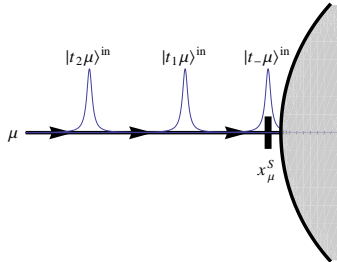


Figure A.18: Zoom into source lead μ : Sketch of spatial distribution of wave packet states $|t_-\mu\rangle^{\text{in}}$, $|t_1\mu\rangle^{\text{in}}$, $|t_2\mu\rangle^{\text{in}}$ with $t_2 > t_1 > t_-$.

This is a wave packet in source channel μ which propagates towards contact x_μ^S , arriving there at time t , see Fig. A.18. After entering the system it may split and spread in some complicated way. Similarly, the outgoing state $|t\lambda\rangle^{\text{out}}$ may be distributed in some complicated manner inside the system, however tuned

such that at time t it arrives at drain contact x_λ^D and continues propagation as a single wave packet in drain channel λ . Summarizing,

$$e^{-iH_0(t-t_-)} |t\mu\rangle^{\text{in}} \equiv \sqrt{v_\mu} |x_\mu^S\rangle, \quad e^{-iH_0(t-t_+)} |t\lambda\rangle^{\text{out}} \equiv \sqrt{v_\lambda} |x_\lambda^D\rangle \quad (\text{A.6})$$

are wave packets residing at contacts x_μ^S , x_λ^D , and thus being independent of t_\mp and t .

Making the assumption that interaction, counting etc. is switched on and off adiabatically such that $H(t') = H_0$ for $t' \notin [t_-, t_+]$, we now argue that the same simple relations hold when taking the full Hamiltonian $H(t)$ into account,

$$U^\alpha(t, t_-) |t\mu\rangle^{\text{in}} = \sqrt{v_\mu} |x_\mu^S\rangle, \quad U^\alpha(t, t_+) |t\lambda\rangle^{\text{out}} = \sqrt{v_\lambda} |x_\lambda^D\rangle. \quad (\text{A.7})$$

These relations are a direct consequence of (A.6) and the fact that potential φ^α is restricted spatially and temporally: For $t > t' > t_-$ incoming wave packet $U(t', t_-) |t\mu\rangle$ is completely contained in the source lead where we assume φ^α to be absent. For $t < t' < t_-$ potential $\varphi^\alpha(t')$ is again ineffective since not switched on yet. Therefore, $U(t, t_-) |t\mu\rangle^{\text{in}} = e^{-iH_0(t-t_-)} |t\mu\rangle$ for all t . The reasoning is analogous for outgoing states.

We are now able to give the operator $fU^+(t_+, t_-)^\dagger U^-(t_+, t_-)$ in the wave-packet representation. For source channels μ, μ' the matrix elements read

$$\begin{aligned} &^{\text{in}}\langle t\mu | fU^+(t_+, t_-)^\dagger U^-(t_+, t_-) | t'\mu' \rangle^{\text{in}} \\ &= \sum_{\mu''} \int dt'' f_{\mu\mu''}(t, t'') \sum_\lambda \int dt''' ^{\text{in}}\langle t''\mu'' | U^+(t_+, t_-)^\dagger | t'''\lambda \rangle^{\text{out}} ^{\text{out}}\langle t'''\lambda | U^-(t_+, t_-) | t'\mu' \rangle^{\text{in}}. \end{aligned} \quad (\text{A.8})$$

Since the leads are populated by the reservoirs such that the occupation number of the *incoming* states is fixed, $^{\text{in}}\langle \epsilon\mu | f | \epsilon'\mu' \rangle^{\text{in}} = \delta_{\mu\mu'} \delta(\epsilon - \epsilon') f_\mu(\epsilon)$, the distribution function in time domain simplifies to

$$f_{\mu\mu'}(t, t') \equiv \langle t\mu | f | t'\mu' \rangle = \delta_{\mu\mu'} \int \frac{d\epsilon}{2\pi} e^{-i\epsilon(t-t')} f_\mu(\epsilon).$$

The matrix elements of the time-evolution operator further reduce to

$$^{\text{out}}\langle t\lambda | U(t_+, t_-) | t'\mu \rangle^{\text{in}} = ^{\text{out}}\langle t\lambda | U(t_+, t) U(t, t') U(t', t_-) | t'\mu \rangle^{\text{in}} = \sqrt{v_\lambda v_\mu} \langle x_\lambda^D | U(t, t') | x_\mu^S \rangle \equiv S_{\lambda\mu}(t, t') \quad (\text{A.9})$$

which defines the scattering matrix $S = S[\varphi]$.

In the wave-packet representation Eq. (A.5) can be written

$$J[\varphi] = e^{i\mathcal{A}_f[\varphi]} = \det [\mathbb{1} - f + S^{+\dagger} S^- f]$$

where the determinant is to be taken with respect to source lead indices and arrival times. The log of this determinant appears in our general result stated in Eq. (12). The retarded and advanced part of polarization operator which are present in Eq. (12) are not reproduced within the method of this section since they represent itself the quantum anomaly. Their structure does not depend on the actual nonequilibrium state of the system and can be deduced from the analysis of the fermion action in the absence of tunneling as it was discussed in section 2.1.

Appendix A.3. Construction of Scattering Matrix

According to (A.9) the scattering matrix element $S_{\lambda\mu}(t, t')$ is the transition amplitude for a peak residing in the (incoming) lead μ at time t' to a peak residing in the (outgoing) lead λ at time t . One expects that it is the summed amplitude for all possible trajectories which connect μ with λ . We will briefly demonstrate this assuming that the scatterer is a network of simple blocks which are connected to each other via “interface channels” which may be “outgoing” with respect to one block and “incoming” with respect to a neighboring one. The electronic state residing in the interface channel λ is denoted by $|x_\lambda\rangle$. It corresponds to a wave packet which is leaving one of the blocks and about to enter another one. We further assume that the blocks

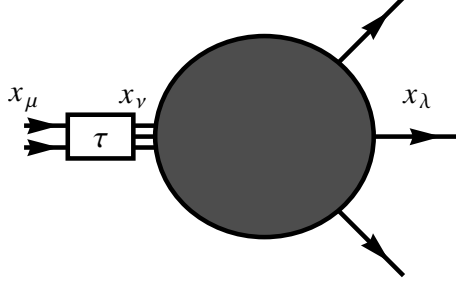


Figure A.19: Sketch of the system: A block characterized by the dwell time τ is connected to some part of the system (the shaded blob) via interface states $|x_\nu\rangle$.

be simple enough such that each of them can be characterized by a unique dwell time τ (possibly different for each block), i.e. a wave packet which enters the block at time t will definitely leave it at (exactly) $t + \tau$, through whatever channel: $U(t + \tau, t) |x_i\rangle = \sum_f u_{fi}(t) |x_f\rangle$ where $|x_i\rangle$ is an incoming interface state and the sum extends over outgoing interface states $|x_f\rangle$. This defines the functions $u_{fi}(t)$ and the scattering matrix elements

$$s_{fi}(t', t) \equiv \delta(t' - t - \tau) \sqrt{\frac{v_i}{v_f}} u_{fi}(t) \quad (\text{A.10})$$

where we have assigned a characteristic velocity v_λ to each interface channel λ . The full scattering matrix $S_{\lambda\mu}(t', t)$ can be constructed out of elements $s_{fi}(t', t)$ with the use of following decomposition property. Consider the situation sketched at Fig. A.19. Because of the decomposition property $U(t', t) = U(t', t + \tau)U(t + \tau, t)$ of the time-evolution operator, the amplitude for the transition from a peak at t in channel μ to one at t' in λ is

$$\sqrt{v_\lambda v_\mu} \langle x_\lambda | U(t', t) | x_\mu \rangle = \sum_\nu \int dt'' \sqrt{v_\lambda v_\mu} \langle x_\lambda | U(t', t'') | x_\nu \rangle s_{\nu\mu}(t'', t). \quad (\text{A.11})$$

Obviously, the inner transition amplitude can be decomposed further in the same manner, and the full scattering matrix element $S_{\lambda\mu}$ turns out to be the sum of amplitudes $A_{\lambda\mu}^{(p)}$, each of them corresponding to a possible path p connecting the incoming state μ with the outgoing one λ . As p passes through a certain number of building blocks, $A_{\lambda\mu}^{(p)}$ is the product of the blocks' scattering matrix elements. For completeness we note that, since each trajectory will end in the outgoing leads, each decomposition will end with

$$\sqrt{v_{\lambda'} v_\lambda} \langle x_{\lambda'} | U(t', t) | x_\lambda \rangle = \delta(t' - t) \delta_{\lambda'\lambda} \quad (\text{A.12})$$

for $\lambda, \lambda' \in \text{out}$.

Simple blocks

Having convinced ourselves of the usefulness of definition (A.10) we turn to simple two examples of building blocks: wires with fluctuating potentials and point scatterers. Simple as they are, a broad class of devices, including quantum wire junctions and electronic interferometers, can be modeled as a network of these construction units, and in the following we will restrict ourselves to such systems.

The corresponding scattering matrices are found by considering the time-evolution of wave packets $\psi(t, x) \equiv \langle x | U(t, t_0) | x_i \rangle$ which satisfy the Schrödinger equation

$$i\partial_t \psi(t) = H(t) \psi(t), \quad \text{with initial condition } \psi(t_0, x) = \delta(x - x_i). \quad (\text{A.13})$$

We list the results here, giving all necessary definitions in the subsequent paragraphs:

Construction unit		Scattering matrix
Chiral wire	$x_i \xrightarrow{\varphi} x_f$	$\mathcal{M}^\alpha(t', t) = e^{i\vartheta_{fi}^\alpha(t')} \Delta(t', t)$
Point scatterer	$i \rightarrow \text{---} \circ \text{---} f$ s_{fi}	$s_{fi}(t', t) = s_{fi} \delta(t' - t)$

Chiral wire with fluctuating potential. A possible block is a chiral non-dispersive wire where fermions propagate with constant velocity v in a fluctuating potential $\varphi^\alpha(t, x)$. Similar to the leads wires are described by a single coordinate x , extending from x_i to x_f , such that the dwell time is $\tau = \frac{x_f - x_i}{v}$. It is taken into account by the “delay operator” $\Delta(t', t) \equiv \delta(t' - t - \tau)$. The presence of the potential leads to accumulation of phase

$$\vartheta_{fi}(t) = -v^{-1} \int_{x_i}^{x_f} dx' \varphi(x', t - (x - x')/v). \quad (\text{A.14})$$

The wire connects exactly one incoming to one outgoing channel and the scattering matrix has just one entry $\mathcal{M}(t', t)$ in channel space.

Point scatterer. Another possible construction unit is the point scatterer which connects one-dimensional incoming (index i) and outgoing (index f) channels such that scattering occurs instantaneously (dwell time $\tau = 0+$). The scatterer is characterized by the unitary time-independent scattering matrix s_{fi} . If all channels λ have a linear dispersion with constant velocity v_λ , then according to (A.13) the wave packet incident from channel i (at time t_0) is

$$\psi(t, x, \lambda) = \delta_{\lambda i} \delta(x_i + v_i(t - t_0) - x) + \sum_f \delta_{\lambda f} s_{fi} \sqrt{\frac{v_f}{v_i}} \delta(x_f + v_f(t - t_0) - x), \quad t \approx t_0.$$

Since the state extends over several channels the wave function is a function of both channel index λ and channel coordinate x , and the sum is to be taken over all outgoing channels f .

Counting Fields. Up to now we have not addressed the issue of counting fields, claiming that they can be treated on the same footing as fluctuating potentials, a statement to be proven in this section.

The number of electrons which flow through a certain point \tilde{x} in the time interval $\tilde{t}_0 < t < \tilde{t}$ is described quantum-mechanically by the operator $N = \int_{\tilde{t}_0}^{\tilde{t}} dt I(t)$. The current operator $I = v\psi^\dagger(\tilde{x})\psi(x)$ becomes time-dependent in Heisenberg representation, $I(t) = e^{iH(t-t_-)} I e^{-iH(t-t_-)}$ (t_- is some reference time at which the initial state of the system is fixed), v is the fermion velocity in the considered channel. According to Levitov and Lesovik [6] the correct generating functional of charge transfer through \tilde{x} is

$$\mathcal{Z}(\chi) = \langle U_{-\chi}(\tilde{t}, \tilde{t}_0)^\dagger U_\chi(\tilde{t}, \tilde{t}_0) \rangle \quad \text{with } U_\chi(\tilde{t}, \tilde{t}_0) = \text{Texp} \left[i \frac{\chi}{2} \int_{\tilde{t}_0}^{\tilde{t}} dt I(t) \right].$$

From the properties $U_\chi(\tilde{t}_0, \tilde{t}_0) = \mathbb{1}$ and $i\partial_{\tilde{t}} U_\chi(\tilde{t}, \tilde{t}_0) = -\frac{\chi}{2} I(\tilde{t}) U_\chi(\tilde{t}, \tilde{t}_0)$ we conclude that

$$U_\chi(\tilde{t}, \tilde{t}_0) = e^{iH(\tilde{t}-t_-)} e^{-i(H-\frac{\chi}{2}I)(\tilde{t}-\tilde{t}_0)} e^{-iH(\tilde{t}_0-t_-)}$$

is a possible alternative representation. Thus,

$$\mathcal{Z}(\chi) = \left\langle T_C \exp \left[-i \int_C dt' H_\chi(t') \right] \right\rangle$$

is the Keldysh partition sum with respect to the Hamiltonian $H_\chi^\alpha(t) \equiv H + v \int dx A_\chi^\alpha(x, t) \psi^\dagger(x) \psi(x)$ where time integration and ordering is to be understood along the Keldysh contour \mathcal{C} and we defined the local vector potential $A_\chi^\alpha(t, x) = \alpha \frac{\chi(t)}{2} \delta(x - \tilde{x})$ with the “time-dependent” counting field $\chi(t') \equiv \chi \theta(\tilde{t} - t') \theta(t' - \tilde{t}_0)$.

The corresponding scattering matrix reads $s^\alpha(t', t) = \delta(t' - t) e^{-i\frac{\alpha}{2}\chi(t)}$ and can be incorporated in the total scattering matrix.

Appendix B. Alternative Derivation of the Action for 1D Systems

In this appendix we sketch an alternative derivation of the action $\mathcal{A}_f[\varphi]$ which holds for one-dimensional (1D) systems. As shown in Fig. B.20 they may consist of several channels. Either direction of propagation is the same in all of them (in case of which the setup is referred to as “chiral”) or there are two distinct possible directions: “right” (+) and “left” (-). The derivation generalizes that of Ref. [8] and some of the arguments given already there will be not reiterated here.

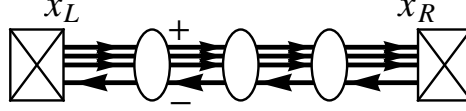


Figure B.20: Exemplary 1D system with 3 right-moving (+) and 1 left-moving (-) channels and 3 scatterers. The system extends $x_L < x < x_R$.

We use a single coordinate system $x_L < x < x_R$ to describe all channels with left (right) contact position $x_{L(R)}$, i.e. velocities in right-(left-)moving channels are positive (negative): v_F ($-v_F$). The fermionic action is

$$\mathcal{A}_f[\psi, \bar{\psi}, \mathcal{V}] = \int dx \int_C dt \Psi^\dagger (i\partial_t + i\tau_3 v_F \partial_x - \Sigma - \mathcal{V}) \Psi$$

where $\Psi = (\psi_\mu^\alpha)$ are vectors of Grassmannian fields with Keldysh and channel/direction indices α and μ , resp. τ are Pauli matrices in direction space, v_F is Fermi velocity, Σ is the self-energy correction due to the coupling to the reservoirs (see below), and \mathcal{V} denotes the (temporally and spatially local) potential under the influence of which the electrons traverse the system. The latter may be the static scattering, Hubbard-Stratonovich or counting potential.

To obtain the integrated action \mathcal{A} , first its variation with respect to \mathcal{V} is considered,

$$i\delta\mathcal{A} = - \int dx \int dt \text{Tr}_\tau \left[\delta\mathcal{V}^-(t, x) G^T(x, t - 0; x, t) - \delta\mathcal{V}^+(t, x) G^{\tilde{T}}(x, t + 0; x, t) \right] \equiv - \int dx \text{Tr} \delta\mathcal{V}(x) \sigma_3 G(x, x) \quad (\text{B.1})$$

where σ are Pauli matrices in Keldysh space, and the first trace Tr_τ is taken over Keldysh and channel indices, while the “full” trace Tr is additionally taken over real time. The full fermionic Green’s function G is needed at coinciding spatial coordinates, where it is discontinuous because of linear dispersion. The above time shift regularization, which takes into account that fermion fields in the action are normal-ordered, is equivalent to the identification

$$G^{T(\tilde{T})}(x, t; x', t') \xrightarrow{x \rightarrow x'} \frac{1}{2iv_F} \left(g^{T(\tilde{T})}(x; t, t') - \delta(t - t') \right) \quad (\text{B.2})$$

with the quasiclassical Green’s function

$$g^{\alpha\beta}(x, t, t') = iv_F \left(G^{\alpha\beta}(x + 0, x; t, t') + G^{\alpha\beta}(x - 0, x; t, t') \right).$$

Appendix B.1. Transfer matrices

The Green’s function $G(x_1, x_2)$ is related to $G(x'_1, x'_2)$ via the single-particle transfer matrices $\mathcal{M}(x, x')$ for spatial evolution from x' to x : $G^{\alpha\beta}(x_1, x_2) = \mathcal{M}^\alpha(x_1, x'_1) G^{\alpha\beta}(x'_1, x'_2) \mathcal{M}^\beta(x'_2, x_2)^\dagger$ or, for quasiclassical Green’s functions, $g^{\alpha\beta}(x) = \mathcal{M}^\alpha(x, x') g^{\alpha\beta}(x') \mathcal{M}^\beta(x, x')^\dagger$. Defining $\mathcal{U}^\alpha(x; t, t') = iv_F^{-1} \delta(t - t') \tau_3 (i\partial_{t'} - \mathcal{V}^\alpha(x, t'))$ (or more clearly in energy representation $\mathcal{U}^\alpha(x)(\epsilon, \epsilon') = iv_F^{-1} \tau_3 (2\pi\delta(\epsilon - \epsilon') \epsilon - \mathcal{V}^\alpha(x, \epsilon - \epsilon'))$), the transfer matrices are given by

$$\mathcal{M}^\alpha(x, x') = \begin{cases} \mathcal{O}_{x_1} \exp \left[\int_{x'}^x dx_1 \mathcal{U}^\alpha(x_1) \right], & x \geq x', \\ \tilde{\mathcal{O}}_{x_1} \exp \left[\int_x^{x'} dx_1 \mathcal{U}^\alpha(x_1) \right], & x \leq x', \end{cases}$$

where \mathcal{O}_x ($\tilde{\mathcal{O}}_x$) orders subsequent operators with respect to their space coordinate x , smaller (larger) coordinates ordered to the right. Consequently, transfer matrices are diagonal in Keldysh space (with \mathcal{M}^α being only related to \mathcal{V}^α) and satisfy

$$\delta\mathcal{M}^\alpha(x_R, x_L) = \int_{x_L}^{x_R} dx \mathcal{M}^\alpha(x_R, x) [-iv_F^{-1}\tau_3\delta\mathcal{V}^\alpha(x)] \mathcal{M}^\alpha(x, x_L). \quad (\text{B.3})$$

For short, we will also write for the total transfer matrix $\mathcal{M} \equiv \mathcal{M}(x_R, x_L)$. Note that in chiral systems considered in Ref. [8] scattering matrices S can be used. While coinciding with the transfer matrices in chiral systems, they differ in non-chiral ones, the two being related via

$$S = \tau_3 (\tau_+ + \mathcal{M}\tau_-)^{-1} (\mathcal{M}\tau_+ + \tau_-) \tau_3 \quad (\text{B.4})$$

with the projectors $\tau_\pm = (\tau_0 \pm \tau_3)/2$ in direction space. In chiral, say right-moving, systems $\tau_3 = \tau_+ = \mathbb{1}$, $\tau_- = 0$ and indeed $S = \mathcal{M}$. Generally, S is unitary, $SS^\dagger = \mathbb{1}$, \mathcal{M} is pseudo-unitary, $\mathcal{M}(x, x')\tau_3\mathcal{M}(x, x')^\dagger = \tau_3$. By defining $\bar{g} \equiv \sigma_3 g \tau_3$ spatial evolution amounts for the similarity transformation

$$\bar{g}(x) = \mathcal{M}(x, x')\bar{g}(x')\mathcal{M}(x, x')^{-1}.$$

The factor σ_3 ensures the normalization property $\bar{g}(x)^2 = \mathbb{1}$.

Using (B.2), (B.3) and $\bar{g}(x) = \mathcal{M}(x, x_L)\bar{g}(x_L)\mathcal{M}(x_R, x_L)^{-1}\mathcal{M}(x_R, x)$ the variation of the action (B.1) can be simplified to

$$\begin{aligned} i\delta\mathcal{A} &= - \int dx \text{Tr} \tau_3 \delta\mathcal{V}(x) \frac{1}{2iv_F} (\bar{g}(x) - \sigma_3\tau_3) \\ &= - \frac{1}{2} \int dx \text{Tr} [-iv_F^{-1}\tau_3\delta\mathcal{V}(x)] \mathcal{M}(x, x_L)\bar{g}(x_L)\mathcal{M}(x_R, x_L)^{-1}\mathcal{M}(x_R, x) + \text{const.} \\ &= - \frac{1}{2} \text{Tr} \bar{g}(x_L)\mathcal{M}^{-1}\delta\mathcal{M} + \text{const.} \end{aligned} \quad (\text{B.5})$$

where we absorb all contributions to the action which are independent of distribution functions in “const.”. We will show later on that they vanish.

Appendix B.2. Reservoir Green's Functions

In a next step, $\bar{g}(x_L)$ is expressed in terms of the quasiclassical Green's function

$$g_{L(R)}(t - t') = \begin{pmatrix} g_{L(R)}^T & g_{L(R)}^< \\ g_{L(R)}^> & g_{L(R)}^{\tilde{T}} \end{pmatrix}_{t-t'} = \begin{pmatrix} \mathbb{1} - 2f_{L(R)} & -2f_{L(R)} \\ 2(\mathbb{1} - f_{L(R)}) & \mathbb{1} - 2f_{L(R)} \end{pmatrix}_{t-t'} \quad (\text{B.6})$$

of the left (right) reservoirs (with distribution functions $f_{L(R)}$ which may have a non-trivial channel structure $f_{L(R)\mu}$). The Green's functions $\bar{g}_i = \sigma_3 \bar{g}_i \tau_3$, $i = L, R$, are related to each other via a similarity transformation as follows: First, introducing the Keldysh matrices

$$L \equiv \frac{1}{\sqrt{2}} \begin{pmatrix} \mathbb{1} & -\mathbb{1} \\ \mathbb{1} & \mathbb{1} \end{pmatrix}, \quad \tilde{U}_i = \begin{pmatrix} \mathbb{1} & (\mathbb{1} - 2f_i) \\ 0 & -\mathbb{1} \end{pmatrix} = \tilde{U}_i^{-1} \quad (\text{B.7})$$

one easily finds

$$L\bar{g}_i L^{-1} = \begin{pmatrix} \mathbb{1} & 2(\mathbb{1} - 2f_i) \\ 0 & -\mathbb{1} \end{pmatrix} \tau_3 = \tilde{U}_i^{-1} \sigma_3 \tau_3 \tilde{U}_i \quad (\text{B.8})$$

and hence

$$\bar{g}_i = U_i^{-1} \sigma_3 \tau_3 U_i \quad \text{with} \quad U_i = \tilde{U}_i L = \frac{1}{\sqrt{2}} \begin{pmatrix} 2f_i^> & -2f_i^< \\ -\mathbb{1} & -\mathbb{1} \end{pmatrix} \quad (\text{B.9})$$

with $f_i^< = f_i$, $f_i^> = \mathbb{1} - f_i$. Thus we have proven

$$\bar{g}_R = U^{-1} \bar{g}_L U \quad \text{with} \quad U = U_L^{-1} U_R. \quad (\text{B.10})$$

To relate the Green's function $\bar{g}(x_L)$ inside the system to its counterparts in the reservoirs one assumes that the dynamics inside the leads is governed by some relaxation process, say isotropization of momentum direction due to scattering off static white noise disorder. This is described by the self-energy contribution

$$\Sigma(t_1, x_1; t_2, x_2) = \delta(x_1 - x_2) \left(-\frac{i}{2\tau_{\text{rel}}} \right) \times \begin{cases} g_L(t_1, t_2), & x_1, x_2 < x_L \\ g_R(t_1, t_2), & x_1, x_2 > x_R \end{cases}.$$

Here τ_{rel} denotes the relaxation time. The requirement that $G(x + \Delta x, x)$ vanish for infinite distances Δx yields the boundary conditions[8],

$$(\mathbb{1} + \bar{g}_L)(\mathbb{1} - \bar{g}(x_-)) = 0, \quad (\mathbb{1} - \bar{g}_R)(\mathbb{1} - \bar{g}(x_+)) = 0, \quad (\text{B.11})$$

again with $\bar{g} \equiv \sigma_3 g \tau_3$. Defining $\bar{\mathcal{M}} \equiv U \mathcal{M}$ the second equation is equivalent to $0 = (\mathbb{1} - \bar{\mathcal{M}}^{-1} \bar{g}_L \bar{\mathcal{M}})(\mathbb{1} + \bar{g}(x_L))$. Combining it with the first equation gives

$$0 = (2\mathbb{1} + \bar{g}_L - \bar{\mathcal{M}}^{-1} \bar{g}_L \bar{\mathcal{M}}) - (\bar{g}_L + \bar{\mathcal{M}}^{-1} \bar{g}_L \bar{\mathcal{M}}) \bar{g}(x_L) \quad (\text{B.12})$$

and by inversion

$$\bar{g}(x_L) = \mathbb{1} + 2(\mathbb{1} - \bar{g}_L) (\bar{g}_L \bar{\mathcal{M}} + \bar{\mathcal{M}} \bar{g}_L)^{-1} \bar{\mathcal{M}} \quad (\text{B.13})$$

where we have made use of $\bar{g}_L^2 = \mathbb{1}$.

To rewrite this expression we choose a specific basis representation. Since $\bar{g}_L^2 = \mathbb{1}$ there exists one in which $\bar{g}_L = \text{diag}(\mathbb{1}, -\mathbb{1})$. In the very same representation we write

$$\bar{\mathcal{M}} = \begin{pmatrix} \bar{\mathcal{M}}_{11} & \bar{\mathcal{M}}_{12} \\ \bar{\mathcal{M}}_{21} & \bar{\mathcal{M}}_{22} \end{pmatrix}.$$

Then we have $\bar{g}_L \bar{\mathcal{M}} + \bar{\mathcal{M}} \bar{g}_L = 2 \text{diag}(\bar{\mathcal{M}}_{11}, -\bar{\mathcal{M}}_{22})$, which is readily inverted, as well as $\mathbb{1} + \bar{g}_L = 2 \text{diag}(\mathbb{1}, 0)$, $\mathbb{1} - \bar{g}_L = 2 \text{diag}(0, \mathbb{1})$, and (B.13) gives

$$\bar{g}(x_L) = \begin{pmatrix} \mathbb{1} & 0 \\ -2\bar{\mathcal{M}}_{22}^{-1} \bar{\mathcal{M}}_{21} & -\mathbb{1} \end{pmatrix}. \quad (\text{B.14})$$

Defining

$$\mathcal{D} \equiv (\mathbb{1} + \bar{g}_L)/2 + \bar{\mathcal{M}}(\mathbb{1} - \bar{g}_L)/2 \quad (\text{B.15})$$

one may show that

$$\bar{g}(x_L) = \mathbb{1} - (\mathbb{1} - \bar{g}_L) \mathcal{D}^{-1} \bar{\mathcal{M}} \quad (\text{B.16})$$

is equivalent to (B.14). We have thus expressed $\bar{g}(x_L)$ entirely in terms of $\bar{g}_{L(R)}$ and the transfer matrix $\mathcal{M}(x_R, x_L)$.

Substituting this result into (B.5) and using $\mathcal{M}(x_R, x_L)^{-1} \delta \mathcal{M}(x_R, x_L) = \bar{\mathcal{M}}^{-1} \delta \bar{\mathcal{M}}$ yields

$$\begin{aligned} i\delta\mathcal{A} &= \frac{1}{2} \text{Tr}(\mathbb{1} - \bar{g}_L) \mathcal{D}^{-1} \delta \bar{\mathcal{M}} + \text{const.} = \text{Tr} \mathcal{D}^{-1} \delta \mathcal{D} + \text{const.} \\ &\Rightarrow i\mathcal{A} = \text{Tr} \text{Ln} \mathcal{D} + \text{const.} = \text{Tr} \text{Ln} \left[\frac{\mathbb{1} + \bar{g}_L}{2} + \bar{\mathcal{M}} \frac{\mathbb{1} - \bar{g}_L}{2} \right] + \text{const.} \end{aligned} \quad (\text{B.17})$$

Appendix B.3. Role of Drain Distribution Functions

So far we have not been concerned with the channel structure explicitly and merely stated that there are 2 directions of motion, right(+) and left(-), each of which is realized by a certain (not necessarily equal) number of channels (possibly even zero in chiral systems). In both left and right reservoirs to each channel μ was assigned a distribution function $f_{L\mu}$ and $f_{R\mu}$. For a right-(left-)moving channel $f_{R\mu}$ ($f_{L\mu}$) is the *drain* distribution function and one naturally wonders whether it should have an effect on the chiral fermions as long as the latter have not entered the drain reservoirs. We show here that this is not the case.

To this end we introduce the block decomposition with respect to channel indices, e.g.

$$\mathcal{M} = \begin{pmatrix} \mathcal{M}_{++} & \mathcal{M}_{+-} \\ \mathcal{M}_{-+} & \mathcal{M}_{--} \end{pmatrix}, \quad f_i = \begin{pmatrix} f_{i+} & \\ & f_{i-} \end{pmatrix}, \quad i = L, R, \quad (\text{B.18})$$

where e.g. \mathcal{M}_{+-} , f_{i+} , f_{i-} still may have channel structure $(\mathcal{M}_{+-})_{\mu\nu}$, $(f_{i+})_\mu$, $(f_{i-})_\nu$, however, with μ (ν) extending exclusively over right-(left-)moving channels.

Introducing

$$Q \equiv U_R \mathcal{M} U_L^{-1} = \begin{pmatrix} Q_{11} & Q_{12} \\ Q_{21} & Q_{22} \end{pmatrix} = \begin{pmatrix} f_R^> \mathcal{M}^- + f_R^< \mathcal{M}^+ & -2f_R^> \mathcal{M}^- f_L^< + 2f_R^< \mathcal{M}^+ f_L^> \\ -\frac{1}{2} \mathcal{M}^- + \frac{1}{2} \mathcal{M}^+ & \mathcal{M}^- f_L^< + \mathcal{M}^+ f_L^> \end{pmatrix} \quad (\text{B.19})$$

and the projectors

$$P_+ = \frac{1}{2}(1 + \sigma_3 \tau_3) = \begin{pmatrix} \tau_+ & 0 \\ 0 & \tau_- \end{pmatrix}, \quad P_- = \frac{1}{2}(1 - \sigma_3 \tau_3) = \begin{pmatrix} \tau_- & 0 \\ 0 & \tau_+ \end{pmatrix} \quad (\text{B.20})$$

the action (B.17) reads

$$i\mathcal{A} = \ln \text{Det} (P_+ + QP_-) + \text{const.} = \ln \text{Det} (P_+ + P_- QP_-) + \text{const.}$$

where

$$P_- QP_- = \begin{pmatrix} \tau_- Q_{11} \tau_- & \tau_- Q_{12} \tau_+ \\ \tau_+ Q_{21} \tau_- & \tau_+ Q_{22} \tau_+ \end{pmatrix}.$$

Writing out the direction structure explicitly yields

$$i\mathcal{A} = \ln \text{Det} \begin{pmatrix} f_{R-}^> \mathcal{M}_{--}^- + f_{R-}^< \mathcal{M}_{--}^+ & -2f_{R-}^> \mathcal{M}_{-+}^- f_{L+}^< + 2f_{R-}^< \mathcal{M}_{-+}^+ f_{L+}^> \\ -\frac{1}{2} \mathcal{M}_{+-}^- + \frac{1}{2} \mathcal{M}_{+-}^+ & \mathcal{M}_{++}^- f_{L+}^< + \mathcal{M}_{++}^+ f_{L+}^> \end{pmatrix} + \text{const.}$$

This proves that the action depends only on f_{L+} and f_{R-} , i.e. the source distribution functions.

Appendix B.4. Tracing out Keldysh Structure

We now return to the expression (B.17). Since we already know that the result does not depend on $f_{L,-}$ and $f_{R,+}$ we may make the choice $f_{L,-} = f_{R,-}$ and $f_{R,+} = f_{L,+}$. In other words, we put $\bar{g}_L = \bar{g}_R = \text{diag}(\bar{g}_{L+}, \bar{g}_{R-}) \equiv \bar{g}_{\text{in}} \equiv \sigma_3 g_{\text{in}} \tau_3$. As suggested by the subindex g_{in} contains the source (or incoming) distribution functions. It can be parametrized analogously to (B.9),

$$\sigma_3 g_{\text{in}} = U_{\text{in}}^{-1} \sigma_3 U_{\text{in}} \quad \text{with } U_{\text{in}} = \frac{1}{\sqrt{2}} \begin{pmatrix} 2f^> & -2f^< \\ -\mathbb{1} & -\mathbb{1} \end{pmatrix} \quad (\text{B.21})$$

with f being the matrix of source distribution functions. Since U is not needed anymore and hence $\bar{\mathcal{M}} = \mathcal{M}$, we recall the definition of \mathcal{D} given by Eq. (B.15) and of scattering matrix S (B.4) and obtain

$$\mathcal{D} = \frac{\mathbb{1} + \sigma_3 g \tau_3}{2} + \mathcal{M} \frac{\mathbb{1} - \sigma_3 g \tau_3}{2} = (\tau_+ + \mathcal{M} \tau_-) \tau_3 U_{\text{in}}^{-1} \left[\frac{\mathbb{1} + \sigma_3}{2} + U_{\text{in}} S U_{\text{in}}^{-1} \frac{\mathbb{1} - \sigma_3}{2} \right] U_{\text{in}}. \quad (\text{B.22})$$

With

$$\tilde{Q} \equiv U_{\text{in}} S U_{\text{in}}^{-1} = \begin{pmatrix} Q^{--} & Q^{-+} \\ Q^{+-} & Q^{++} \end{pmatrix} = \begin{pmatrix} f^{>} S^- + f^{<} S^+ & -2f^{>} S^- f^{<} + 2f^{<} S^- f^{>} \\ -\frac{1}{2} S^- + \frac{1}{2} S^+ & S^- f^{<} + S^+ f^{>} \end{pmatrix}$$

the action (B.17) is

$$i\mathcal{A} = \ln \text{Det } \mathcal{D} + \text{const.} = \ln \text{Det } Q^{++} + \text{const.} = \text{Tr Ln } [\mathbb{1} - f + S^{+\dagger} S^- f] + \text{const.} \quad (\text{B.23})$$

Up to anomalous terms, representing the R- and A-parts of the polarization operator, and contributions which are independent of distribution functions f , this proves Eq. (12)

Appendix B.5. Constant contributions

What are the “const.”-contributions to the action we keep ignoring? All that we know so far about them is their independence of distribution function f . According to (B.23) they can be recovered by substituting $f = 0$ in the *full* action (where “const.” is not neglected). So let us put $f \equiv 0$ in the rest of this section and recalculate the full action. Eq. (B.13) can be evaluated explicitly now, yielding $g^T(x_L) = g_0^-(x_L)$ and $g^{\tilde{T}}(x_L) = g_0^+(x_L)^\dagger$ with

$$g_0(x_L) = \begin{pmatrix} \mathbb{1} & 0 \\ 2S_{-+} & \mathbb{1} \end{pmatrix} = \mathbb{1} + 2 \begin{pmatrix} 0 & 0 \\ A_{-+}(x_L) & 0 \end{pmatrix}$$

where $A_{\nu\mu}(x; t', t)$ is defined as the amplitude for a μ -wave packet at position x and time t to end up as a ν -wave packet at time t' and the same position x (cf. Sect. Appendix A.3). The above relation between $g^{T/\tilde{T}}$ and g_0^\mp holds for all positions x with $g_0^\alpha(x) \equiv \mathcal{M}^\alpha(x, x_L) g_0^\alpha(x_L) \mathcal{M}^\alpha(x, x_L)^\dagger$. To calculate the latter we define (for given x) the “scattering matrix”

$$s \equiv \tau_3 (\tau_+ + \mathcal{M}(x, x_L) \tau_-)^{-1} (\mathcal{M}(x, x_L) \tau_+ + \tau_-) \tau_3$$

of the region between x_L and x which takes into account paths extending only within this region. Using the

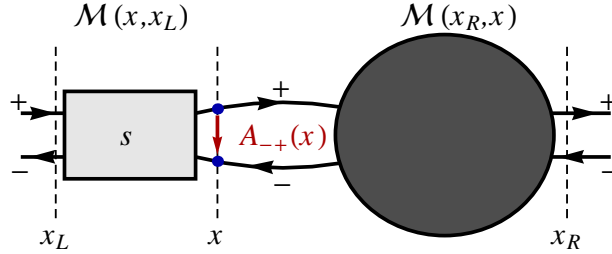


Figure B.21: Spatial evolution of g from x_L to x with $\mathcal{M}(x, x_L)$; s is the corresponding “scattering matrix”; the shaded blob represents the rest of the system. In contrast to s , paths contributing to $A_{-+}(x)$ may extend throughout the entire system.

recursion relations (see Fig. B.21)

$$\begin{aligned} S_{-+} &= s_{-+} + s_{--} A_{-+}(x) s_{++}, \\ A_{++}(x) &= s_{+-} A_{-+}(x), \quad A_{+-}(x) = s_{+-} + s_{+-} A_{-+}(x) s_{+-}, \quad A_{--}(x) = A_{-+}(x) s_{+-} \end{aligned}$$

one obtains

$$g_0(x) = \mathbb{1} + 2 \begin{pmatrix} A_{++}(x) & A_{+-}(x) \\ A_{-+}(x) & A_{--}(x) \end{pmatrix}. \quad (\text{B.24})$$

For a smooth potential $\mathcal{V}(x)$ all paths contributing to $A_{\nu\mu}(x)$ have a non-vanishing flight time such that $A_{\nu\mu}(x; t, t) = 0$. At point scatterers, which are a mere idealization, the Green’s function $g(x)$ is not well-defined and we stay sufficiently far away from them. Concluding, for equal times the Green’s function (B.2) vanishes. Substituting this result into Eq. (B.1) yields $\delta\mathcal{A}|_{f \equiv 0} = 0$, hence $\text{const.} = \mathcal{A}|_{f \equiv 0}$ is indeed a physically irrelevant constant.

Appendix C. Weak Tunneling Regularization

In general, the scattering matrix $S^\alpha = S[\varphi^\alpha]$ depend on time in a complicated manner which makes the exact evaluation of the functional determinant (12) unfeasible. In this section we present an approximation scheme which applies for systems with weak tunneling. A tunneling action \mathcal{A}_t is derived by subtracting a clean action \mathcal{A}_0 from the full one \mathcal{A} . By construction \mathcal{A}_t is small and may be therefore expanded. The crucial step, the separation of actions, can be performed at zero temperature where reservoirs may have differing chemical potentials. As it will turn out, interaction effectively leads to a dressing of the point scatterers by phases Φ .

Appendix C.1. Clean Limit

The clean limit was discussed in Sect. 2.1. The action \mathcal{A}_0 is obtained from (12) by replacing S by the clean scattering matrix $S_*^\alpha = \text{diag}(e^{i\vartheta_1^\alpha} \Delta_1, \dots, e^{i\vartheta_N^\alpha} \Delta_N) \equiv e^{i\vartheta^\alpha} \Delta$ with the delay operators Δ_μ and the phases ϑ_μ accumulated along the complete paths $x_\mu^S \rightarrow x_\mu^D$.

The main step in the quest of the tunneling action

$$\mathcal{A}_t = \mathcal{A} - \mathcal{A}_0 = i\text{Tr} \text{Ln} \left[(\mathbb{1} - \bar{f} + S^{+\dagger} S^- \bar{f}) (\mathbb{1} - \bar{f} + S_*^{+\dagger} S_*^- \bar{f})^{-1} \right]$$

is the inversion of the second bracket, a problem which is already dealt with in Ref. [54]. Since S_* is diagonal in channel space, the operator can be inverted for each channel separately. So we consider

$$(\mathbb{1} - \bar{f} + S_*^{+\dagger} S_*^- \bar{f})_{\mu\mu} = \mathbb{1} - f_\mu + \Delta_\mu^{-1} e^{i(\vartheta_\mu^- - \vartheta_\mu^+)} \Delta_\mu f_\mu$$

where $\Delta_\mu(t', t) = \delta(t' - t - \tau_\mu)$ is an appropriate time delay operator. Note that it commutes with the stationary distribution function f_μ . For zero temperature we follow Ref.[54], according to which the inversion problem can be reformulated in terms of a certain Riemann-Hilbert problem, which is solved by defining the phases ϑ_μ^\wedge and ϑ_μ^\vee by

$$\vartheta_\mu^{\wedge\vee}(t) \equiv \frac{i}{2\pi} \int dt' \frac{\vartheta_\mu^-(t') - \vartheta_\mu^+(t')}{t_\pm - t'} \equiv - \int dt' [B(t - t') \mp \delta(t - t')] [\vartheta_\mu^-(t') - \vartheta_\mu^+(t')], \quad (\text{C.1})$$

with $t_\pm \equiv t \pm i0$. They satisfy $\vartheta^\wedge - \vartheta^\vee = \vartheta^- - \vartheta^+$, hence $\vartheta^- - \vartheta^\wedge = \vartheta^+ - \vartheta^\vee \equiv \bar{\vartheta}$, and $f_\mu e^{i\vartheta_\mu^\wedge} f_\mu = e^{i\vartheta_\mu^\wedge} f_\mu$, $f_\mu e^{i\vartheta_\mu^\vee} f_\mu = f_\mu e^{i\vartheta_\mu^\vee}$. Thus, one obtains

$$(\mathbb{1} - f_\mu + \Delta_\mu^{-1} e^{i(\vartheta_\mu^- - \vartheta_\mu^+)} \Delta_\mu f_\mu)^{-1} = \Delta_\mu^{-1} \left[e^{-i\vartheta_\mu^\vee} (\mathbb{1} - f_\mu) + e^{-i\vartheta_\mu^\wedge} f_\mu \right] e^{i\vartheta_\mu^\vee} \Delta_\mu,$$

and, taking now the full channel structure into account,

$$\mathcal{A}_t = -i\text{Tr} \text{Ln} \left[\mathbb{1} - \bar{f} + \tilde{S}^{+\dagger} \tilde{S}^- \bar{f} \right] = i \sum_{n=1}^{\infty} \frac{1}{n} \text{Tr} \left[(\mathbb{1} - \tilde{S}^{+\dagger} \tilde{S}^-) \bar{f} \right]^n$$

with the “regularized” scattering matrix

$$\tilde{S}^\mp \equiv e^{-i\bar{\vartheta}} S^\mp \Delta^{-1} e^{-i\vartheta^{\wedge\vee}} \Delta. \quad (\text{C.2})$$

Defining in energy representation $N(\omega) = -\theta(-\omega)$ as the zero temperature limit of the Bose distribution function, we note that the function B introduced in (C.1) is the “generalized” distribution function $B(\omega) = 1 + 2N(\omega)$ ubiquitous in bosonic Keldysh formalism. This fact allows us to endow the phases with a Keldysh structure. We address this issue in the next section before turning to the computation of the regularized scattering matrix in the subsequent one.

Appendix C.2. Phases and Keldysh Structure

Before we turn to the computation of the regularized scattering matrix let us consider the Keldysh structure of the phases ϑ . To this end we consider the clean path $x_\mu^S \rightarrow x_\mu^D$ containing the point x . An electron propagating from the source reservoir x_μ^S to x (arrival time t) accumulates the phase

$$\vartheta_{\text{in},\mu}^\alpha(t, x) \equiv -v_\mu^{-1} \int_{x_\mu^S}^x dx' \varphi^\alpha(x', t - (x - x')/v_\mu) = -D_{0\mu}^r \varphi_\mu^\alpha(x, t); \quad (\text{C.3})$$

likewise when traveling from x (departure time t) to the drain reservoir x_μ^D it accumulates

$$\vartheta_{\text{out},\mu}^\alpha(t, x) \equiv -v_\mu^{-1} \int_x^{x_\mu^D} dx \varphi^\alpha(x, t + (x' - x)/v_\mu) = D_{0\mu}^a \varphi_\mu^\alpha(x, t) \quad (\text{C.4})$$

where we introduced the retarded/advanced bare electron-hole pair propagators

$$D_{0\mu}^{r/a}(t; x', x) = \pm \theta(\pm t) \delta(x' - (x + v_\mu t))$$

along the the clean path. Quite obviously, the phase accumulated along the complete clean path satisfies

$$\vartheta_\mu^\mp(t) = \vartheta_{\mu,\text{in}}^\mp(x, t - (x_\mu^D - x)/v_\mu) + \vartheta_{\mu,\text{out}}^\mp(x, t - (x_\mu^D - x)/v_\mu) = - (D_{0\mu}^r - D_{0\mu}^a) \varphi_\mu^\mp(x, t - (x_\mu^D - x)/v_\mu). \quad (\text{C.5})$$

The propagators $D_{0\mu}^{r/a}$ directly make reference to propagation velocity v_μ and thus encode spectral (kinematic) properties of the electron-hole pairs. As usual they lack information about the system's state which one expects to be contained in the missing Keldysh component $D_{0\mu}^k$ of the propagator. In this sense the phases ϑ are related to the potential φ via the linear operator D_0 which does not have the full Keldysh structure.

To overcome this “deficiency” we recall the definition made in the previous section

$$\bar{\vartheta}_\mu = \vartheta_\mu^\mp - \vartheta_\mu^{\wedge\vee} = \frac{1}{2}(B + \mathbb{1})\vartheta_\mu^- - \frac{1}{2}(B - \mathbb{1})\vartheta_\mu^+. \quad (\text{C.6})$$

Combining now (C.5) and (C.6) and using the stationarity of $B(t, t') = B_\mu(t - t')$ we obtain

$$\bar{\vartheta}_\mu(t + (x_\mu^D - x)/v_\mu) = -\frac{1}{2}(B + \mathbb{1})(D_{0\mu}^r - D_{0\mu}^a) \varphi_\mu^-(x, t) + \frac{1}{2}(B - \mathbb{1})(D_{0\mu}^r - D_{0\mu}^a) \varphi_\mu^+(x, t) \quad (\text{C.7})$$

With that the phase that an electron, traveling along a piece of wire between x_1 and x_2 , accumulates is

$$\begin{aligned} \vartheta_{\mu 21}^\mp(t) &= -\vartheta_{\mu,\text{out}}^\mp(x^2, t) + \vartheta_{\mu,\text{out}}^\mp(x^1, t - (x^2 - x^1)/v_\mu) \\ &\equiv \Theta_\mu^\mp(x^2, t) - \Theta_\mu^\mp(x^1, t - (x^2 - x^1)/v_\mu) \end{aligned}$$

with the phases

$$\begin{aligned} \Theta_\mu^\mp(x, t) &\equiv -\vartheta_{\mu,\text{out}}^\mp(x, t) + \bar{\vartheta}_\mu(t + (x_\mu^D - x)/v_\mu) \\ &= -\frac{1}{2}[(B + \mathbb{1})D_{0\mu}^r - (B \mp \mathbb{1})D_{0\mu}^a] \varphi_\mu^-(x, t) + \frac{1}{2}[(B - \mathbb{1})D_{0\mu}^r - (B \mp \mathbb{1})D_{0\mu}^a] \varphi_\mu^+(x, t) \\ &= -\left[D_{0\mu}^{T/>} \varphi_\mu^-(x, t) - D_{0\mu}^{>/\bar{T}} \varphi_\mu^+(x, t)\right]. \end{aligned} \quad (\text{C.8})$$

We thus have managed to rewrite the scattering matrix of chiral wires $\mathcal{M}^\alpha(x_2, x_1) = e^{i\vartheta_{21}^\alpha} \Delta(x_2, x_1) = e^{i\Theta^\alpha(x_2)} \Delta(x_2, x_1) e^{i\Theta^\alpha(x_1)}$ in terms of phases with full Keldysh structure. Formally we started with expressions which did not contain any distribution functions whatsoever and somewhat artificially included them by redefining phases. The usefulness of such construction will become apparent in the next section.

Appendix C.3. Construction of “Regularized” Scattering Matrix

We have previously shown that the full scattering matrix S can be constructed out of simpler units. We prove in this subsection that the same statement holds for the regularized scattering matrix \tilde{S} .

Since the full scattering matrix elements are amplitude sums $S_{\nu\mu}^\alpha = \sum_p A_{\nu\mu}^{(p)\alpha}$ over all paths p connecting x_μ^S with x_ν^D , definition (C.2) directly implies that $\tilde{S}_{\nu\mu}^\mp = \sum_p \tilde{A}_{\nu\mu}^{(p)\mp}$ is the sum of the *regularized* amplitudes

$$\tilde{A}_{\nu\mu}^{(p)\mp} \equiv e^{-i\tilde{\vartheta}_\nu} A_{\nu'\mu}^{(p)\mp} \Delta_\mu^{-1} e^{-i\vartheta_\mu^{\wedge\nu}} \Delta_\mu = e^{-i\Theta_\nu^\mp(x_\nu^D)} A_{\nu\mu}^{(p)\mp} e^{i\Theta_\mu^\mp(x_\mu^S)} \quad (\text{C.9})$$

over the same paths p with phases $\Theta_{\mu(\nu)}$ along the clean paths $x_\mu^S \rightarrow x_\mu^D$ and $x_\nu^S \rightarrow x_\nu^D$. Note that $\vartheta_{\nu,\text{out}}^\mp(x_\nu^D, t) = 0$ and $\vartheta_{\mu,\text{out}}^\mp(x_\mu^S, t) = \vartheta_\mu^\mp(t + (x_\mu^D - x_\mu)/v_\mu)$, and thus definition (C.8) implies $\Theta_\nu^\mp(x_\nu^D, t) = \tilde{\vartheta}_\nu(t)$ and $\Theta_\mu^\mp(x_\mu^S, t) = -\vartheta_\mu^{\wedge\nu}(t + (x_\mu^D - x_\mu^S)/v_\mu)$.

We now consider a generic path p which starts at incoming lead channel μ , winds through an alternating sequence of wires and point scatterers (numbered $1, 2, \dots, N$ with positions x_1, x_2, \dots, x_N), eventually ends in outgoing channel ν' . The corresponding full amplitude is

$$\begin{aligned} A_{\nu\mu}^{(p)\mp} &= \mathcal{M}_\mu^\mp(x_\nu^D, x^N) s_{\nu\lambda}^N \dots s_{\rho\kappa}^2 \mathcal{M}_\kappa^\mp(x^2, x^1) s_{\kappa\mu}^1 \mathcal{M}_\mu^\mp(x^1, x_\mu^S) \\ &= e^{i\Theta_\nu^\mp(x_\nu^D)} \Delta_\nu(x_\nu^D, x^N) e^{-i\Theta_\nu^\mp(x^N)} s_{\nu\lambda}^N \dots s_{\rho\kappa}^2 e^{i\Theta_\kappa^\mp(x^2)} \Delta_\kappa(x^2, x^1) e^{i\Theta_\kappa^\mp(x^1)} s_{\kappa\mu}^1 e^{i\Theta_\mu^\mp(x^1)} \Delta_\mu(x^1, x_\mu^S) e^{-i\Theta_\mu^\mp(x_\mu^S)} \end{aligned}$$

and simply becomes

$$\tilde{A}_{\nu\mu}^{(p)\mp} = \Delta_\nu(x_\nu^D, x^N) e^{-i\Theta_\nu^\mp(x^N)} s_{\nu\lambda}^N \dots e^{i\Theta_\kappa^\mp(x^2)} \Delta_\kappa(x^2, x^1) e^{i\Theta_\kappa^\mp(x^1)} s_{\kappa\mu}^1 e^{i\Theta_\mu^\mp(x^1)} \Delta_\mu(x^1, x_\mu^S)$$

upon regularization. This implies that regularization of the amplitudes amounts to regularization of the scattering matrices of the building blocks: The effect of fluctuating potentials (and counting fields) is removed from all wires and incorporated in the tunneling phases

$$\Phi_{\nu\mu}^\mp(x^j, t) \equiv \Theta_\mu^\mp(x^j, t) - \Theta_\nu^\mp(x^j, t)$$

which dress the point scattering amplitudes $s_{\nu\mu}^j$. This result is summarized in the table below:

Construction unit	Regularized scattering matrix
Chiral wire	$\Delta(t', t)$
Point scatterer	$\tilde{s}_{\nu\mu}^\alpha(t', t) = s_{\nu\mu}^\alpha e^{i\Phi_{\nu\mu}^\alpha(t, \bar{x})} \delta(t' - t)$

Appendix D. Second Order Expansion

We prove the second order expansion (21) in tunneling strength (“tun”) starting from (20). Obviously, $\mathcal{A}_{\nu\mu} \equiv \sum_\lambda (\tilde{S}_{\lambda\nu}^+)^\dagger \tilde{S}_{\lambda\mu}^-$ is the sum over all paths winding forward and along the forward Keldysh branch (i.e. with potentials φ^-) from source μ to some drain λ and then *backwards* along the backward branch (with potentials φ^+) to source ν (for short: “source $\mu \rightarrow$ drain $\lambda \xrightarrow{+}$ source ν ”). The backward part \bar{p}^+ is obtained by time-reversal of a physical, forward path p^+ (source $\nu \xrightarrow{+}$ drain λ) with amplitude $\tilde{A}_{\lambda\mu}^{(p^+)}$ and has amplitude $\tilde{A}_{\nu\lambda}^{\bar{p}^+} \equiv \tilde{A}_{\lambda\nu}^{(p^+)\dagger}$ (note that hermitian conjugation, \dagger , reverses the order of partial amplitudes in the product). Denoting with p^- the forward part of $p = p^- \oplus \bar{p}^+$, the total amplitude is $\tilde{A}_{\nu\mu}^{(p)} \equiv \tilde{A}_{\lambda\nu}^{(p^+)\dagger} \tilde{A}_{\lambda\mu}^{(p^-)}$.

In the chosen order of accuracy we only take paths with a total of 2 or less tunneling events into account. The expanded tunneling action is $\mathcal{A}_t = \mathcal{A}_1 + \mathcal{A}_2$ with

$$\mathcal{A}_1 \equiv i \text{Tr} \sum_\mu (\mathbb{1} - \mathcal{A})_{\mu\mu} f_\mu = i \sum_\mu \text{Tr} \left[f_\mu - \sum_{p_1} \tilde{A}_{\mu\mu}^{(p_1)} f_\mu \right], \quad (\text{D.1})$$

$$\mathcal{A}_2 \equiv \frac{i}{2} \text{Tr} \sum_{\mu \neq \nu} \mathcal{A}_{\mu\nu} f_\nu \mathcal{A}_{\nu\mu} f_\mu = \frac{i}{2} \sum_{\mu \neq \nu} \sum_{p_2=p_2' \oplus p_2''} \text{Tr} \tilde{A}_{\mu\nu}^{(p_2'')} f_\nu \tilde{A}_{\nu\mu}^{(p_2')} f_\mu. \quad (\text{D.2})$$

The sum \sum_p in (D.1) extends over paths p_1 : “source $\mu \xrightarrow{-} \text{drain } \nu \xrightarrow{+} \text{source } \mu$ ” with 2 or less tunneling events (obviously the number has to be even), while the sum in (D.2) extends over paths $p_2 = p'_2 \oplus p''_2$:

$$\underbrace{\text{“source } \mu \xrightarrow{-} \text{drain } \kappa \xrightarrow{+} \text{source } \nu \xrightarrow{-} \text{drain } \lambda \xrightarrow{+} \text{source } \mu \text{”}}_{p'_2},$$

or equivalently, $\underbrace{\text{“source } \nu \xrightarrow{-} \text{drain } \lambda \xrightarrow{+} \text{source } \mu \xrightarrow{-} \text{drain } \kappa \xrightarrow{+} \text{source } \nu \text{”}}_{p_2}$

where the equivalence is ensured by the cyclic invariance of the trace. Since $\mu \neq \nu$ subpaths p'_2 and p''_2 each contain at least one tunneling event, i.e. in our approximation *exactly one*. Depending on whether tunneling occurs on the forward or backward Keldysh branch $\kappa, \lambda = \mu$ or ν . It is quite obvious that no matter how often a path evolves in time forward and backward (once for \mathcal{A}_1 , twice for \mathcal{A}_2), as long as it starts and ends in the same reservoir and contains exactly 2 tunneling events, it exactly involves 2 different channels $\mu \neq \nu$. We will use this fact for a systematic classification of all paths.

To warm up we consider first the simplest (and least interesting) paths, which contribute to \mathcal{A}_1 and are of the form “source $\mu \xrightarrow{-} \text{drain } \mu \xrightarrow{+} \text{source } \mu$ ” without any tunneling taking place. Time delay operators are canceled exactly (since forward and backward paths coincide geometrically) and no phases are accumulated (since after regularization they are carried only by the tunneling amplitudes). The total amplitude is thus a product of forward scattering amplitudes $s_{\mu\mu}^j$ of scatterers j along the clean path $x_\mu^S \rightarrow x_\mu^D$:

$$\prod_j |s_{\mu\mu}^j|^2 = \prod_j \left(\mathbb{1} - \sum_{\nu \neq \mu} |s_{\nu\mu}^j|^2 \right) = \mathbb{1} - \sum_j \sum_{\nu \neq \mu} |s_{\nu\mu}^j|^2 + \mathcal{O}(\text{tun}^4). \quad (\text{D.3})$$

All other relevant paths contain exactly 2 tunneling events. Not surprisingly there is a whole plethora of them and we are well advised to proceed systematically. To this end and according to the observation made before we classify these paths with respect to the pair (μ, ν) of different channels $\mu \neq \nu$ involved and the two scatterers i and j (possibly $i = j$) at which tunneling $\mu \rightarrow \nu$ and $\nu \rightarrow \mu$ respectively occurs. Note that in this classification classes $(ij; \mu\nu)$ and $(ji; \nu\mu)$ are identical. What classes $(ij; \mu\nu)$ are possible, of course, depends on the topology of the considered network (since e.g. not all scatterers are even connected to a given channel μ). But, as we will show, once a class is fixed, its contribution to \mathcal{A}_t is essentially independent of topology!

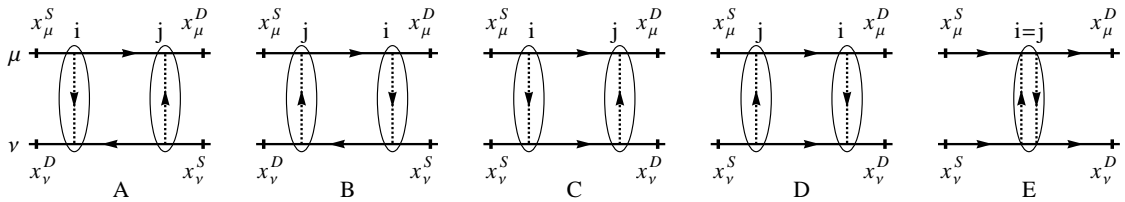


Figure D.22: The 5 topologically distinct configurations for class $(ij; \mu\nu)$. All channels except for μ, ν and all scatterers except for i, j (“distorted white circles”) are dropped. Scatterers $i \neq j$ are different in A-D which allows for 4 different orderings along channels μ and ν . In E tunneling occurs twice at the same scatterer $i = j$.

Fig. D.22 shows the 5 topologically distinct configurations of channels μ, ν and scatterers i, j for given class $(ij; \mu\nu)$. Arrows at the scatterers indicate direction of tunneling. All scatterers except for i, j are dropped. They are involved only in forward scattering events and thus lead to corrections $\mathcal{O}(\text{tun}^3)$. In this way propagation from source x_μ^S to scatterer i just leads to an amplitude $\Delta_{i,\mu,\text{in}}$ which accounts for the

finite flight time $\tau_{\mu,\text{in}}^i$. Analogously we define $\Delta_{j,\mu,\text{in}}$ and the same for ν , and further

$$\begin{aligned}\mathcal{X}_i^- &\equiv \Delta_{i,\nu,\text{in}}^{-1} \bar{s}_{\nu\mu}^{i-} \Delta_{i,\mu,\text{in}} = \Delta_{i,\nu,\text{in}}^{-1} e^{-i\Phi_{\mu\nu}^-(x^i)} \Delta_{i,\mu,\text{in}} s_{\nu\mu}^i, \\ \mathcal{X}_i^+ &\equiv \Delta_{i,\nu,\text{in}}^{-1} (s_{\mu\nu}^{i+})^\dagger \Delta_{i,\mu,\text{in}} = \Delta_{i,\nu,\text{in}}^{-1} e^{-i\Phi_{\mu\nu}^+(x^i)} \Delta_{i,\mu,\text{in}} \bar{s}_{\mu\nu}^i, \\ \mathcal{X}_j^- &\equiv \Delta_{j,\mu,\text{in}}^{-1} \bar{s}_{\mu\nu}^{j-} \Delta_{j,\nu,\text{in}} = \Delta_{j,\mu,\text{in}}^{-1} e^{i\Phi_{\mu\nu}^-(x^j)} \Delta_{j,\nu,\text{in}} s_{\mu\nu}^j, \\ \mathcal{X}_j^+ &\equiv \Delta_{j,\mu,\text{in}}^{-1} (s_{\nu\mu}^{j+})^\dagger \Delta_{j,\nu,\text{in}} = \Delta_{j,\mu,\text{in}}^{-1} e^{i\Phi_{\mu\nu}^+(x^j)} \Delta_{j,\nu,\text{in}} \bar{s}_{\nu\mu}^j.\end{aligned}$$

For paths of given type p_1 or p_2 fixing the Keldysh branches on which the 2 tunneling events $\mu \rightarrow \nu$ (at i), $\nu \rightarrow \mu$ (at j) take place characterizes the corresponding paths uniquely provided they exist. Whether they exist or not depends on topology. Remarkably, they always do if the 2 tunneling events are required to occur on *different* Keldysh branches. Fig. D.23 shows the paths for $i : \mu \rightarrow \nu$ occurring on the forward, $j : \nu \rightarrow \mu$

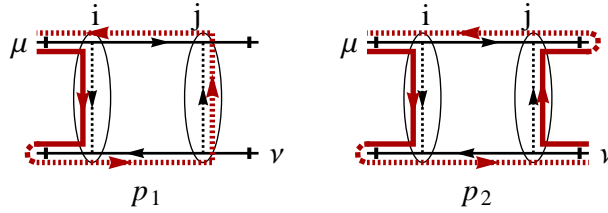


Figure D.23: Paths for topology A with $i : \mu \rightarrow \nu$ on the forward, $j : \nu \rightarrow \mu$ on the backward branch. The forward parts are represented by solid thick lines; the backward parts by dashed lines. The first path is of type p_1 , the second one of type p_2 .

on the backward branch for configuration A. Similar paths can be drawn for all other configurations. As an example, we consider the first path in Fig. D.23 which is of type p_1 . It starts at source μ , tunnels at i on the forward branch, arrives at drain ν , evolves backwards, tunnels at j on the backward branch and returns to source μ . Its amplitude is $\tilde{A}_{\mu\mu}^{(p_1)} = \mathcal{X}_j^+ \mathcal{X}_i^-$. The contribution of both paths to \mathcal{A}_t is

$$\mathcal{A}_{ij;\mu\nu}^< = -i\text{Tr} [\mathcal{X}_j^+ \mathcal{X}_i^- f_\mu - \mathcal{X}_j^+ f_\nu \mathcal{X}_i^- f_\mu] = -i\text{Tr} [e^{-i\Phi_{\mu\nu}^-(x^i)} \Pi_{ij;\mu\nu}^< e^{i\Phi_{\mu\nu}^-(x^j)}]$$

where tunneling polarization operators $\Pi_{ij;\mu\nu}$ are defined in (22) and we have made use of $s_{\mu\nu}^j = -\bar{s}_{\nu\mu}^j + \mathcal{O}(\text{tun}^2)$. Similarly $\mathcal{A}_{ij;\mu\nu}^>$ with $\Pi_{ij;\mu\nu}^>$ is obtained by considering paths with tunneling at i on the backward, at j on the forward branch. As mentioned previously the very same paths can be drawn for all topologies and yield the same action.

The story is less neat if both tunneling events occur on the same Keldysh branch: While p_2 -type contributions to $\mathcal{A}_{ij;\mu\nu}^T$ and $\mathcal{A}_{ij;\mu\nu}^{\bar{T}}$ are still independent from topology, p_1 -type contributions are not as universal. Taking all paths carefully into account results in the table below

	$\Pi_{ij;\mu\nu}^T(t)/[-s_{\nu\mu}^i \bar{s}_{\nu\mu}^j]$	$\Pi_{ij;\mu\nu}^{\bar{T}}(t)/[-s_{\nu\mu}^i \bar{s}_{\nu\mu}^j]$
A	$-\tilde{f}_\mu^<(t) \tilde{f}_\nu^<(-t)$	$\tilde{f}_\mu^>(t) \tilde{f}_\nu^<(-t) + \tilde{f}_\mu^<(t) \tilde{f}_\nu^>(-t) + \tilde{f}_\mu^<(t) \tilde{f}_\nu^<(-t)$
B	$\tilde{f}_\mu^>(t) \tilde{f}_\nu^<(-t) + \tilde{f}_\mu^<(t) \tilde{f}_\nu^>(-t) + \tilde{f}_\mu^<(t) \tilde{f}_\nu^<(-t)$	$-\tilde{f}_\mu^<(t) \tilde{f}_\nu^<(-t)$
C	$\tilde{f}_\mu^<(t) \tilde{f}_\nu^>(-t)$	$\tilde{f}_\mu^>(t) \tilde{f}_\nu^<(-t)$
D	$\tilde{f}_\mu^>(t) \tilde{f}_\nu^<(-t)$	$\tilde{f}_\mu^<(t) \tilde{f}_\nu^>(-t)$
E	$-f_\mu^<(t) f_\nu^<(-t) + \frac{1}{2}(f_\mu^<(t) + f_\nu^<(-t))\delta(t)$	$-f_\mu^>(t) f_\nu^>(-t) + \frac{1}{2}(f_\mu^<(t) + f_\nu^<(-t))\delta(t)$

with $\tilde{f}_\mu^{\gtrless}(t) \equiv f_\mu^{\gtrless}(t + \tau_{\mu,\text{in}}^i - \tau_{\mu,\text{in}}^j)$, $\tilde{f}_\nu^{\gtrless}(t) \equiv f_\nu^{\gtrless}(t - \tau_{\nu,\text{in}}^i + \tau_{\nu,\text{in}}^j)$. We have incorporated the tunneling-free contribution (D.3) into the case E which amounts to the $\delta(t)$ -terms.

Quite miraculously, using the symmetry relation $f_{\mu/\nu}^{\gtrless}(t) = -f_{\mu/\nu}^{\lessgtr}(t)$ for $t \neq 0$, one can show that (23) holds, i.e. $\Pi_{ij;\mu}^{T/\bar{T}}$ can be represented in a form which is independent of topology. We exemplify the proof,

which is a straightforward calculation, on configuration A. In this situation, $\tau_{\mu,\text{in}}^j > \tau_{\mu,\text{in}}^i$ and $\tau_{\nu,\text{in}}^i > \tau_{\nu,\text{in}}^j$ and thus $\tilde{f}_\mu^>(t) = -\tilde{f}_\mu^<(t)$ for $t > 0$ and $\tilde{f}_\nu^>(-t) = -\tilde{f}_\nu^<(-t)$ for $t < 0$, hence,

$$\begin{aligned} -\tilde{f}_\mu^<(t)\tilde{f}_\nu^<(-t) &= \theta(t)\tilde{f}_\mu^>(t)\tilde{f}_\nu^<(-t) + \theta(-t)\tilde{f}_\mu^<(t)\tilde{f}_\nu^>(-t), \\ \tilde{f}_\mu^>(t)\tilde{f}_\nu^<(-t) + \tilde{f}_\mu^<(t)\tilde{f}_\nu^>(-t) + \tilde{f}_\mu^<(t)\tilde{f}_\nu^<(-t) &= \theta(-t)\tilde{f}_\mu^>(t)\tilde{f}_\nu^<(-t) + \theta(t)\tilde{f}_\mu^<(t)\tilde{f}_\nu^>(-t), \end{aligned}$$

proving our statement. In the case E it is necessary to drop a constant (albeit infinite) and thus physically irrelevant contribution to the action to obtain (23) or (24). (See similar discussion after Eq. (24))

Appendix E. Saddle-Point Approximation

We prove here the formulas of Sect. 2.4. To keep things readable we resort on a rather symbolic notation, in which the contributions to the exponent in (26) read

$$\mathcal{A}_0[\varphi] = \frac{1}{2}\varphi V^{-1}\varphi - \varphi \varrho_0, \quad \mathcal{A}_t[\varphi] = -ie^{-i\Phi(1)}\Pi_{12}e^{i\Phi(2)}, \quad \mathcal{A}_J[\varphi] = -J\varphi$$

with the tunneling phases $\Phi = -\mathcal{D}\varphi$ being linear functionals of φ . The saddle-points of $\mathcal{A}_0 + \mathcal{A}_t + \mathcal{A}_J$ and $\mathcal{A}_0 + \mathcal{A}_J$ are denoted φ_{**} and φ_* . We show first that up to the chosen accuracy $\mathcal{O}(\text{tun}^2)$ the former is not needed and calculation of the latter is sufficient, using that $\varphi_* - \varphi_{**} = \mathcal{O}(\text{tun}^2)$. A Gaussian expansion of the full action around φ_{**} reads

$$(\mathcal{A}_0 + \mathcal{A}_t + \mathcal{A}_J)[\varphi] \approx (\mathcal{A}_0 + \mathcal{A}_t + \mathcal{A}_J)[\varphi_{**}] + \frac{1}{2}(\varphi - \varphi_{**}) \delta^2(\mathcal{A}_0 + \mathcal{A}_t + \mathcal{A}_J)[\varphi_{**}] (\varphi - \varphi_{**}). \quad (\text{E.1})$$

Note that the first order term vanishes due to φ_{**} being the full saddle-point. We now successively replace φ_{**} by φ_* in the above expression. Expansion around φ_{**} and using $\delta^2(\mathcal{A}_0 + \mathcal{A}_J)[\varphi_{**}] = V^{-1} = \delta^2(\mathcal{A}_0 + \mathcal{A}_J)[\varphi_*]$ yields

$$\begin{aligned} (\mathcal{A}_0 + \mathcal{A}_t + \mathcal{A}_J)[\varphi_*] &= (\mathcal{A}_0 + \mathcal{A}_t + \mathcal{A}_J)[\varphi_{**}] + \mathcal{O}(\text{tun}^4), \\ \delta^2(\mathcal{A}_0 + \mathcal{A}_t + \mathcal{A}_J)[\varphi_*] &= \delta^2(\mathcal{A}_0 + \mathcal{A}_t + \mathcal{A}_J)[\varphi_{**}] + \mathcal{O}(\text{tun}^4). \end{aligned}$$

Writing $\varphi - \varphi_{**} = (\varphi - \varphi_*) + (\varphi_* - \varphi_{**})$ and using again $\varphi_* - \varphi_{**} = \mathcal{O}(\text{tun}^2)$ Eq. (E.1) thus becomes

$$\begin{aligned} (\mathcal{A}_0 + \mathcal{A}_t + \mathcal{A}_J)[\varphi] &\approx (\mathcal{A}_0 + \mathcal{A}_t + \mathcal{A}_J)[\varphi_*] + \frac{1}{2}(\varphi - \varphi_*) \delta^2(\mathcal{A}_0 + \mathcal{A}_t + \mathcal{A}_J)[\varphi_*] (\varphi - \varphi_*) \\ &\quad + (\varphi_* - \varphi_{**}) \delta^2(\mathcal{A}_0 + \mathcal{A}_t + \mathcal{A}_J)[\varphi_*] (\varphi - \varphi_{**}). \end{aligned} \quad (\text{E.2})$$

Only the last term, which is linear in $\varphi - \varphi_*$, contains φ_{**} . To proceed, we define $h \equiv (\varphi_* - \varphi_{**}) \delta^2(\mathcal{A}_0 + \mathcal{A}_t + \mathcal{A}_J)[\varphi_*] = \mathcal{O}(\text{tun}^2)$ and perform the functional integration (26) in Gaussian approximation (E.2):

$$\begin{aligned} \int \mathcal{D}\varphi e^{i(\mathcal{A}_0 + \mathcal{A}_t + \mathcal{A}_J)[\varphi]} &\approx e^{i(\mathcal{A}_0 + \mathcal{A}_t + \mathcal{A}_J)[\varphi_*]} (\text{Det } \delta^2(\mathcal{A}_0 + \mathcal{A}_t + \mathcal{A}_J)[\varphi_*])^{-1/2} \\ &\quad \times \exp\left[-\frac{i}{2}h \underbrace{\delta^2(\mathcal{A}_0 + \mathcal{A}_t + \mathcal{A}_J)[\varphi_*]}_{=\mathcal{O}(\text{tun}^4)} h\right] \\ &= e^{i(\mathcal{A}_0 + \mathcal{A}_J)[\varphi_*]} \exp\left[i\mathcal{A}_t[\varphi_*] - \frac{1}{2}\text{Tr Ln } (\mathbb{1} + V\delta^2\mathcal{A}_t[\varphi_*])\right]. \end{aligned} \quad (\text{E.3})$$

Hence, φ_{**} dropped out completely. The first exponential satisfies $e^{i(\mathcal{A}_0 + \mathcal{A}_J)[\varphi_*]} = \langle e^{i\mathcal{A}_J[\varphi]} \rangle_0$ where $\langle \dots \rangle_0$ denotes the average with respect to the free action $\mathcal{A}_0[\varphi]$. This is shown using $\langle \varphi \rangle_0 = \bar{\varphi} \equiv V\varrho_0$ and $\langle (\varphi - \bar{\varphi})(\varphi - \bar{\varphi}) \rangle_0 = iV$. Since $\mathcal{A}_0[\varphi]$ is Gaussian we have the simple relation

$$\langle e^{i\mathcal{A}_J[\varphi]} \rangle_0 = \langle e^{-iJ\varphi} \rangle_0 = \exp\left[-iJ\bar{\varphi} - \frac{1}{2}\langle [J(\varphi - \bar{\varphi})]^2 \rangle\right] = e^{-iJ\bar{\varphi} - \frac{i}{2}JVJ}.$$

On the other hand it is $i(\mathcal{A}_0 + \mathcal{A}_J)[\varphi_*] = -\frac{i}{2}(\varrho_0 + J)V(\varrho_0 + J) = -\frac{i}{2}JVJ - iJ\bar{\varphi} - \frac{i}{2}\varrho_0 V\varrho_0$. I.e. up to the last term $-\frac{i}{2}\varrho_0 V\varrho_0$, which is canceled by normalization, we have

$$e^{i(\mathcal{A}_0 + \mathcal{A}_J)[\varphi_*]} = e^{-iJ\bar{\varphi} - \frac{i}{2}JVJ} = \left\langle e^{i\mathcal{A}_J[\varphi]} \right\rangle_0$$

which proves (29).

To deal with the second exponential in (E.3) we expand the logarithm to leading order in V (again, a Gaussian expansion),

$$\begin{aligned} i\mathcal{A}_t[\varphi_*] - \frac{1}{2}\text{Tr Ln}(\mathbb{1} + V\delta^2\mathcal{A}_t[\varphi_*]) &\approx i\mathcal{A}_t[\varphi_*] - \frac{1}{2}\text{Tr } V\delta^2\mathcal{A}_t[\varphi_*] = i\mathcal{A}_t[\varphi_*] + \underbrace{i\langle\delta\mathcal{A}_t[\varphi_*](\varphi - \bar{\varphi})\rangle_0}_{=0} \\ &+ \frac{i}{2}\langle(\varphi - \bar{\varphi})\delta^2\mathcal{A}_t[\varphi_*](\varphi - \bar{\varphi})\rangle_0 \approx i\langle\mathcal{A}_t[\varphi - \bar{\varphi} + \varphi_*]\rangle_0. \end{aligned}$$

Defining the phases $\bar{\Phi} = -\mathcal{D}\bar{\varphi}$, $\Phi_* = -\mathcal{D}\varphi_*$ it is

$$\langle\mathcal{A}_t[\varphi - \bar{\varphi} + \varphi_*]\rangle_0 = -i\left\langle e^{-i[\Phi(1) - \bar{\Phi}(1) + \Phi_*(1)]} \Pi_{12} e^{i[\Phi(2) - \bar{\Phi}(2) + \Phi_*(2)]} \right\rangle_0 = -ie^{-i\Phi_*(1)} \tilde{\Pi}_{12} e^{i\Phi_*(2)},$$

i.e. Eq. (30), where $\tilde{\Pi}_{12} \equiv e^{i(D_\Phi(1,2) - D_\Phi(0,0))}\Pi_{12}$ are the renormalized tunneling polarization operators with the phase-phase correlator

$$D_\Phi(1, 2) = -i\langle(\Phi(1) - \bar{\Phi}(1))(\Phi(2) - \bar{\Phi}(2))\rangle_0 = (\mathcal{D}V\mathcal{D})(1, 2).$$

References

- [1] A. Kamenev, A. Levchenko, *Advances in Physics* **58**, 197 (2009).
- [2] A. Kamenev, *Field Theory of Non-Equilibrium Systems* (Cambridge University Press, Cambridge, 2011).
- [3] T. Giamarchi, *Quantum Physics in One Dimension* (Oxford University Press, 2004).
- [4] D.B. Gutman, Y. Gefen, and A. D. Mirlin, *Europhys. Letters* **90**, 37003 (2010); *Phys. Rev. B* **81**, 085436 (2010).
- [5] A. Grishin, I.V. Yurkevich, I.V. Lerner, *Phys. Rev. B* **69**, 165108 (2004) and references therein.
- [6] L.S. Levitov and G.B. Lesovik, *JETP Lett.* **58**, 230 (1993); L.S. Levitov, H. Lee, and G.B. Lesovik, *J. of Math. Phys.* **37**, 4845 (1996); D.A. Ivanov, H. Lee, and L.S. Levitov, *Phys. Rev. B* **56**, 6839 (1997).
- [7] Klich, I. in *Quantum Noise in Mesoscopic Physics* (ed. Nazarov, Y. V.) 397-402 (NATO Science Series, Kluwer, Dordrecht, 2003).
- [8] I. Snyman and Y.V. Nazarov, *Phys. Rev. B* **77**, 165118(2008).
- [9] S. Ngo Dinh, D.A. Bagrets, and A.D. Mirlin, *Phys. Rev. B* **81**, 081306(R) (2010).
- [10] S. Ngo Dinh and D.A. Bagrets, *Phys. Rev. B* **85**, 073403 (2012).
- [11] J.T. Chalker, and P.D. Coddington, *J. Phys. C* **21** 2665 (1988).
- [12] I.E. Dzyaloshinskii, K.B. Larkin, *JETP* **38**, 202 (1973)
- [13] U. Eckern, G. Schön, V. Ambegaokar, *Phys. Rev. B* **30**, 6419 (1984).
- [14] L.S. Levitov and A.V. Shtyov, *Sov. Phys. JETP* **66**, 214 (1997).
- [15] Y.-Fu Chen *et al.*, *Phys. Rev. Lett.* **102**, 036804 (2009).
- [16] C. Altimiras, H. le Sueur, U. Gennser, *et al.*, *Nature Physics*, **6** 34 (2010).
- [17] H. le Sueur, C. Altimiras, U. Gennser, *et al.*, *Phys. Rev. Lett.* **105** 056803 (2010).
- [18] H. le Sueur, C. Altimiras, U. Gennser, *et al.*, *Phys. Rev. Lett.* **105** 226804 (2010).
- [19] C. Nayak *et al.*, *Rev. Mod. Phys.* **80**, 1083 (2008).
- [20] D.B. Chklovskii, K.A. Matveev, and B.I. Shklovskii, *Phys. Rev. B* , **47**, 12605 (1993).
- [21] N.R. Cooper and J.T. Chalker, *Phys. Rev. B* **48**, 4530 (1993).
- [22] A.K. Evans, L.I. Glazman, and B.I. Shklovskii, *Phys. Rev. B* **48**, 11120 (1993).
- [23] With the logarithmic accuracy this result can be deduced from the mutual capacitance per length of two parallel coplanar strips of the widths b_i which are separated at distance a from each other, $C_{12} = (1/4\pi)K(\sqrt{1-k^2})/K(k)$, where $k^2 = k_1 k_2$, $k_i = a/(2b_i + a)$ and K is elliptic integral of the first kind. See e.g. K.J Binns, P.J. Lawrenson, *Analysis and computation of electric and magnetic field problems*, Oxford, New York, Pergamon Press (1973).
- [24] A. Furusaki and K.A. Matveev, *Phys. Rev. B* **52**, 16676 (1995).
- [25] D. A. Bagrets and Yu. V. Nazarov, *Phys. Rev. Lett.* **94** 056801 (2005).
- [26] D. T. McClure *et al.*, *Phys. Rev. Lett.* **103**, 206806 (2009).
- [27] Y. Yamauchi *et al.*, *Phys. Rev. B* **79**, 161306(R) (2009).
- [28] Yiming Zhang *et al.*, *Phys. Rev. B* **79**, 241304(R) (2009).

- [29] N. Ofek *et al.*, Proc. Natl. Acad. Sci. USA **107**, 5276 (2010).
- [30] Y. Ji, Y. C. Chung, D. Sprinzak, M. Heiblum, D. Mahalu, and H. Shtrikman, Nature (London) **422**, 415 (2003).
- [31] I. Neder, M. Heiblum, Y. Levinson, D. Mahalu, and V. Umansky, Phys. Rev. Lett. **96**, 016804 (2006).
- [32] I. Neder, M. Heiblum, D. Mahalu, and V. Umansky, Phys. Rev. Lett. **98**, 036803 (2007).
- [33] I. Neder, F. Marquardt, M. Heiblum, D. Mahalu, and V. Umansky, Nat. Phys. **3**, 534 (2007).
- [34] P. Roulleau, F. Portier, D. C. Glatthli, P. Roche, A. Cavanna, G. Faini, U. Gennser, and D. Mailly, Phys. Rev. B **76**, 161309(R)(2007).
- [35] P. Roulleau, F. Portier, D. C. Glatthli, P. Roche, A. Cavanna, G. Faini, U. Gennser, and D. Mailly, Phys. Rev. Lett. **100**, 126802(2008).
- [36] P. Roulleau, F. Portier, P. Roche, A. Cavanna, G. Faini, U. Gennser, and D. Mailly, Phys. Rev. Lett. **101**, 186803 (2008); *ibid* **102**, 236802 (2009).
- [37] P.-A. Huynh, F. Portier, H. le Sueur, G. Faini, U. Gennser, D. Mailly, F. Pierre, W. Wegscheider, P. Roche, arXiv:1202.3591.
- [38] L. V. Litvin, H.-P. Tranitz, W. Wegscheider, and C. Strunk, Phys. Rev. B **75**, 033315 (2007).
- [39] L. V. Litvin, A. Helzel, H.-P. Tranitz, W. Wegscheider, and C. Strunk, Phys. Rev. B **78**, 075303 (2008).
- [40] L. V. Litvin, A. Helzel, H.-P. Tranitz, W. Wegscheider, and C. Strunk, Phys. Rev. B **81**, 205425 (2010).
- [41] E. Bieri, M. Weiss, O. Göktas, M. Hauser, C. Schönenberger, and S. Oberholzer, Phys. Rev. B **79**, 245324 (2009).
- [42] I. Neder and E. Ginossar, Phys. Rev. Lett. **100**, 196806 (2008).
- [43] E.V. Sukhorukov and V.V. Cheianov, Phys. Rev. Lett. **99**, 156801 (2007).
- [44] J.T. Chalker, Y. Gefen, and M.Y. Veillette, Phys. Rev. B **76**, 085320 (2007).
- [45] I.P. Levkivskyi and E.V. Sukhorukov, Phys. Rev. B **78**, 045322 (2008).
- [46] Seok-Chan Youn, Hyun-Woo Lee, and H.-S. Sim, Phys. Rev. Lett. **100**, 196807 (2008).
- [47] D.L. Kovrizhin and J.T. Chalker, Phys. Rev. B **80**, 161306 (2009); *ibid*, **81**, 155318 (2010).
- [48] M. Schneider, D. A. Bagrets, A. D. Mirlin, Phys. Rev. B **84**, 075401 (2011).
- [49] C. de C. Chamon, D. E. Freed, S. A. Kivelson, S. L. Sondhi, and X. G. Wen, Phys. Rev. B **55**, 2331 (1997).
- [50] B. Rosenow and B. I. Halperin, Phys. Rev. Lett. **98**, 106801 (2007).
- [51] B. I. Halperin *et al.*, Phys. Rev. B **83**, 155440 (2011).
- [52] S. Ngo Dinh, D.A. Bagrets, and A.D. Mirlin, to be published.
- [53] D.B. Gutman, Y. Gefen, and A. D. Mirlin, J. Phys. A: Math. Theor. **44**, 165003 (2011); I. V. Protopopov, D. B. Gutman, and A.D. Mirlin, arXiv:1203.6418
- [54] B. Braunecker, Phys. Rev. B **73**, 075122(2006).
- [55] R. Landauer, Physica D **38**, 226(1987); Th. Martin and R. Landauer, Phys. Rev. B **45**, 1742(1992).